

Approximate string matching in the high-throughput sequencing era

Dissertation zur Erlangung des Grades eines
Doktors der Naturwissenschaften (Dr. rer. nat.)
vorgelegt von

Enrico Siragusa



am Fachbereich Mathematik und Informatik
der Freien Universität Berlin

Berlin 2014

Datum des Disputation: **XX.XX.2014**

Gutachter:

Prof. Dr. Knut Reinert, *Freie Universität Berlin, Deutschland*

Prof. Dr. XXX XXX, XXX, XXX

Abstract

Abstract...

CONTENTS

1. Introduction	1
1.1 High-throughput sequencing	1
1.1.1 Protocols and applications	2
1.1.2 Analysis pipelines	3
1.2 Outline	5
1.2.1 Approximate string matching	5
1.2.2 Read mapping	5
 Part I Approximate string matching	 7
2. Stringology preliminaries	9
2.1 Definitions	9
2.2 Alignments	10
2.3 Distance functions	11
2.4 Optimal alignments	12
2.5 String matching	13
2.5.1 Online methods	14
2.5.2 Indexed methods	14
2.5.3 Filtering methods	17
3. Indexed methods	19
3.1 Classic full-text indices	20
3.1.1 Suffix array	20
3.1.2 q -Gram index	23
3.2 Succinct full-text indices	25
3.2.1 Burrows-Wheeler transform	26
3.2.2 Rank dictionaries	28
3.2.3 FM-index	31
3.3 Algorithms	33
3.3.1 Bounded top-down traversal	33
3.3.2 Exact pattern matching	33
3.3.3 Backtracking k -mismatches	34
3.3.4 Backtracking k -differences	35
3.3.5 Multiple backtracking	37

4. Filtering methods	41
4.1 Exact seeds	42
4.2 Approximate seeds	44
4.2.1 Parameterization	44
4.2.2 Redundancy	45
4.3 Contiguous q -grams	46
4.4 Gapped q -grams	47
4.4.1 Characteristic functions	48
4.4.2 Full-sensitivity	49
4.4.3 Optimal threshold	49
4.4.4 Maximum error	51
4.4.5 Specificity	51
4.4.6 Optimal gapped q -grams	52
4.5 Verification methods	53
4.5.1 Banded Myers' bit-vector algorithm	53
4.5.2 Increased bit-parallelism using SIMD instructions	53
 Part II Read mapping	 55
5. Background	57
5.1 High-throughput sequencing data	57
5.1.1 Read sequences	57
5.1.2 Phred base quality scores	57
5.2 Data analysis paradigms	58
5.2.1 Best-mapping	59
5.2.2 All-mapping	60
5.3 Limits of high-throughput sequencing	61
5.3.1 Genome mappability	61
5.3.2 Genome mappability score	62
5.4 Popular read mappers	63
5.4.1 Bowtie	64
5.4.2 BWA	65
5.4.3 Soap	65
5.4.4 SHRiMP	66
5.4.5 RazerS	66
5.4.6 mr(s)Fast	66
5.4.7 GEM	66
6. Masai	69
6.1 Engineering	70
6.1.1 Filtration	70
6.1.2 Indexing	71
6.1.3 Verification	73
6.2 Evaluation	73
6.2.1 Rabema benchmark on simulated data	74
6.2.2 Variant detection on simulated data	75
6.2.3 Performance on real data	77

6.2.4	Filtration efficiency	78
6.3	Discussion	79
7.	Yara	81
7.1	Engineering	81
7.1.1	Ad-hoc filtration	81
7.1.2	Stratified filtration	82
7.1.3	Paired-end and mate-pair protocols	83
7.1.4	Mapping qualities	84
7.1.5	Indexing	84
7.2	Evaluation	84
7.2.1	Experimental setup	85
7.2.2	Accuracy on simulated data	85
7.2.3	Rabema benchmark on simulated and real data	86
7.2.4	Throughput on real data	86
A.	Dictionary search and join	89
A.1	Online methods	89
A.2	Indexed methods	90
A.3	Filtering methods	90
B.	Read mappers parameterization	91
B.1	Masai evaluation	91
B.2	Yara evaluation	92
C.	Declaration	93
	Bibliography	94

The sequencing of the whole human genome, consisting of three billion base pairs of DNA, has been one of the major scientific achievements of the last decades. Very surprisingly, this milestone has been achieved twice, by two independent groups. The three billion dollars publicly funded *Human Genome Project* (HGP) in February 2001 published the first draft covering more than 96% of the euchromatic part of the human genome [?], and finally the full sequence in April 2003. The privately funded company *Celera Genomics* concurrently published a 2.91 billion base pair consensus sequence of the euchromatic portion of the human genome [?]. These two groups also contributed to characterize the entire genomes of other model organisms, such as mice [?], fruit flies [?], nematode worms and yeasts.

These achievements are not only due to the efforts of molecular biologists but also of computer scientists. Indeed, both groups used sequencing technologies based on the *shotgun* approach. Shotgun sequencing consists of chopping long DNA fragments up into smaller segments and then generating *reads* of these short nucleotide sequences. Then, it is left up to *bioinformatics* to reassemble these reads and produce a holistic representation of the original genome.

These early sequencing projects used *capillary electrophoresis* based on the *Sanger sequencing* method [?]. This sequencing technology is capable of reading DNA with high fidelity but at low speed: it produces reads of an average length of 700 bp at a throughput of about 150 Kbp/h. Moreover, in order to produce an assembly with high fidelity, DNA must be sequenced multiple times to obtain a manyfold *coverage*. At this pace, the sequencing of the human genome took years and many million dollars. Nonetheless, the success of those huge sequencing projects did not mark the end of the sequencing era, but its beginning.

1.1 High-throughput sequencing

Since then, sequencing technology steadily improved and evolved into what is now called *high-throughput sequencing* (HTS), or *next-generation sequencing* (NGS). In 2004, *454 Life Science* commercialized the *Genome Sequencer FLX*, an instrument based on large-scale parallel *pyrosequencing*, capable of sequencing DNA under the form of 400 bp reads at a throughput of 20–30 Mbp/h. High-throughput sequencing was born.

In 2006, Solexa released its *1G Genetic Analyzer*, based on a massively parallel tech-

nique of *reversible terminator-based sequencing*. The instrument produced reads as short as 30 bp, at lower accuracy than Sanger sequencing, but at very high-throughput: it allowed *resequencing* a human genome in three months for about \$100,000. Following this success, Solexa was acquired by *Illumina*, which is nowadays the market leader. At the beginning of 2014, Illumina announced the *HiSeq X Ten*, allowing the sequencing of many human whole-genomes at \$1,000 each, in less than three days.

Over the last decade, other sequencing instruments hit the market with mixed success, e.g. the *SOLiD* system of *Applied Biosystems*, as well as the *third-generation sequencing* *Ion Torrent* instruments by *Life Technologies* and the *RS II* by *Pacific Bioscience*. I return to sequencing technologies in chapter 5.1, to give more insights on the kind of data produced and understand the problematics linked with their analysis.

In the following of this section, I continue to provide the context of this work. I first introduce most relevant *applications* of HTS and then explain how HTS *analysis pipelines* proceed. Then, I outline the structure of this work and state my contributions to this field.

1.1.1 Protocols and applications

In the last years, HTS has become an invaluable method of investigation for molecular biologists. Abundant and cost-effective production of sequencing data permits viewing not only genomic DNA but also transcripts and epigenetic features at unprecedented single-base resolution. For instance, applications of HTS include genotyping and discovery of structural variation (from DNA-seq); assessments of gene expression and alternative splicing events, analysis of microRNAs, discovery of novel non-coding RNAs (through RNA-seq); prediction of transcription factor binding-sites, analysis of methylation patterns (using ChIP-seq). Some HTS applications are already oriented towards clinical settings, e.g. in the context of mendelian disorders and cancer diagnostic.

Whole genome and exome-seq

Whole genome sequencing (WGS, DNA-reseq) allows discovery of genetic variations across the whole genome. These may be in the form of single nucleotide variants (SNVs), small insertions or deletions (indels), or large structural variants such as transversions, translocations, and copy number variants (CNVs). *Whole exome sequencing* (WES, exome-seq) is a cost-effective yet powerful alternative to WGS. This protocol consists in the targeted sequencing of the *exome*, i.e. the protein coding subset of the human genome.

RNA-seq

RNA sequencing (RNA-seq) is a protocol to sequence the *transcriptome*, i.e. the set of RNA molecules of an organism, including mRNAs, rRNAs, tRNAs, and other non-coding RNAs. Actual HTS technologies perform deep-sequencing of RNA molecules after they have been reverse-transcribed into cDNA. RNA-seq provides a myriad of information on gene expression, alternative splicing, intron/exon boundaries, untranslated regions (UTRs), and genetic variation with single-base accuracy.

ChIP-seq

Chromatin immunoprecipitation with next-generation sequencing (ChIP-seq) is a protocol that allows the selective sequencing of genomic DNA bound by a specific protein. The process isolates chromatin-protein complexes and shears them by sonication. Subsequently, immunoprecipitation with a protein-specific antibody pulls down genomic DNA sequences bound by a specific protein. These DNA sequences are finally sequenced by HTS. ChIP-seq is used to study the mechanisms of gene regulation. Through this sequencing protocol it is possible to determine global methylation patterns, identify transcription factor binding sites, histone modifications, chromatin remodelling proteins.

1.1.2 Analysis pipelines

The analysis of HTS data consists of numerous steps, ranging from the initial instrument specific data processing to the final application specific interpretation of the results. It is conventional wisdom to subdivide such data analysis pipelines in three stages of *primary*, *secondary*, and *tertiary* analysis. The primary stage of analysis consists of instrument specific processes for generation, collection, and processing of raw sequencing data. The secondary stage reconstructs the original sequence of the donor genome by applying sequence analysis methods to the raw sequencing data. The tertiary stage characterizes features of the donor genome specific to the sequencing application e.g. genetic variations in exome-seq, then provides interpretations e.g. by aggregating multiple samples and performing data mining.

Primary analysis

Primary analysis consists of instrument specific steps to call base pairs and compute quality metrics. The base caller processes instrumental signals and assigns a base to each peak, i.e. A, C, G, T, or N. The software assigns a quality value to each called base, estimating the probability of a base calling error. On early generation instruments, users could provide their own base calling tool. Now this process happens automatically on special hardware (e.g. FPGAs or GPUs) bundled within the instrument. The result of primary analysis is a standard *FASTQ* file containing DNA read sequences and their associated quality scores in *Phred* format (see section ??).

Secondary analysis

Secondary analysis aims at reconstructing the original sequence of the donor genome. There are two main *plans* to reassemble the original genome: (A) *de novo* assembly, and (B) *reference-guided* assembly (commonly called *read mapping*). *De novo* methods essentially scaffold the reads by performing *overlap alignments* [?] or equivalently by constructing *de Bruijn graphs* [?]. Computational methods in plan A are very involved, as they require finding a *shortest common superstring*, which is a NP-complete problem [?]. The knowledge of a *reference genome*, highly similar to the donor, simplifies the problem and opens the door to plan B. The reads are simply aligned to the reference, tolerating

a few base pair errors. It is worth mentioning that some combinations of plans A and B have been proposed in [??].

Plan B is always preferred in resequencing projects, as it is more computationally viable than plan A and directly provides a way to assess genetic variation w.r.t. a reference genome. In this manuscript, I follow only plan B and present methods that work within this specific plan. Nonetheless, many of the algorithmic components that I expose in the first part of this manuscript are ubiquitous in bioinformatics, thus applicable, if not already applied, to plan A. According to plan B, the secondary analysis step consists of three tasks: *quality control*, *read mapping*, and *pile up*.

Quality control (Q/C) checks the quality of raw reads. Reads produced by current HTS technologies contain sequencing artefacts, in form of single miscalled bases or stretches of oligonucleotides. In order to circumvent this problem, various techniques have been developed, ranging from the simple *trimming* of low quality read stretches to sophisticated methods of *read error correction* [?]. Nonetheless, sometimes Q/C is simply omitted.

Read mapping takes care of aligning the reads to the reference genome. Read mappers adopt state of the art *approximate string matching* methods to efficiently analyze the deluge of data produced by HTS instruments. Approximate matching accounts for two kinds of errors: residual sequencing artefacts not removed by Q/C, and small genetic variations in the donor genome to which reads belong. Thus, the read mapper must take into account errors when mapping reads.

Mapped reads, often stored in de-facto standard BAM files, are *piled up* in order to construct a *consensus sequence* of the donor genome. The height of the pileup denotes the sequencing depth at each locus in the donor genome, thus the average height corresponds to the average sequencing coverage; higher depth implies more confidence in the consensus sequence of the donor genome and thus more accuracy in tertiary analysis.

Tertiary analysis

Tertiary analysis aims at interpreting the deluge of information provided by secondary analysis. This pipeline stage groups a wide range of analyses specific to the sequencing application. In many pipelines, downstream analysis performs data mining over aggregated data coming from multiple samples.

Within DNA resequencing, *genotyping* consists of determining the variations between the donor and the reference genome. The result of *variant calling* is usually a VCF file annotating the variations of the donor genome. Subsequently, *genome-wide association studies* (GWAS) associate genetic variants with phenotypic traits by examining *single-nucleotide polymorphisms* (SNPs), variants relatively common among individuals of the same population.

In RNA-seq, tertiary analysis consists of computing transcripts abundance by measuring *reads per kilobase per million mapped reads* (RPKM) [?]. Subsequently, relative gene expression is determined by comparing multiple RNA samples. In ChIP-seq, this stage consists of calling peaks in correspondence of mapped reads, determining which peaks identify feasible transcription factor binding sites, then interesting sites affecting

gene regulation.

1.2 Outline

In this work, I present novel methods for the efficient and accurate mapping of high-throughput sequencing reads, based on state of the art approximate string matching algorithms and data structures. Read mapping is an ubiquitous and non-trivial task in all resequencing applications. Efficiency is required to keep the pace of HTS technologies constantly increasing their throughput. Accuracy is required to provide data analysis with single-base resolution.

I decided to subdivide this work in two parts: part I is about approximate string matching, while part II is about read mapping. The initial ingenuity of approximate string matching methods turns out to be beneficial in the design of an accurate method for read mapping.

1.2.1 Approximate string matching

In chapter 2, I introduce basic stringology concepts.

In chapter 3, I expose indexed methods for approximate string matching.

In chapter 4, I expose filtering methods for approximate string matching.

1.2.2 Read mapping

In chapter 5, I return to read mapping. I give a solid background.

In chapter 6, I present my first attempt at engineering a read mapping tool.

In chapter 7, I present Yara, a state of the art read mapping tool.

Part I

APPROXIMATE STRING MATCHING

We now introduce fundamental definitions and problems of stringology, in order to keep the manuscript self-contained. We provide a summary of notations at the end of this manuscript. The reader familiar with basic stringology can skip this chapter and proceed to chapter ??.

2.1 Definitions

Let us start by introducing primitive objects of stringology: alphabets and strings. An *alphabet* is a finite ordered set of symbols (or characters); a *string* (or word) over an alphabet is a finite sequence of symbols from that alphabet. We denote the length of a string s by $|s|$, and by ϵ the empty string s.t. $|\epsilon| = 0$.

Definition 2.1. Given an alphabet Σ , we define $\Sigma^0 = \{\epsilon\}$ as the set containing the empty string, Σ^n as the set of all strings over Σ of length n , and $\Sigma^* = \cup_{n=0}^{\infty} \Sigma^n$ as the set of all strings over Σ . Finally, we call any subset of Σ^* a language over Σ .

Definition 2.2. We define the concatenation operator of two strings as $\cdot : \Sigma^* \times \Sigma^* \rightarrow \Sigma^*$. Given two strings $x \in \Sigma^m$ with $x = x_1x_2 \dots x_m$ and $y \in \Sigma^n$ with $y = y_1y_2 \dots y_n$, their concatenation $x \cdot y$ (simply denoted xy) is the string $z \in \Sigma^{m+n}$ consisting of the symbols $x_1x_2 \dots x_my_1y_2 \dots y_n$.

Definition 2.3. A string x is a *prefix* of y iff there is some string z s.t. $y = x \cdot z$; analogously, x is a *suffix* of y iff there is some string z s.t. $y = z \cdot x$; moreover, x is a *substring* of y iff there is some string w, z s.t. $y = w \cdot x \cdot z$. We denote by $y_{1\dots i}$ the prefix of y ending at position $i \in \mathbb{N}$, by $y_{i\dots n}$ (or simply $y_{i\dots}$) the suffix of y beginning at position $i \in \mathbb{N}$, and by $y_{i\dots j}$ the substring of y within positions $i \leq j \in \mathbb{N}$.

Definition 2.4. Given an alphabet Σ of size σ , we define the function $\rho : \Sigma \rightarrow [1 \dots \sigma]$ denoting the *lexicographic rank* of any alphabet symbol, s.t. $\rho(a) < \rho(b) \Leftrightarrow a < b$ for any distinct $a, b \in \Sigma$.

Definition 2.5. We define the *lexicographical order* $<_{lex}$ between two non-empty strings x, y as $x <_{lex} y \Leftrightarrow x_1 < y_1$, or $x_1 = y_1$ and $x_{2\dots} <_{lex} y_{2\dots}$.

Definition 2.6. We define a *string collection* as an ordered multiset $\mathbb{S} = \{s^1, s^2, \dots, s^c\}$ of non necessarily distinct strings over a common alphabet Σ . We denote by $\|\mathbb{S}\| = \sum_{i=1}^c |s^i|$

the total length of the string collection. We also extend the notation of prefix, suffix and substring to multisets, e.g. $S_{(a,i) \dots (a,j)}$ denotes the substring $s_{i \dots j}^a$.

Definition 2.7. We call *terminator symbol* a symbol $\$ \notin \Sigma$ s.t. $\rho(\$) < \rho(a)$ for any $a \in \Sigma$.

Definition 2.8. Given a string s over Σ , we call *padded string* the concatenation of s with a terminator symbol $\$$.

Definition 2.9. Given a string collection \mathbb{S} over Σ , we call *padded string collection* the collection consisting of strings $s^i \in \mathbb{S}$ padded with terminator symbols $\i s.t. $\rho(\$^i) < \rho(\$^j) \Leftrightarrow i < j$.

2.2 Alignments

The next step is to define the minimal set of edit operations to transform one string into another: substitutions, insertions and deletions. Given two strings x, y of equal length n , the string x can be transformed into the string y by substituting (or replacing) all symbols x_i s.t. $x_i \neq y_i$ into y_i , for $1 \leq i \leq n$. If the given strings have different lengths, insertion and deletion of symbols from x become necessary to transform it into y . Therefore, given any two strings x, y , we define an edit transcript for x, y any finite sequence of substitutions, insertions and deletions transforming x into y . See Figure 2.1 for an example.

Figure 2.1: Example of edit transcript transforming the string $x = AAAAA$ into $y = CCCCC$. The transcript character M indicates a match, R a replacement, I an insertion, and D a deletion.

x	G C T N T G G G C A T T A T G G C C A T T T T T																								
$transcript$	M	M	M	R	M	M	D	M	M	M	M	M	R	M	M	M	M	I	M	M	M	M	R	M	
y	{ G C T A T G G C A T T G T G G C C C A T T T A T }																								

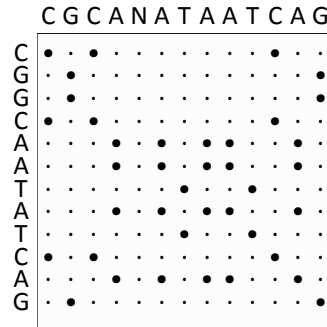
An alignment is an alternative yet equivalent way of visualizing a transformation between strings. While an edit transcript provides an explicit sequence of edit operations transforming one string into another, an alignment relates pairs of corresponding symbols between two strings. Because some symbols in one string are not related to any symbol in the other string, i.e. some symbols are inserted or removed, we first need to introduce a gap symbol $-$, which is not part of the string alphabet Σ . Subsequently, we can define the alignment of two strings of length m, n over Σ to be a string of length between $\min\{m, n\}$ and $m + n$ over the pair alphabet $(\Sigma \cup \{-\}) \times (\Sigma \cup \{-\})$.

Example 2.1. An alignment of the strings $x = AAAAA$ and $y = CCCCC$ is given by the string $z = \begin{pmatrix} A \\ A \end{pmatrix} \begin{pmatrix} A \\ - \end{pmatrix} \begin{pmatrix} A \\ C \end{pmatrix} \begin{pmatrix} G \\ G \end{pmatrix}$

A dotplot is a way to visualize any alignment between two strings and highlight their similarities. Given two strings x, y of length m, n , a dotplot is a $m \times n$ matrix containing a

dot at position (i, j) iff the symbol x_i matches symbol y_j . We define a dotplot trace to be a monotonical path in the matrix connecting non-decreasing positions of the matrix. A dotplot trace corresponds to an alignment and vice versa. In a trace, match and mismatch columns of the corresponding alignment appear as diagonal stretches, while insertions and deletions are horizontal or vertical stretches. See Figure 2.2.

Figure 2.2: Example of dotplot of the strings $x = AAAA$ and $y = CCCC$. The highlighted trace corresponds to the alignment of example 2.1.



2.3 Distance functions

We can assign a cost to any alignment and to its associated edit transformation by defining a weight function $\omega : (\Sigma \cup \{-\}) \times (\Sigma \cup \{-\}) \rightarrow \mathbb{R}_0^+$, where:

- $\omega(\alpha, \beta)$ for all $(\alpha, \beta) \in \Sigma \times \Sigma$ defines the cost of substituting α with β ,
- $\omega(\alpha, -)$ for all $\alpha \in \Sigma$ defines the cost of deleting the symbol α ,
- $\omega(-, \beta)$ for all $\beta \in \Sigma$ defines the cost of inserting the symbol β ,

and by defining the total cost $C(z)$ of an alignment z between two strings as the sum of the weights of all its alignment symbols:

$$C(z) = \sum_{i=0}^{|z|} \omega(z_i) \quad (2.1)$$

Consequently, we can define the distance function $d : \Sigma^* \times \Sigma^* \rightarrow \mathbb{R}_0^+$ by taking the minimum cost over all possible alignments of x, y :

$$d(x, y) = \sum_{z \in A(x, y)} C(z) \quad (2.2)$$

In particular, the edit or *Levenshtein distance* between two strings $x, y \in \Sigma^*$ is defined as the function $d_E : \Sigma^* \times \Sigma^* \rightarrow \mathbb{N}_0$ counting the *minimum* number of edit operation necessary to transform x into y . It is obtained by defining for all $(\alpha, \beta) \in \Sigma \times \Sigma$, $\omega(\alpha, \beta) = 1$ iff

$\alpha \neq \beta$ and 0 otherwise, and $\omega(\alpha, -)$ and $\omega(-, \beta)$ as 1. The *Hamming distance* between two strings $x, y \in \Sigma^n$ is defined as the function $d_H : \Sigma^n \times \Sigma^n \rightarrow \mathbb{N}_0$ counting the number of substitutions necessary to transform x into y . We obtain it by defining $\omega(\alpha, \beta)$ as in the edit distance, and by setting all $\omega(\alpha, -)$ and $\omega(-, \beta)$ to be ∞ in order to disallow indels.

Example 2.2. TODO: example of edit and hamming distance.

2.4 Optimal alignments

The problem of finding an optimal alignment between two strings is equivalent to the problem of finding their minimum distance [Gusfield, 1997]. A solution to this optimization problem can be efficiently computed via dynamic programming (DP). Below we describe the three essential components of the DP approach: the recurrence relation, the DP table, and the traceback.

Given two strings x, y of length m, n , for all $1 \leq i \leq m$ and $1 \leq j \leq n$ we define with $d(x_{1..i}, y_{1..j})$ the distance between their prefixes $x_{1..i}$ and $y_{1..j}$. The base conditions of the recurrence relation are:

$$d(\epsilon, \epsilon) = 0 \quad (2.3)$$

$$d(x_{1..i}, \epsilon) = \sum_{l=1}^i \omega(x_l, -) \text{ for all } 1 \leq i \leq m \quad (2.4)$$

$$d(\epsilon, y_{1..j}) = \sum_{l=1}^j \omega(-, y_l) \text{ for all } 1 \leq j \leq n \quad (2.5)$$

and the recursive case is defined as follows:

$$d(x_{1..i}, y_{1..j}) = \min \begin{cases} d(x_{1..i-1}, y_{1..j}) & + \omega(x_i, -) \\ d(x_{1..i}, y_{1..j-1}) & + \omega(-, y_j) \\ d(x_{1..i-1}, y_{1..j-1}) & + \omega(x_i, y_j) \end{cases} \quad (2.6)$$

We can compute the above recurrence relation in time $\mathcal{O}(nm)$ using a dynamic programming table D of $(m+1) \times (n+1)$ cells, where cell $D[i, j]$ stores the value of $d(x_{1..i}, y_{1..j})$. The sole distance without any alignment can be computed in space $\mathcal{O}(\min\{n, m\})$, as we only need column $D[: j - 1]$ to compute column $D[: j]$ (or row $D[i - 1 :]$ to compute $D[i :]$) and we can fill the table D either column-wise or row-wise¹. An optimal alignment can be computed in time $\mathcal{O}(m + n)$ via *traceback* on the table D : We start in the cell $D[m, n]$ and go backwards (either left, up-left, or up) to the previous cell by deciding which condition of equation 2.6 yielded the value of $D[m, n]$.

¹ Note that D can be filled also diagonal-wise or antidiagonal-wise.

Figure 2.3: DP table representing the computation of the edit distance $d_E(x_{1..5}, y_{1..4})$.

ϵ	C	G	C	A	N	A	T	A	A	T	C	A	G	
ϵ	0	1	2	3	4	5	6	7	8	9	10	11	12	13
C	0	1	2	3	4	5	6	7	8	9				
G	0	1	2	3	4	5	6	7	8	9				
G	0	1	2	3	4	5	6	7	8	9				
C	0	1	2	3	4	5	6	7	8	9				
A	0	1	2	3	4	5	6	7	8	9				
A	0	1	2	3	4	5	6	7	8	9				
T	0	1	2	3	4	5	6	7	8	9				
T														
A														
T														
C														
A														
G														

2.5 String matching

We now define *exact string matching*, one of the most fundamental problem in stringology.

Definition 2.10. [Gusfield, 1997] Given a string p of length m , called the *pattern*, and a string t of length n , called the *text*, the exact string matching problem is to find all occurrences of pattern p into text t .

This problem has been extensively studied from the theoretical standpoint and is well solved in practice [Faro and Lecroq, 2013]. Nonetheless, the definition of distance functions between strings let us generalize exact string matching into a more challenging problem: *approximate string matching*.

Definition 2.11. Given a text t , a pattern p , and a *distance threshold* $k \in \mathbb{N}$, the approximate string matching problem is to find all occurrences of p into t within distance k .

The approximate string matching problem under the Hamming distance is commonly referred as the *k-mismatches* problem and under the edit distance as the *k-differences* problem. For *k-mismatches* and *k-differences*, it must hold $k > 0$ as the case $k = 0$ corresponds to exact string matching, and $k < m$ as a pattern occurs at any position in the text if we substitute all its m characters.

Definition 2.12. Under the edit or Hamming distance, we define the *error rate* as $\epsilon = \frac{k}{m}$, with $0 < \epsilon < 1$ given the above conditions.

String matching problems are subdivided in two categories, *online* and *offline*, depending on which string, the pattern or the text, is given first. Algorithms for online string matching work by preprocessing the pattern and scanning the text from left to right (or right to left). Algorithms for offline string matching are instead allowed to preprocess the text, hence they build an index of the text beforehand to speed up subsequent searches. In practice, if the text is long, static and searched frequently, provided the necessary amount of memory for text indexing, offline methods outperform online methods in terms of runtime.

It goes without saying that offline string matching algorithms are tightly bound to text indexing data structures. Almost all of these algorithms require a *full-text index*, i.e. a data structure representing all substrings of the text. Very often, such *full-text index* is the *suffix tree* [?], a fundamental data structure in stringology. Among its virtues [?], the suffix tree natively provides exact string matching in optimal time and also approximate string matching via backtracking [?]. Often the suffix tree finds its use within hybrid *filtering methods* rather than on its own.

Filtering methods first discard uninteresting portions of the text and subsequently use a conventional method to verify only narrow areas. These methods work either online or offline. Online filtering methods try to jump over the text while scanning it, while offline filtering methods use an index to place anchors in the text. Any filtering method then requires an online verification method. Filtering methods outperform *native* online and indexed methods for a vast range of inputs, e.g. when the error rate is low, and are thus very appealing from a practical standpoint. Nonetheless, filtering methods are just opportunistic combinations of native online and indexed methods.

In the following of this section, I give a quick overview of the fundamental algorithms and data structures adopted in string matching methods. This overview serves as an introduction to the indexed and filtering methods presented in the next chapters. For an extensive treatment of this subject, the reader is referred to complete surveys on online [Navarro, 2001] and indexed [Navarro *et al.*, 2001] approximate string matching methods.

2.5.1 Online methods

The dynamic programming algorithm ?? to compute the distance of two strings can be easily turned into a string matching algorithm. Since an occurrence of the pattern can start and end anywhere in the text, k -differences consists of computing the edit distance between the pattern and any substring of the text. The problem can be thus solved by computing the edit distance between the text and the pattern without penalizing leading and trailing deletions in the text.

Consider equation 2.6 and pose $x = p$ and $y = t$. Since an occurrence of the pattern can start anywhere in the text, we change the initialization of the top row $D[0 :]$ of the DP matrix according to the condition:

$$d(\epsilon, y_{1..j}) = 0 \text{ for all } 1 \leq j \leq n \quad (2.7)$$

and since an occurrence of the pattern can end anywhere in the text, we check all cells $D[m, j]$ for all $1 \leq j \leq n$ in the bottom row of D for the condition $D[m, j] \leq k$.

2.5.2 Indexed methods

Here I introduce *suffix tries*, idealized data structures to index full-texts. Moreover, I define a set of generic operations to traverse suffix tries in a top-down fashion. In chapter 3, I will expose various data structures replacing suffix tries in practice. The generic

Figure 2.4: DP table representing the match of $p = \dots$ in $t = \dots$

	ϵ	C	G	C	A	N	A	T	A	A	T	C	A	G	A	A	A
ϵ	0	0	0	0	0	0	0	0	0	0	0	0	0	0	0	0	0
C	1	1	2	3	4	5	6	7	8	9							
G	2	1	2	3	4	5	6	7	8	9							
G	3	1	2	3	4	5	6	7	8	9							
C	4	1	2	3	4	5	6	7	8	9							
A	5	1	2	3	4	5	6	7	8	9							
A	6	1	2	3	4	5	6	7	8	•							

traversal operations here introduced lead to the formulation of generic algorithms solving string matching problems on any of these data structures.

Trie

Consider a padded string collection \mathbb{S} (definition 2.9) consisting of c strings. Note that padding is necessary to ensure that no string $s^i \in \mathbb{S}$ is a prefix of another string $s^j \in \mathbb{S}$.

Definition 2.13. The trie \mathcal{S} of \mathbb{S} is a lexicographically ordered tree data structure having one node designated as the root and c leaves, denoted as $l_1 \dots l_c$, where leaf l_i points to string s^i . The entering edge of any node of \mathcal{S} is labeled with a symbol in Σ , while the entering edge of any leaf of \mathcal{S} is labeled with a terminator symbol. Any path from the root to a leaf l_i spells the string s^i , including its terminator symbol $\i .

Suffix trie

We define the suffix trie as the trie of all suffixes of a string.

Definition 2.14. Given a padded string s (definition 2.8) of length n , the suffix trie \mathcal{S} of s has n leaves where leaf l_i points to suffix $s_{i..n}$.

We generalize the suffix trie to index string collections.

Definition 2.15. Given a padded string collection \mathbb{S} (definition 2.9), any leaf of the *generalized suffix trie* is labeled with a pair (i, j) where i points to the string $s^i \in \mathbb{S}$ and $1 \leq j \leq n_i$ points to one of the n_i suffixes of s^i . Thus each path from the root to a leaf (i, j) spells the suffix $\mathbb{S}_{(i,j) \dots}$.

Note that the suffix trie so defined contains $\mathcal{O}(n^2)$ nodes, yet we only consider the suffix trie as an idealized data structure to expose our algorithms. The optimal data structure to represent in linear space all suffixes of a given string is the *suffix tree* [Morrison, 1968]. However, the suffix tree comes with the restriction that internal nodes must have more than one child and with the property that edges can be labeled by strings of arbitrary length (see Figure 2.5). This latter property slightly complicates the exposition of our string matching algorithms but it does not affect their runtime complexity nor their result. For this reason, in the following of this manuscript we always consider w.l.o.g. suffix tries instead of suffix trees.

Figure 2.5: Suffix trie and suffix tree for the string ANANAS\$.



Figure 2.6: Generalized suffix trie for the string collection $\mathcal{S} = \{ \text{ANANAS}_1, \text{CACAO}_2 \}$.



Top-down traversal

We now give a set of generic operations to traverse tries in a top-down fashion. Given a trie \mathcal{T} , we define the following operations inspecting any pointed node x of \mathcal{T} :

- $\text{ISROOT}(x)$ returns true iff the pointed node is the root;
- $\text{ISLEAF}(x)$ returns true iff all outgoing edges are labeled by terminator symbols;
- $\text{LABEL}(x)$ returns the symbol labeling the edge entering x ;
- $\text{OCCURRENCES}(x)$ returns the list of positions pointed by leaves below x ;

and the following operations moving from pointed node x , and returning true on success and false otherwise:

Algorithm 2.1 $\text{goDOWN}(x)$

Input x : pointer to a suffix trie node
Output boolean indicating success
1: **if** $\text{ISLEAF}(x)$ **then**
2: **return false**
3: **if** $\text{goDOWN}(x, \min_{\text{lex}} \Sigma)$ **then**
4: **return true**
5: **else**
6: **return** $\text{goRIGHT}(x)$

Algorithm 2.2 $\text{goRIGHT}(x)$

Input x : pointer to a suffix trie node
Output boolean indicating success
1: **if not** $\text{ISROOT}(x)$ **then**
2: **while** $c \leftarrow \text{next}_{\text{lex}} \Sigma, \text{LABEL}(x)$ **do**
3: $\text{goUP}(x)$
4: **if** $\text{goDOWN}(x, c)$ **then**
5: **return true**
6: **return false**

- $\text{goDOWN}(x)$ moves to the lexicographically smallest child of x ;
- $\text{goDOWN}(x, c)$ moves to the child of x whose entering edge is labeled by c ;
- $\text{goRIGHT}(x)$ moves to the lexicographically next child of x ;
- $\text{goUP}(x)$ moves to the parent node of x .

Time complexities of the above operations depend on the data structure implementing the trie. Usually LABEL is $\mathcal{O}(1)$, both variants of goDOWN and goRIGHT can be $\mathcal{O}(1)$ or logarithmic in n , OCCURRENCES can be linear in the number of occurrences, goUP is $\mathcal{O}(1)$ but with an additional $\mathcal{O}(n)$ space complexity to stack all parent nodes. Note that is always possible to implement goDOWN and goRIGHT by relying on goDOWN a symbol and goUP , but their complexity becomes $\mathcal{O}(\sigma)$. In chapter 3, we consider various data structures to implement suffix tries, we show how to implement these operations and give their complexities.

2.5.3 Filtering methods

Filtering methods work in two stages: they first discard uninteresting portions of the text and subsequently use a conventional method to verify the remaining portions. These methods yield practical algorithms with good *average* running times. Whenever filtration is effective, the conventional method is applied to a relatively small portion of the text. In this case, the additional filtration stage pays off. Conversely, under some extreme circumstances, it pays off to directly apply the conventional method to the whole text.

Filtering methods for string matching work under the assumption that patterns occur in the text with a *low average probability*. For k -differences, the occurrence probability is a function of the error rate ϵ , in addition to the alphabet size σ , and can be computed or estimated under the assumption of the text being generated by a specific random source. Under the uniform Bernoulli model, where each symbol of Σ occurs with probability $\frac{1}{\sigma}$, Navarro and Baeza-Yates [2000] estimate that $\epsilon < 1 - \frac{1}{\sigma}$ is a conservative bound on the error rate which ensures few matches, and for which filtering algorithms are effective. For higher error rates, non-filtering methods, either online or offline, work better.

Filtering methods apply combinatorial criteria to determine which portions of the text are relevant and must be retained. These criteria are in general valid for both on-

line and offline variants of the problem. In practice, one specific criterion might be more convenient for one variant of the problem rather than the other. The combinatorial criterion underlying a filter is of paramount importance as it provides guarantees on filtration efficiency, both in terms of sensitivity and specificity.

Lossless versus lossy filters

A filter is said to be *lossless* or *full-sensitive* if it guarantees not to discard any occurrence of the pattern in the text, otherwise it is called *lossy*. Practical applications, e.g. read mapping, often do not require strictly lossless filtration. Nonetheless, a predictable or controlled lossy filter helps to interpret the results and insure their quality. For this reason, I focus on criteria yielding filters which are lossless or lossy in a predictable fashion.

Seeds versus q -grams

In this manuscript, I consider two classes of combinatorial filtering methods: those based on *seeds* and those based on *q -grams*. The first class of filters partition the pattern into *non-overlapping* factors called seeds. Application of the pigeonhole principle yields full-sensitive partitioning strategies. Instead, filters based on *q -grams* consider all *overlapping* substrings of the pattern having length q , the so-called *q -grams*. Simple lemmata give lower bounds on the number of *q -grams* that must be present in a narrow window of the text, as necessary condition for an approximate occurrence of the pattern.

Suffix trees are elegant data structures but they are rarely used in practice. Although suffix trees provides optimal construction and query time, their high space consumption prohibits practical applicability to large string collections. A practical study on suffix trees [Kurtz, 1999] reports that efficient implementations achieve sizes between $12n$ and $20n$ bytes per character. For instance, two years before completing the sequencing of the human genome, Kurtz conjectured the resources required for computing the suffix tree for the complete human genome (consisting of about $3 \cdot 10^9$ bp) in 45.31 GB of memory and nine hours of CPU time, and concluded that “it seems feasible to compute the suffix tree for the entire human genome on some computers”.

We might be tempted to think that such memory requirements are not anymore a limiting factor as, at the time of writing, standard personal computers come with 32 GB of main memory. Indeed, over the last decades, the semiconductors industry followed the exponential trends dictated by Moores’ law and yielded not only exponentially faster microprocessors but also larger memories. Unfortunately, memory latency improvements have been more modest, leading to the so called memory wall effect [Wilkes, 1995]: data access times are taking an increasingly fraction of total computation times. Thus, if in 1973 Knuth wrote that “space optimization is closely related to time optimization in a disk memory”, forty years later we can simply say that space optimization is closely related to time optimization.

Over the last years, a significant effort has been devoted to the engineering of more space-efficient data structures to replace the suffix tree in practical applications. In particular, much research has been done into designing succinct (or even compressed) data structures providing efficient query times using space proportional to that of the uncompressed (or compressed) input. Thanks to this research, we are able to index the human genome in as little as 3.5 GB of memory and at the same time improve query time over classic indices.

In this chapter, we introduce some classic full-text indices (suffix arrays and q -gram indices) and subsequently a succinct full-text index (an uncompressed variant of the original FM-index). Afterwards we give generic approximate string matching algorithms working on any of these data structures.

3.1 Classic full-text indices

3.1.1 Suffix array

The key idea of the suffix array [Manber and Myers, 1990] is that most information explicitly encoded in a suffix trie is superfluous for pattern matching. We can omit the explicit representation of suffix trie's internal nodes and outgoing edges. Leaves pointing to the sorted suffixes are sufficient to perform exact pattern matching or even trie traversals. Indeed, we can compute on the fly any path from the root to an internal node via binary search over the leaves. In this way, we are willing to pay an additional logarithmic time complexity to reduce space by a linear factor.

We define the suffix array and later show how to emulate suffix trie traversal.

Definition 3.1. The suffix array of a string s of length n is defined as an array A containing a permutation of the interval $[1, n]$, such that $s_{A[i]...n} <_{lex} s_{A[i+1]...n}$ for all $1 \leq i < n$.

Figure 3.1: Suffix array for the string ANANAS\$.

i	$A[i]$	$s_{A[i]...n}$
1	7	\$
2	1	ANANAS\$
3	3	ANAS\$
4	5	AS\$
5	2	NANAS\$
6	4	NAS\$
7	6	S\$

We define the generalized suffix array to index string collections, analogously to the generalized suffix trie introduced in section 2.5.2.

Definition 3.2. The generalized suffix array of a padded string collection \mathbb{S} (definition 2.9), consisting of c strings of total length n , is defined as an array A of length n containing a permutation of all pairs (i, j) where i points to a string $s^i \in \mathbb{S}$ and $1 \leq j \leq n_i$ points to one of the n_i suffixes of s^i . Pairs are ordered such that $\mathbb{S}_{A[i]...} <_{lex} \mathbb{S}_{A[i+1]...}$ for all $1 \leq i < n$.

We can construct the suffix array in $\mathcal{O}(n)$ time, for instance using the [Kärkkäinen and Sanders, 2003] algorithm, or using non-optimal but practically faster algorithms, e.g. [Schürmann and Stoye, 2007]. The space consumption of the suffix array is $n \log n$ bits. When $n < 2^{32}$, a 32 bit integer is sufficient to encode any value in the range $[1, n]$. Consequently, the space consumption of suffix arrays for texts shorter than 4 GB is $4n$ bytes.

[Weese, 2013] gives a generalization of Kärkkäinen and Sanders algorithm to construct the generalized suffix array in $\mathcal{O}(n)$ time. The space consumption of the generalized suffix array is $n \log cn^*$ bits, where $n^* = \max n_i$. For instance, the human genome

Figure 3.2: Generalized suffix array for the string collection $\mathbb{S} = \{ \text{ANANAS}\$_1, \text{CACAO}\$_2 \}$.

i	$A[i]$	$\mathbb{S}_{A[i] \dots}$
1	(1, 7)	$\$_1$
2	(2, 6)	$\$_2$
3	(2, 2)	$\text{ACAO}\$_2$
4	(1, 1)	$\text{ANANAS}\$_1$
5	(1, 3)	$\text{ANAS}\$_1$
6	(2, 4)	$\text{AO}\$_2$
7	(1, 5)	$\text{AS}\$_1$
8	(2, 1)	$\text{CACAO}\$_2$
9	(2, 3)	$\text{CAO}\$_2$
10	(1, 2)	$\text{NANAS}\$_1$
11	(1, 4)	$\text{NAS}\$_1$
12	(2, 5)	$\text{O}\$_2$
13	(1, 6)	$\text{S}\$_1$

GRCh38 is a collection of 24 sequences, among whose the largest one consists of 248 Mbp. Hence, to represent the generalized suffix array of GRCh38 we use pairs of 1 + 4 bytes. Our suffix array of GRCh38 fits in 15 GB of memory and we are able to construct it in about one hour on a modern computer [Weese, 2013].

Top-down traversal

We now concentrate on implementing suffix trie functionalities. Any suffix trie node is univocally identified by an interval of the suffix array A . Thus, while traversing the trie, we maintain the interval $[l, r]$ associated to the pointed node. In addition, we also remember the depth d of the pointed node. Recall from section 2.5.2 that any leaf node is defined by an interval containing only terminator symbols. The edge label entering any internal node at depth d is defined by the d -th symbol in any suffix $\mathbb{S}_{A[i]}$ with $i \in [l, r]$. The occurrences below any node correspond by definition to the interval $[l, r]$ of A . Summing up, we represent the pointed node x by the integers $\{l, r, d\}$ and define the following operations on it:

- $\text{ISLEAF}(x)$ returns true iff $A[x.r] + x.d = n_{A[x.r]}$;
- $\text{LABEL}(x)$ returns $\mathbb{S}_{A[x.l] + x.d}$;
- $\text{OCCURRENCES}(x)$ returns $A[x.l \dots x.r]$.

Binary search is the key to implement function goDown a symbol. Functions L (algorithm 3.1) and R (algorithm 3.2) compute in $\mathcal{O}(\log n)$ binary search steps the position in A of the left and right interval corresponding to the child node following the edge labeled by a given symbol c . Note that line 6 of algorithms 3.1–3.2 may involve a comparison

Algorithm 3.1 $L(x, c)$

Input x : pointer to a suffix array node
 c : character to query

Output integer denoting the left interval

```

1:  $l_1 \leftarrow x.l$ 
2:  $l_2 \leftarrow x.r$ 
3: while  $l_1 < l_2$  do
4:    $i \leftarrow \lfloor \frac{l_1 + l_2}{2} \rfloor$ 
5:   if  $\mathbb{S}_{A[i]+x.d} <_{lex} c$  then
6:      $l_1 \leftarrow i + 1$ 
7:   else
8:      $l_2 \leftarrow i$ 
9: return  $l_1$ 

```

Algorithm 3.2 $R(x, c)$

Input x : pointer to a suffix array node
 c : character to query

Output integer denoting the right interval

```

1:  $r_1 \leftarrow x.l$ 
2:  $r_2 \leftarrow x.r$ 
3: while  $r_1 < r_2$  do
4:    $i \leftarrow \lfloor \frac{r_1 + r_2}{2} \rfloor$ 
5:   if  $\mathbb{S}_{A[i]+x.d} \leq_{lex} c$  then
6:      $r_1 \leftarrow i + 1$ 
7:   else
8:      $r_2 \leftarrow i$ 
9: return  $r_1$ 

```

Algorithm 3.3 $\text{goRoot}(x)$

Input x : pointer to a suffix array node

```

1:  $x \leftarrow \{1, n, 0\}$ 

```

Algorithm 3.4 $\text{goDown}(x, c)$

Input x : pointer to a suffix array node
 c : character to query

Output boolean indicating success

```

1: if  $\text{ISLEAF}(x)$  then
2:   return false
3:  $x.d \leftarrow x.d + 1$ 
4:  $x.l \leftarrow L(x, c)$ 
5:  $x.r \leftarrow R(x, c)$ 
6: return  $x.l < x.r$ 

```

beyond the end of strings in \mathbb{S} , however we defined t_i as the empty word ϵ if $i > |t|$ and $\epsilon <_{lex} c$ for all $c \in \Sigma$.

We now implement goDown (algorithm 3.5) and goRight (algorithm 3.6) to have time complexity independent of the alphabet size σ . Indeed, the time complexity of goDown and goRight is $\mathcal{O}(\log n)$, as they rely on a single call of R . In this way, the time complexity of exact string matching algorithm 3.15 is $\mathcal{O}(m \log n)$.

Note that we can iterate down the trie spelling a full pattern within a single call of L and R : in line 6 of algorithms 3.1–3.2, instead of comparing a single character, it suffices to compare the full pattern to the current suffix. However, the worst case runtime of algorithm 3.15 remains $\mathcal{O}(m \log n)$, as each step of the binary search now requires a full lexicographical comparison between the pattern and any suffix of the text, which is performed in $\mathcal{O}(m)$ time in the worst case. As shown in [Manber and Myers, 1990], we can decrease the worst case runtime to $\mathcal{O}(m + \log n)$ at the expense of additional $n \log n$ bits, by storing the precomputed longest common prefixes (LCP) between any two consecutive suffixes $\mathbb{S}_{A[i] \dots}, \mathbb{S}_{A[i+1] \dots}$ for all $1 \leq i < n$. Alternatively, we can reduce the *average case*

Algorithm 3.5 $\text{goDOWN}(x)$

Input x : pointer to a suffix array node
Output boolean indicating success
1: **if** $\text{ISLEAF}(x)$ **then**
2: **return false**
3: $x.d \leftarrow x.d + 1$
4: $x.l \leftarrow R(x, \epsilon)$
5: $c_l \leftarrow S_{A[x.l]+x.d}$
6: $c_r \leftarrow S_{A[x.r]+x.d}$
7: **if** $c_l \neq c_r$ **then**
8: $x.r \leftarrow R(x, c_l)$
9: **return** $x.l < x.r$

Algorithm 3.6 $\text{goRIGHT}(x)$

Input x : pointer to a suffix array node
Output boolean indicating success
1: **if** $\text{ISROOT}(x)$ **then**
2: **return false**
3: $c_l \leftarrow S_{A[x.l]+x.d}$
4: $c_r \leftarrow S_{A[x.r]+x.d}$
5: **if** $c_l \neq c_r$ **then**
6: $x.l \leftarrow x.r$
7: $x.r \leftarrow R(x, c_l)$
8: **return** $x.l < x.r$

runtime to $\mathcal{O}(m + \log n)$ without storing any additional information, by using the MLR heuristic [Manber and Myers, 1990]. In practice, the MLR heuristic outperforms the SA + LCP algorithm, due to the higher cost of fetching additional data from the LCP table.

3.1.2 q -Gram index

If we restrict the traversal of our idealized suffix trie to a fixed depth q , we can remove the logarithmic factor introduced by the suffix array. The idea is to supplement the suffix array A with a so-called q -gram directory: an additional array D of length $\Sigma^q + 1$, storing the suffix array ranges computed by algorithm ?? for any possible word of length q .

With the aim of addressing q -grams in the directory D , we impose a canonical code on q -grams through a bijective function $h : \Sigma^q \rightarrow [1 \dots \sigma^q]$ defined as in [Knuth, 1973]:

$$h(p) = 1 + \sum_{i=1}^q \rho_0(p_i) \cdot \sigma^{q-i} \quad (3.1)$$

where $p \in \Sigma^q$ is any q -gram and ρ_0 is the zero-based lexicographic rank defined on Σ (recall the lexicographic rank function ρ from definition 2.4 and pose $\rho_0(x) = \rho(x) - 1$). This allows us to store in and retrieve from $D[h(p)]$, for each q -gram $p \in \Sigma^q$, the left suffix array interval returned by algorithm 3.1, i.e. $D[h(p)] = L(1, n, p)$. Note that the right interval returned by algorithm 3.2 is equivalent to the left interval of the lexicographical successor q -gram and therefore available in $D[h(p) + 1]$.

The downside of the q -gram index is that in practice it is only applicable to small alphabet and pattern sizes. For instance, parameters $|\Sigma| = 4$ and $q = 14$ require a q -gram directory consisting of 268 M entries that, using a 32 bits encoding, consume 1 GB of memory.

Figure 3.3: q -Gram index for the string ANANAS over the alphabet $\Sigma = \{A, N, S\}$.

p	h	$D[h]$	i	$A[i]$	$S_{A[i]...n}$
AA	1	2	1	7	\$
AN	2	2	2	1	ANANAS\$
AS	3	4	3	3	ANAS\$
NA	4	5	4	5	AS\$
NN	5	6	5	2	NANAS\$
NS	6	6	6	4	NAS\$
SA	7	6	7	6	S\$
SN	8	6			
SS	9	6			
	10	6			

Algorithm 3.7 $L(x, c)$

Input x : pointer to a q -gram node
 c : character to query
Output integer denoting the left interval
1: $x.l_h \leftarrow x.l_h + \rho_0(c) \cdot \sigma^{x.d}$
2: **return** $D[x.l_h]$

Algorithm 3.8 $R(x, c)$

Input x : pointer to a q -gram node
 c : character to query
Output integer denoting the right interval
1: $x.r_h \leftarrow x.r_h - \rho_0(c) \cdot \sigma^{x.d}$
2: **return** $D[x.r_h]$

Top-down traversal

We now extend suffix array traversal operations to use the q -gram directory D . Again, we maintain the current range $[l, r]$ and the current depth d . In addition, while traversing the trie, we maintain the interval $[l_h, r_h]$ in D and, in order to answer $\text{LABEL}(x)$, the label e of the edge entering the current node. Summing up, we represent the pointed node x by the elements $\{l, r, d, l_h, r_h, e\}$. We define the basic node operations as follows:

- $\text{ISLEAF}(x)$ returns true iff $x.d = q$;
- $\text{LABEL}(x)$ returns $x.e$;
- $\text{OCCURRENCES}(x)$ returns $A[x.l \dots x.r]$.

We define functions L and R to use the directory D instead of A and obtain goDown in $\mathcal{O}(1)$. Note how the canonical code assigned by h preserves the lexicographical ordering for all words not longer than q , i.e. $v <_{\text{lex}} w$ iff $h(v) < h(w)$ for all $v, w \in \Sigma^{\leq q}$.

Exact string matching algorithm 3.15 runs in time $\mathcal{O}(q)$, nonetheless we can improve it to perform $\mathcal{O}(1)$ lookups in D . It suffices to compute the canonical code of the pattern in one step, as shown in algorithm 3.11.

Algorithm 3.9 $\text{GO_ROOT}(x)$

Input x : pointer to a q -gram node
 1: $x \leftarrow \{1, n, 0, 1, \sigma^q, \epsilon\}$

Algorithm 3.10 $\text{GO_DOWN}(x, c)$

Input x : pointer to a q -gram node
 c : character to query
Output boolean indicating success
 1: **if** $\text{ISLEAF}(x)$ **then**
 2: **return false**
 3: $x.d \leftarrow x.d + 1$
 4: $x.e \leftarrow c$
 5: $x.l \leftarrow L(x, x.e)$
 6: $x.r \leftarrow R(x, x.e)$
 7: **return** $x.l < x.r$

Algorithm 3.11 $\text{EXACT_SEARCH}(t, p)$

Input t : pointer to the root node of the q -gram index of the text
 p : string to query
Output list of all occurrences of the pattern in the text
 1: $l \leftarrow D[h(p)]$
 2: $r \leftarrow D[h(p) + 1]$
 3: **report** $A[l \dots r]$

If the patterns are shorter or equal to the fixed length q , we access the suffix array only to locate the occurrences, as the directory D alone is sufficient to count the occurrences. In this case, the total ordering of the text suffixes in the suffix array can be relaxed to prefixes of length q . This gives us a twofold advantage, as we can: (i) construct the suffix array more efficiently using bucket sorting and (ii) maintain leaves in each bucket sorted by their relative text positions. The latter property allows to compress the suffix array bucket-wise e.g. using Elias δ encoding [Elias, 1975] or to devise cache-oblivious strategies to process the occurrences [Hach *et al.*, 2010].

If the patterns are longer than q , the q -gram index is still usable. We can devise a hybrid algorithm that uses the directory D to conduct the search up to depth q and later continue with binary searches on the suffix array. This hybrid index cuts the most expensive binary searches and increases memory locality. Furthermore, this hybrid index becomes useful whenever the suffix array is too big to fit in main memory and has to reside in external memory.

3.2 Succinct full-text indices

The Burrows-Wheeler transform (BWT) [Burrows and Wheeler, 1994] is a transformation defining a permutation of an input string. The transformed string exposes two important properties: reversibility and compressibility. The former property allows us to

reconstruct the original string from its BWT, the latter property makes the transformed string more amenable to compression. Thanks to these two properties, the BWT has been recognized as a fundamental method for text compression and practically used in the bzip2 [Seward, 1996] tool.

More recently, Ferragina and Manzini proposed the BWT as a tool for full-text indexing. They showed in [Ferragina and Manzini, 2000] that the BWT alone allows to perform exact pattern matching and engineered in [Ferragina and Manzini, 2001] a compressed full-text index called FM-index. Over the last years, the FM-index has been widely employed under different re-implementations by many popular Bioinformatics tools e.g. Bowtie [Langmead *et al.*, 2009] and BWA [Li and Durbin, 2009], and is now considered a fundamental method for the indexing of genomic sequences.

In the next subsections we give the fundamental ideas behind the BWT and the FM-index. Subsequently, we discuss our succinct FM-index implementations covering strings and string collections.

3.2.1 Burrows-Wheeler transform

Let s be a padded string (definition 2.8) of length n over an alphabet Σ . In the following we consider the string s to be cyclic and its subscript s_i to be *modular*, e.g. $s_0 = s_n$ and $s_{n+i} = s_i$ for any $i \in \mathbb{N}$. Consider the square matrix consisting of all cyclic shifts of the string s (the i -th cyclic shift has the form $s_{i...n}s_{1...i-1}$) sorted in lexicographical order (see figure 3.4). For convenience, we denote by f the first column $s_{A[i]}$, and by l the last column $s_{A[i]-1}$. Note how the cyclic shifts matrix is related to the suffix array A of s : the i -th cyclic shift is $s_{A[i]...n}s_{1...A[i]-1}$.

Definition 3.3. The BWT of s is the string obtained concatenating the symbols in the last column of the cyclic shifts matrix of s , i.e. it is the string $l = s_{A[i]-1}$.

Figure 3.4: Burrows-Wheeler transform for the string ANANAS\$.

i	$A[i]$	$s_{A[i]}$		$s_{A[i]-1}$
1	7	\$	ANANA	S
2	1	A	NANAS	\$
3	3	A	NAS\$A	N
4	5	A	S\$ANA	N
5	2	N	ANAS\$	A
6	4	N	AS\$AN	A
7	6	S	\$ANAN	A

We easily generalize the BWT to string collections. Indeed, definition 3.3 still holds if we consider a padded string collection \mathbb{S} (definition 2.9) and its cyclic shifts matrix sorted in lexicographical order.

The cyclic shifts matrix is conceptual and we do not have to construct it explicitly to derive the BWT of a text. We can obtain the BWT in linear time by scanning the suffix array A and assigning to the i -th BWT symbol the text character $s_{A[i]-1}$. Various direct BWT construction algorithms working within $o(n)$ bits plus constant space have been recently proposed [Bauer *et al.*, 2013; Crochemore *et al.*, 2013], as constructing the suffix array is not desirable due to its space consumption of $n \log n$ bits.

Inversion

We now describe how to invert the BWT to reconstruct the original text. Inverting the BWT means being able to know where any BWT character occurs in the original text. To this extent, we introduce two permutations $LF : [1, n] \rightarrow [1, n]$ and $\Psi : [1, n] \rightarrow [1, n]$, with $LF = \Psi^{-1}$, where the value of $LF(i)$ gives the position j in f where character l_i occurs and the value $\Psi(j)$ gives back the position i in l where f_j occurs. Figure 3.5 illustrates.

Figure 3.5: Functions LF and Ψ for the string ANANAS\$. Note how $LF(\Psi(i)) = \Psi(LF(i)) = i$ for any i . Also note how the i -th occurrence of any character c in l is the i -th occurrence of c in f .

i	$\Psi(i)$	$LF(i)$	$s_{A[i]}$	$s_{A[i]-1}$
1	2	7	\$	ANANA
2	5	1	A	NANAS
3	6	(5)	A	NAS\$A
4	7	6	A	S\$ANA
5	(3)	2	(N)	ANAS\$
6	4	3	N	AS\$AN
7	1	4	S	\$ANAN

We recover s_i as $f_{\Psi^{i-1}(j)}$, where the iterated Ψ is defined as

$$\begin{aligned}\Psi^0(j) &= j \\ \Psi^{i+1}(j) &= \Psi(\Psi^i(j))\end{aligned}\tag{3.2}$$

Conversely, we recover \bar{s}_i as $s_{LF^{i-1}(j)}$, where the iterated LF is defined as

$$\begin{aligned}LF^0(j) &= j \\ LF^{i+1}(j) &= LF(LF^i(j))\end{aligned}\tag{3.3}$$

We recover the string s by starting in f at the position of \$ and following the cycle defined by the permutation Ψ . Or we recover the reverse string \bar{s} by starting in l at the position of \$ and following the cycle defined by the permutation LF .

Inverting the generalized BWT works in the same way. Indeed, permutations Ψ and LF are composed of c cycles, where each cycle corresponds to a distinct string in the

Figure 3.6: Recovering the string ANANAS\$ from the permutation Ψ . Here we depict only the first two steps of the inversion recovering AN.

$s_{A[i]}$	i	$\Psi(i)$
\$	1	2
(A)	2	5
A	3	6
A	4	7
(N)	5	3
N	6	4
S	7	1

collection. We recover s^i by starting at the position of $\i and following the cycle of Ψ (or LF) associated to s^i .

Permutation LF

The permutation LF is conceptual: we do not have to represent it explicitly but we can deduce it from the BWT l with the help of some additional character counts. This is possible due to two simple observations on the cyclic shifts matrix [Burrows and Wheeler, 1994; Ferragina and Manzini, 2000]:

- for all $i \in [1, n]$, the character l_i precedes the character f_i in the original string s ;
- for all characters $c \in \Sigma$ the i -th occurrence of c in f corresponds to the i -th occurrence of c in l .

These observation are obvious since $f = s_{A[i]}$ and $l = s_{A[i]-1}$ (see figure 3.4). Given the above observations, we define the permutation LF as [Burrows and Wheeler, 1994; Ferragina and Manzini, 2000]:

$$LF(i) = C(l_i) + Occ(l_i, i) \quad (3.4)$$

where we denote with $C : \Sigma \rightarrow [1, n]$ the total number of occurrences in s of all characters alphabetically smaller than c , and with $Occ : \Sigma \times [1, n] \rightarrow [1, n]$ the number of occurrences of character c in the prefix $l_{1..i}$.

The key problem of representing the permutation LF is how to represent function Occ , as function C can be easily tabulated by a small array of size $\sigma \log n$ bits. In the next subsection we address the problem of representing function Occ efficiently. Subsequently, in subsection 3.2.3 we see how to build a full-text index out of function LF .

3.2.2 Rank dictionaries

We want to answer efficiently the question “how many times a given character c occurs in the prefix $l_{1..i}$?”, ideally in constant time and linear space. The general problem on

arbitrary strings has been tackled by several studies on the succinct representation of data structures [Jacobson, 1989]. Our specific question takes the name of *rank query* and a data structure answering rank queries is called *rank dictionary*.

Definition 3.4. Given a string s over an alphabet Σ and a character $c \in \Sigma$, $\text{rank}_c(s, i)$ returns the number of occurrences of c in the prefix $s_{1..i}$.

The key idea of rank dictionaries is to maintain a succinct (or even compressed) representation of the input string and attach a dictionary to it. By doing so, Jacobson showed how it is possible to answer rank queries in constant time (on the RAM model) using $n + o(n)$ bits for an input binary string of n bits [Jacobson, 1989]. First we consider the binary case $\Sigma_B = \{0, 1\}$ and later we extend it to arbitrary alphabets. In addition, we discuss implementation details that are crucial to obtain practical efficiency.

Binary alphabet

We start by describing a simple rank dictionary answering rank queries in constant time but consuming $2n$ bits and later we extend it to consume only $n + o(n)$ bits. Given the binary string $s \in \Sigma_B$, we partition it in blocks of size b . In the following we assume w.l.o.g. the string length n to be a multiple of b , conversely values in all subsequent formulas must be rounded accordingly.

We attach to the binary string s an array R of length $\frac{n}{b}$, where the i -th entry gives a summary of the number of occurrences of the bit 1 in $s_{1..ib}$, i.e. $R[\frac{i}{b}] = \text{rank}_1(s, \frac{i}{b})$. Note that $\text{rank}_0(s, i) = i - \text{rank}_1(s, i)$ so we consider only $\text{rank}_1(s, i)$. Therefore we are able to rewrite our rank query as:

$$\text{rank}_1(s, i) = R[\frac{i}{b}] + \text{rank}_1(s_{\frac{i}{b} \dots \frac{i}{b} + b}, i \bmod b) \quad (3.5)$$

and answer it in time $\mathcal{O}(b)$ as (i) we fetch in constant time the rank summary from R and (ii) we compute the number of occurrences of the bit 1 within a block of length b . If we pose $b = \log n$, we can compute step ii in $\mathcal{O}(1)$ by means of the four-Russians tabulation technique [?]. Moreover, the array R stores $\frac{n}{\log n}$ positions and each position in s requires $\log n$ bits, so R consumes n bits. Thus, this rank dictionary consumes $2n$ bits.

To squeeze our rank dictionary to consume only $n + o(n)$ bits of space, we add another array R^2 summarizing the ranks on b^2 bits boundaries and let our initial array R store only local positions within the corresponding blocks defined by R^2 . We rewrite $\text{rank}_1(s, i)$ accordingly:

$$\text{rank}_1(s, i) = R^2[\frac{i}{b^2}] + R[\frac{i}{b}] + \text{rank}_1(s_{\frac{i}{b} \dots \frac{i}{b} + b}, i \bmod b) \quad (3.6)$$

Each entry of R now has to represent only b^2 possible values and thus consumes only $2 \log b$ bits. Summing up, this two-levels rank dictionary consumes n bits for the input string, $\mathcal{O}(\frac{n \log n}{b^2})$ bits for R^2 and $\mathcal{O}(\frac{n \log b}{b})$ bits for R . By posing $b = \log n$ we have $\mathcal{O}(\frac{n}{\log n})$ bits for R^2 and $\mathcal{O}(\frac{n \log \log n}{\log n})$ bits for R . Hence, the two-levels rank dictionary consumes $n + o(n)$ bits.

Figure 3.7: Example of rank dictionaries for the string $s = 010101100100$. On the one-level rank dictionary, $b = 4$ and $\text{rank}_1(s, 6) = R[2] + \text{rank}_1(s_{5\dots 8}, 2) = 3$. On the two-levels rank dictionary, $b = 2$ and $\text{rank}_1(s, 6) = R^2[2] + R[3] + \text{rank}_1(s_{6\dots 6}, 1) = 3$.

i	s_i	$R[\frac{i}{b}]$	i	s_i	$R[\frac{i}{b}]$	$R^2[\frac{i}{b^2}]$
1	0	0	1	0	0	0
2	1		2	1		
3	0		3	0	1	
4	1		4	1		
5	0	(2)	5	0	0	(2)
6	1		6	1		
7	1		7	1	1	
8	0		8	0		
9	0	4	9	0	0	4
10	1		10	1		
11	0		11	0	1	
12	0		12	0		

We implemented generic multi-levels rank dictionaries where the block size b is a template parameter adjustable at compile time. Whenever the input string has length inferior to 4 GB, we employ one-level rank dictionaries with $b = 32$ bits or two-levels rank dictionaries with $b = 16$ bits and $b^2 = 32$ bits; otherwise, we employ two-levels rank dictionaries with $b = 32$ bits and $b^2 = 64$ bits, or three-levels rank dictionaries with $b = 16$ bits, $b^2 = 32$ bits and $b^3 = 64$ bits. In order to reduce the number of cache misses, we interleaved the succinct representation of the input string with the lowest level summaries array R . Moreover, we compute step ii in $\mathcal{O}(1)$ using the SSE 4.2 popcnt instruction [Intel, 2011].

Small alphabets

The extension to small alphabets e.g. Σ_{DNA} is easy. Here we show how to extend the one-level rank dictionary. Given an input string s over Σ_{DNA} of size n bits (and thus of length $\frac{n}{\log \sigma}$ symbols), we partition it in blocks of b symbols (which do not correspond to b bits as in the Σ_B case). We supplement each block of s with an occurrences summary for all symbols in Σ , thus we use a matrix R_σ of size $\frac{n}{b} \times \sigma$ entries. We rewrite $\text{rank}_c(s, i)$ as:

$$\text{rank}_c(s, i) = R_\sigma[\frac{i}{b}][\rho(c)] + \text{rank}_c(s_{\frac{i}{b} \dots \frac{i}{b} + b}, i \bmod b) \quad (3.7)$$

where i now is the i -th symbol in s , not the i -th bit as in the Σ_B case.

In order to answer rank queries in constant time, we have to count the number of occurrences of the character c inside a block of length b . We pose $b = \frac{\log n}{\log \sigma}$ symbols, thus

$b = \log n$ bits as in the Σ_B case. The matrix R_σ has $\frac{n}{\log n}$ entries, each one consuming $\sigma \log n$ bits. Thus R_σ consumes $n\sigma$ bits, and the whole rank dictionary $n + n\sigma$ bits.

Figure 3.8: Example of rank dictionaries for the string $s = \text{CCCGCA}$ under the binary encoding $\{A, C, G, T\} = \{00, 01, 10, 11\}$ of the alphabet Σ_{DNA} .

i	$s_{\frac{i}{2}}$	s_i	$R_\sigma[\frac{i}{b}]$	σ
1	C	0	0	A
2		1	0	C
3	C	0	0	G
4		1	0	T
5	C	0	0	A
6		1	2	C
7	G	1	0	G
8		0	0	T
9	C	0	0	A
10		1	3	C
11	A	0	1	G
12		0	0	T

3.2.3 FM-index

We now turn to the problem of implementing a full-text index relying on the permutation LF . This is possible because of the relationship between the cyclic shifts matrix and the suffix array A . First we see how to emulate a top-down traversal of the suffix trie, which is sufficient to count the number of occurrences of any substring in the original text. Later we focus on how to represent the leaves, which are necessary to locate occurrences in the original text.

We represent the pointed node x by the elements $\{l, r, e\}$, where $[l, r]$ represents the current suffix array interval and e is the label of the edge entering the current node.

- $\text{ISLEAF}(x)$ returns true iff $x.l_r = \$$;
- $\text{LABEL}(x)$ returns $x.e$.

Given a padded string collection \mathbb{S} , its BWT plus its associated permutation LF let us recover any substring of $\bar{\mathbb{S}}$. Nonetheless, we want to recover substrings of \mathbb{S} in forward direction, as the suffix trie \mathcal{S} spells all forward substrings of \mathbb{S} . Therefore, given a string \mathbb{S} we consider the BWT of $\bar{\mathbb{S}}$, such that LF let us recover any substring of \mathbb{S} . Now we can use the permutation LF to decode the intervals computed during a suffix trie traversal.

From the root node, we easily obtain the interval of its child node labeled by c as $[C(c), C(c + 1)]$. Now suppose an arbitrary node v of known interval $[b_v, e_v]$ s.t. the path

Algorithm 3.12 GOROOT(x)

Input x : pointer to a FM-index node
 1: $x \leftarrow \{1, n, \epsilon\}$

Algorithm 3.13 GOWDOWN(x, c)

Input x : pointer to a FM-index node
 c : char to query
Output boolean indicating success
 1: **if** ISLEAF(x) **then**
 2: **return false**
 3: $x.l \leftarrow LF(x.l, c)$
 4: $x.r \leftarrow LF(x.r, c)$
 5: $x.e \leftarrow c$
 6: **return** $x.l < x.r$

from the root to v spells the substring s_v ; we want to reach the node w of unknown interval $[b_w, e_w]$ s.t. the path from the root to w spells $c \cdot s_v$ for some $c \in \Sigma$. Thus, we know all prefixes of \mathbb{S} ending with s_v (hence all suffixes of \mathbb{S} starting with s_v) and we are looking for all the prefixes of \mathbb{S} ending with $c \cdot s_v$ (hence all suffixes of \mathbb{S} starting with $s_v \cdot c$). All these characters c are in $l_{b_v \dots e_v}$, since l_i is the character $\mathbb{S}_{A[i]-1}$ preceding the suffix pointed by $A[i]$. Moreover, we know that these characters c are (i) contiguous and (ii) in relative order in f [Ferragina and Manzini, 2000]. If b and e are the first and last position in l within $[b_v, e_v]$ such that $l_b = c$ and $l_e = c$, then $b_w = LF(b)$ and $e_w = LF(e)$. We can rewrite $LF(b)$ as:

$$\begin{aligned}
 LF(b) &= C(l_b) + Occ(l_b, b) \\
 &= C(c) + Occ(c, b) \\
 &= C(c) + Occ(c, b_v - 1) + 1
 \end{aligned} \tag{3.8}$$

Analogously, we can rewrite $LF(e)$ as $C(c) + Occ(c, e_v)$. Therefore, GOWDOWN a symbol computes two values of permutation LF and runs in time $\mathcal{O}(1)$. Conversely, GOWDOWN and GORIGHT run in time $\mathcal{O}(\sigma)$ (see algorithms ??).

In order to locate occurrences we need the suffix array A , yet we do not want to maintain the whole array A . As proposed by Ferragina and Manzini, we maintain a *sampled* suffix array A^ϵ containing positions sampled at regular intervals in the input string. In order to determine if and where we sampled any $A[i]$ in A^ϵ , we maintain a binary rank dictionary S of length n : if $S[i] = 1$, then we sampled $A[i]$ in $A^\epsilon[rank_1(S, i)]$. We obtain any $A[i]$ by finding the smallest $j \geq 0$ such that $LF^j(i)$ is in A^ϵ , and then $A[i] = A[LF^j(i)] + j$.

If we sample one text position out of $\log^{1+\epsilon} n$, for some $\epsilon > 0$, then A^ϵ consumes $\mathcal{O}(\frac{n}{\log^\epsilon n})$ space and OCCURRENCES(x) returns all occurrences in $\mathcal{O}(o \cdot \log^{1+\epsilon} n)$ time [Ferragina and Manzini, 2000]. In practice, we usually sample text positions at rates between 2^{-3} and 2^{-5} . The rank dictionary S consumes always $n + o(n)$ extra space.

3.3 Algorithms

3.3.1 Bounded top-down traversal

Algorithm 3.14 DFS(x, d)

Input x : pointer to the root node of the suffix trie

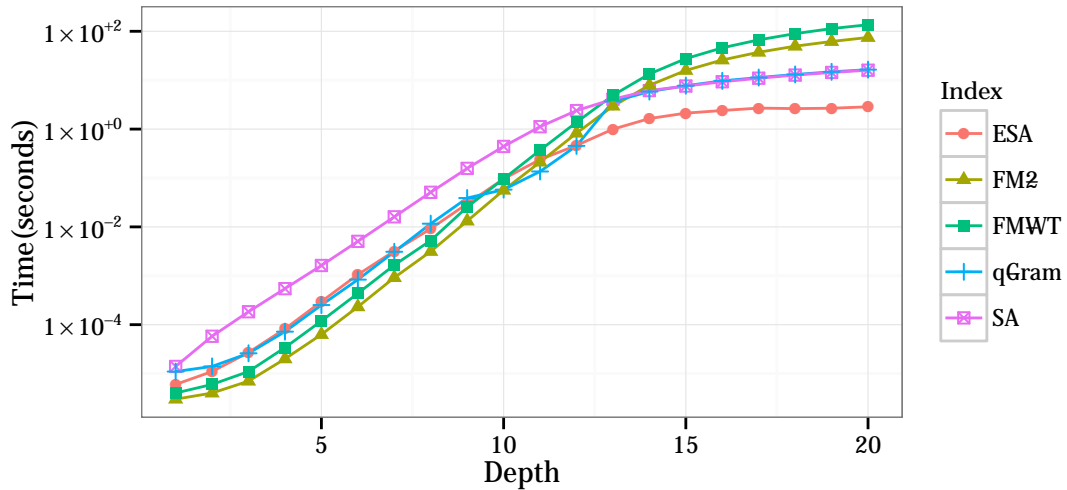
d : integer bounding the traversal depth

```

1: if  $d > 0$  then
2:   if GODOWN( $x$ ) then
3:     repeat
4:       DFS( $x, d - 1$ )
5:     until GORIGHT( $x$ )

```

Figure 3.9: Runtime of bounded top-down traversal of various suffix trie implementations.



3.3.2 Exact pattern matching

Using the above generic top-down traversal operations we are able to formulate generic string matching algorithms. Here we formulate the simple algorithm for exact string matching on a suffix trie. In chapter 3, we give analogous algorithms solving k -mismatches and k -differences by means of a backtracking top-down traversal [Ukkonen, 1993; Baeza-Yates and Gonnet, 1999].

We assume the text t to be indexed by its suffix trie \mathcal{T} . Algorithm 3.15 searches a pattern p by starting in the root node of \mathcal{T} and following the path spelling the pattern. If the search ends up in a node x , each leaf l_i below x points to a distinct suffix $t_{i..n}$ such that

$t_{i..i+m}$ equals p . If we implement `goDown` in constant time and `OCCURRENCES` in linear time, we find all occurrences of p into t in optimal time $\mathcal{O}(m + o)$, where m is the length of p and o its number of occurrences in t .

Algorithm 3.15 EXACTSEARCH(t, p)

Input t : pointer to a suffix trie node
 p : pointer to a pattern

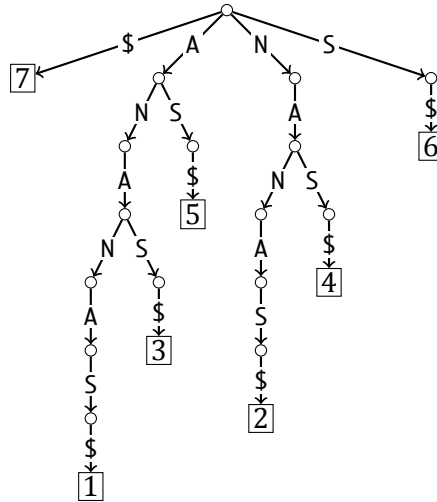
Output list of all occurrences of the pattern in the text

```

1: if ATEND( $p$ ) then
2:     report OCCURRENCES( $t$ )
3: else if goDOWN( $t$ , VALUE( $p$ )) then
4:     goNEXT( $p$ )
5:     EXACTSEARCH( $t, p$ )

```

Figure 3.10: Exact string matching on a suffix tree. The pattern *NA* is searched exactly in the text *ANANAS\$*.



We now benchmark algorithm 3.15.

3.3.3 Backtracking k -mismatches

We can solve k -mismatches by backtracking [Ukkonen, 1993; Baeza-Yates and Gonnet, 1999] on the suffix trie \mathcal{T} , in average time sublinear in n [Navarro and Baeza-Yates, 2000]. A top-down traversal on \mathcal{T} spells incrementally all distinct substrings of t . While traversing each branch of the trie, we incrementally compute the distance between the query and the spelled string. If the computed distance exceeds k , we stop the traversal and proceed on the next branch. Conversely, if we completely spelled the pattern p and we ended

up in a node x , each leaf $l_i \in \mathbb{L}(x)$ points to a distinct suffix $t_{i..n}$ such that $d_H(t_{i..i+m}, p) \leq k$. See algorithm 3.16.

Algorithm 3.16 KMISMATCHES(t, p, e)

Input t : pointer to the root node of the suffix trie of the text
 p : pointer to the root node of the trie of the patterns
 e : integer bounding the number of mismatches

Output list of all occurrences of the pattern in the text

```

1: if  $e = k$  then
2:   EXACTSEARCH( $t, p$ )
3: else if  $e < k$  then
4:   if ATEND( $p$ ) then
5:     report OCCURRENCES( $t$ )
6:   else if GODOWN( $t$ ) then
7:     repeat
8:        $d \leftarrow \omega(\text{LABEL}(t), \text{VALUE}(p))$ 
9:       GONEXT( $p$ )
10:      KMISMATCHES( $t, p, e + d$ )
11:      GOPREVIOUS( $p$ )
12:    until GORIGHT( $t$ )
  
```

3.3.4 Backtracking k -differences

Algorithm for k -differences.

Algorithm 3.17 KDIFFERENCES(t, p, D)

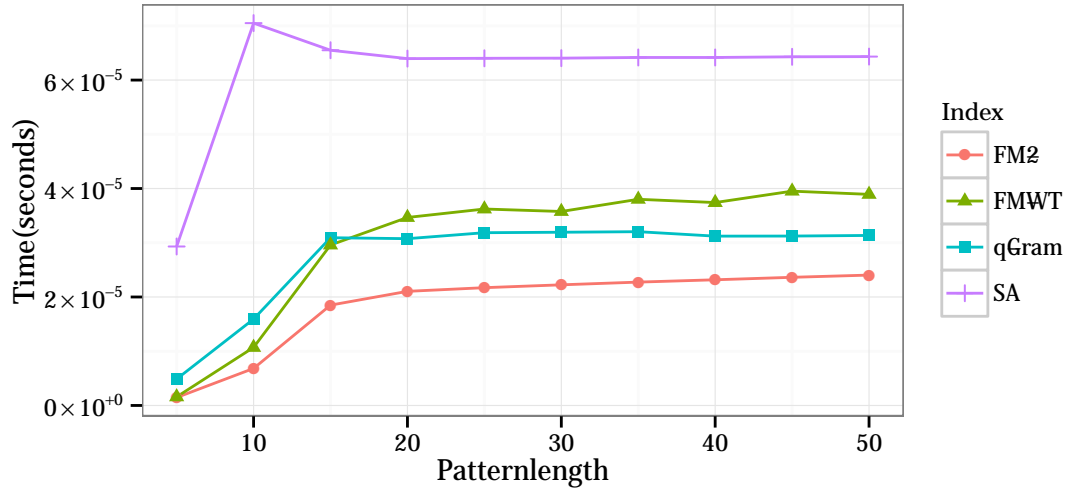
Input t : pointer to the root node of the suffix trie of the text
 p : pointer to the root node of the trie of the patterns
 D : vector of integers

Output list of all occurrences of the pattern in the text

```

1: if  $D[m] \leq k$  then
2:   report OCCURRENCES( $t$ )
3: else if  $\min D \leq k$  then
4:   if GODOWN( $t$ ) then
5:     repeat
6:        $D' \leftarrow \text{DP}(D, \text{LABEL}(t), p)$ 
7:       KDIFFERENCES( $t, p, D'$ )
8:     until GORIGHT( $t$ )
  
```

Figure 3.13: Runtime of k -mismatches on various suffix trie implementations.



3.3.5 Multiple backtracking

We start by giving the simple exact string matching algorithm using suffix trie iterators.

Algorithm 3.18 MULTIPLEEXACTSEARCH(t, p)

Input t : pointer to the root node of the suffix trie of the text
 p : pointer to the root node of the trie of the patterns

Output list of all occurrences of any pattern in the text

- 1: **if** ISLEAF(p) **then**
- 2: **report** OCCURRENCES(t) \times OCCURRENCES(p)
- 3: **else**
- 4: GODOWN(p)
- 5: **repeat**
- 6: **if** GODOWN(t , LABEL(p)) **then**
- 7: MULTIPLEEXACTSEARCH(t, p)
- 8: GOUP(t)
- 9: **until** GORIGHT(p)

Algorithm 3.19 MULTIPLEKMISMATCHES(t, p, e)

Input t : pointer to the root node of the suffix trie of the text
 p : pointer to the root node of the trie of the patterns
 e : integer bounding the number of mismatches

Output list of all occurrences of any pattern in the text

```

1: if  $e = k$  then
2:   MULTIPLEEXACTSEARCH( $t, p$ )
3: else if  $e < k$  then
4:   if ISLEAF( $p$ ) then
5:     report OCCURRENCES( $t$ )  $\times$  OCCURRENCES( $p$ )
6:   else if GODOWN( $t$ ) then
7:     repeat
8:       GODOWN( $p$ )
9:       repeat
10:         $d \leftarrow \omega(\text{LABEL}(t), \text{LABEL}(p))$ 
11:        MULTIPLEKMISMATCHES( $t, p, e + d$ )
12:      until GORIGHT( $p$ )
13:     GOUP( $p$ )
14:   until GORIGHT( $t$ )
  
```

Figure 3.14: Runtime of multiple exact string matching on various suffix trie implementations.

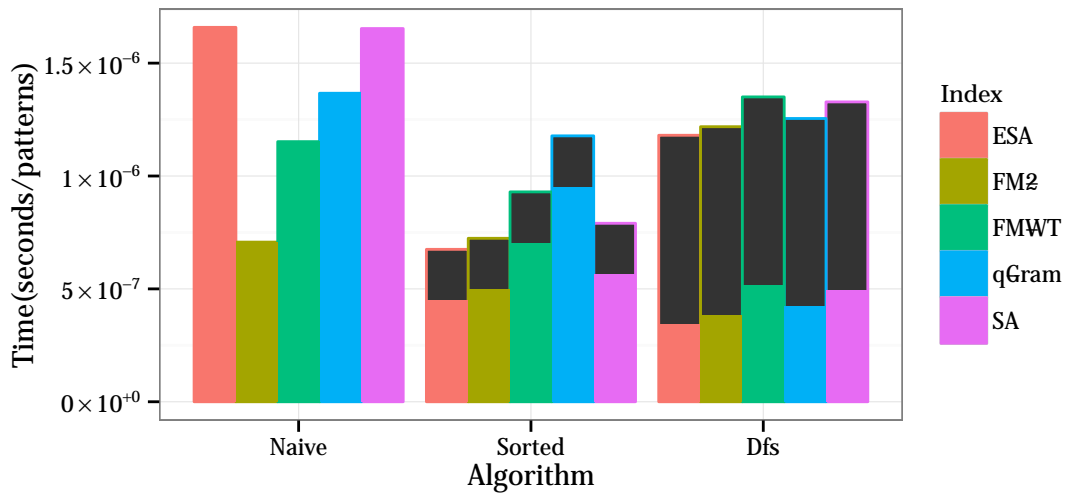
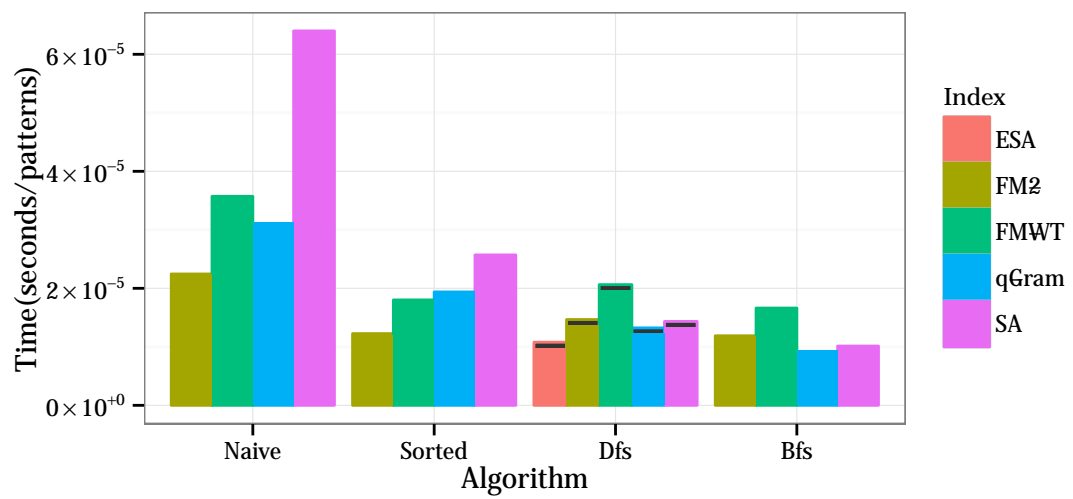


Figure 3.15: Runtime of multiple k -mismatches on various suffix trie implementations.



We now concentrate on designing stronger filters for approximate string matching. Whenever the total time of our filtering algorithm is dominated by verification time, we can think of adopting a stronger filter yielding a lower number of candidate locations to verify. The idea is to improve the total time by means of a significant reduction of verification time, at the expense of a moderate increase in filtration time.

We have already seen in section 2.5.3 an example of such trade-off between filtration speed and strength: non-overlapping seeds versus q -gram filters. The former filters minimize filtration time but yield weak filtration, the latter provide a more involved but stronger filtration. In practice, we know that seeds filters work best at low error rates, while q -gram filters become competitive at higher error rates. Thus we would adopt one or the other filtration method depending on the requested error rate.

The simple analysis of section 2.5.3 show us that filtration specificity is strongly correlated to the parameter q being the seed or q -gram length. Therefore the crux of designing stronger filters lies into increasing the seed or q -gram length while guaranteeing full-sensitivity. To this intent, the following techniques have been proposed in literature: (i) gapped q -grams generalizing contiguous q -grams, (ii) multiple gapped q -grams further generalizing gapped q -grams; (iii) approximate seeds generalizing exact seeds,

The idea of gapped q -grams is to lower the correlation between consecutive q -grams. We have seen in the q -gram lemma 4.3 that one error covers q consecutive q -grams. Thus, the occurrence of a q -gram is strongly correlated to the occurrence of its preceding and following q -grams. Therefore, we introduce *don't care positions* to skip characters at fixed positions inside all q -grams. By doing so, a mismatch does not cover anymore all consecutive q -grams. As less q -grams are now covered by mismatches, we can (i) increase the filtering threshold or (ii) increase the number q of considered characters, in either cases preserving full-sensitivity. Note that however, this concept poorly extends to edit distance, and the design of gapped q -grams is hard.

TODO families.

The idea of approximate seeds is that, to increase seed length, we can factorize the pattern in less than $k + 1$ non-overlapping seeds. The pigeonhole lemma 4.1 however tells us that, by doing so, no seed will be guaranteed to be error-free. Therefore, we are obliged to search the seeds approximately, but within a distance threshold smaller than the original threshold k . We can search approximate seeds with backtracking techniques of section ???. In a nutshell, instead of reducing an approximate search into smaller exact searches, we reduce it into smaller approximate searches.

Problems of exact and approximate seeds filters are that (i) it is not evident which factorization yields optimal filtration, and (ii) they yield duplicate occurrences whenever errors are not distributed in the worst-case combination. Suffix filters are based on tighter pigeonhole lemmas yielding stronger, less redundant, and more adaptive filtration using more efficiently the index. The drawback is that the effort to implement them is slightly higher.

In the following of this chapter we first present (multiple) gapped q -grams and problems associated with their design. Then we move to more practical approximate seeds, which we will adopt later in chapter ?? . Overall, through this chapter:

- we present a framework for the design of (multiple) gapped q -grams consisting of efficient exact and approximate solutions;
- we provide generic parallel implementations of filters based on exact and approximate seeds;
- we evaluate these filtration schemes in practice.

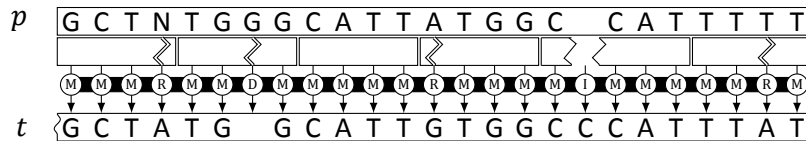
4.1 Exact seeds

We start by considering the case of two arbitrary strings x, y within edit distance k .

Lemma 4.1. [Baeza-Yates and Navarro, 1999] *Let x, y be two strings s.t. $d_E(x, y) = k$. If we partition w.l.o.g. y into $k + 1$ non-overlapping seeds, then at least one seed will occur as a factor of x .*

It is immediate to see that any edit distance error can cover at most one seed, therefore at least one seed of y will not be covered by any seed and occur as a factor of x . Figure 4.1 shows an example.

Figure 4.1: Filtration with exact seeds.



Thus, we solve k -differences by partitioning the pattern into $k + 1$ seeds and searching all seeds into the text, e.g. with the help of a substring index. As Lemma 4.1 gives us a necessary but not sufficient condition, we must verify whether any candidate location induced by an occurrence of some seed corresponds to an approximate occurrence of the pattern in the text. Thus, we verify any substring s of the text of length $|s| \in [m - k, m + k]$ containing one seed of p . Note how we are reducing one approximate search into many smaller exact searches.

How many verifications a seed produces? Let us assume the text to be generated according to the uniform Bernoulli model. The emission probability of any symbol in Σ

is $p = \frac{1}{\sigma}$ and under i.i.d. assumptions the emission (and occurrence) probability of any word of length q is simply

$$\Pr(H > 0) = \frac{1}{\sigma^q} \quad (4.1)$$

thus the expected number of occurrences of a seed of length q in a text of length n is

$$E[H] = \sum_{i=1}^{n-q+1} \Pr(H > 0) = \frac{n-q+1}{\sigma^q} \leq \frac{n}{\sigma^q}. \quad (4.2)$$

Note how lemma 4.1 requires us to partition the pattern into $k+1$ seeds but leaves us free to choose their length. This leads to the question of which is an optimal pattern partitioning, i.e. a partitioning that minimizes the expected number of verifications. We fix¹ the length of all seeds to be

$$q = \left\lfloor \frac{m}{k+1} \right\rfloor \quad (4.3)$$

to minimize the expected number of occurrences of any seed. Under these conditions, the expected number of verifications produced by our seed filter is

$$E[V] = E[H] \cdot (k+1) < \frac{n(k+1)}{\sigma^q} \quad (4.4)$$

We now turn to the effect of the error rate on the runtime of the resulting k -differences algorithm. For which error rate we expect the resulting algorithm to have sublinear runtime? If we use the classic $\mathcal{O}(m^2)$ DP algorithm of section 2.5.1 to verify candidate locations, the expected runtime must be

$$E[V] \cdot m^2 < cn \quad (4.5)$$

for some constant c . By substituting $E[V]$ and solving for q , we obtain

$$q > \log_{\sigma} \frac{m^3}{c} \quad (4.6)$$

and since we chose q as a function of m and k in equation 4.3, it follows that

$$\epsilon = \frac{k}{m} < \frac{m}{\log_{\sigma} m} \quad (4.7)$$

is the error rate for which this k -differences algorithm has expected sublinear runtime.

Nonetheless, texts of practical interest like genomes and natural texts do not fit well the uniform Bernoulli model. On those texts uniform seed length can lead to suboptimal filtration. In section 4.2 we analyze the statistical properties of these texts and the effects of pattern partitioning. Later, in order to obtain more robust filters, we generalize filtration with seeds to consider approximate seeds.

¹ We ignore for simplicity that some seed could have length $\left\lfloor \frac{m}{k+1} \right\rfloor$.

4.2 Approximate seeds

Approximate seeds have been proposed in [Myers, 1994; Navarro and Baeza-Yates, 2000] as a practical and effective generalization of exact seeds, yielding stronger filters both for k -mismatches and k -difference. The key idea of approximate seeds is to reduce an approximate search into *smaller* approximate searches, as opposed to exact seeds reducing an approximate search into smaller exact searches.

Again, we start by considering two arbitrary strings x, y within edit distance k .

Lemma 4.2. [Myers, 1994; Navarro and Baeza-Yates, 2000] *Let x, y be two strings s.t. $d_E(x, y) = k$. If we partition w.l.o.g. y into s non-overlapping seeds s.t. $1 \leq s \leq k + 1$, then at least one seed will occur as a factor of x within distance $\lfloor k/s \rfloor$.*

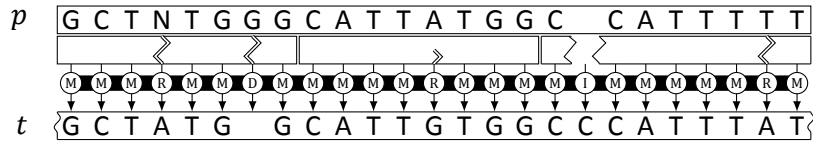
To prove full-sensitivity it suffices to see that, if none of the seeds occurs within its assigned distance, the total distance must be greater than $s \cdot \lfloor k/s \rfloor = k$. Figure 4.2 illustrates.

In order to solve k -mismatches, we partition the pattern p in non-overlapping seeds p^1, p^2, \dots, p^s . According to lemma 4.2, full-sensitivity is guaranteed if we search all seeds p^i within a distance threshold of $\lfloor k/s \rfloor$. Note that we are not obliged to assign the same distance threshold to all seeds. Indeed, we can assign any arbitrary distance threshold k_i to each seed p^i , as long as we satisfy the following inequality

$$s + \sum_{i=1}^s k_i > k. \quad (4.8)$$

We usually tend to distribute evenly distance thresholds because seeds with the highest threshold dominate the overall filtration time. Therefore, we assign to $(k \bmod s) + 1$ seeds distance $\lfloor k/s \rfloor$ and to the remaining seeds distance $\lfloor k/s \rfloor - 1$ [Siragusa *et al.*, 2013]. Also note how we obtain lemma 4.1 for exact seeds by posing $s = k + 1$ and all $k_i = 0$.

Figure 4.2: Filtration with approximate seeds.



4.2.1 Parameterization

With approximate seeds we are free to choose the number of seeds s which gives us $q = \lfloor m/s \rfloor$, or vice versa, if we fix the minimum seed length q then it must hold $s = \lfloor m/q \rfloor$. The resulting filter is flexible, indeed by increasing q filtration becomes more specific at the expense of a higher filtration time. For $s = 1$ we obtain the most specific filtration i.e.

we perform only backtracking and we do not even need to verify the reported locations, while for $s = k + 1$ we obtain the fastest but weakest filtration.

In practice, it is not easy to find which filter parameterization yields an optimal filtration. Both Myers, and Navarro and Baeza-Yates carried out involved analysis to estimate the optimal parameters. Navarro and Baeza-Yates find out that the optimal number of seeds $\Theta(\frac{m}{\log_\sigma n})$ yields an overall time complexity sublinear for an error rate $\epsilon < 1 - \frac{e}{\sqrt{\sigma}}$. Myers reports an analogous sublinear time when $q = \Theta(\log_\sigma n)$ is the seed length. However, these results did not help us in our experiments. The optimal partitioning depends on (i) the full-text index, (ii) the verification algorithm, (iii) the statistical properties of the text. A difference of one from the optimal number of seeds can result in a runtime penalty of an order of magnitude.

4.2.2 Redundancy

Another practical problem of seeds is redundant filtration. Whenever errors are not distributed according to a worst-case combination for lemma 4.1 or 4.2, more than one seed reports the same candidate location. Consider the case of exact seeds: If two errors fall in some seed, then at least two seeds will occur exactly.

In practice, we can choose to avoid redundancy before or after verifying candidate locations. After collecting all candidate locations for a pattern, we have to consider only the induced diagonal positions in the implicit DP matrix. This requires locating and sorting all candidate locations for a pattern. Alternatively, we can prefer to verify directly all candidate locations, e.g. if the verification algorithm is fast and the number of redundant candidate locations is low. Nonetheless, to avoid reporting duplicate occurrences, we have to consider redundant all occurrences either beginning or ending at the same position in the text. This requires memorizing and sorting all occurrences of a pattern.

How many redundant error configurations² are produced by seeds filters? For simplicity we consider exact seeds and combinations of exactly k errors. We have to cover all possible ways of distributing k errors among $k + 1$ seeds, that is $\binom{2k}{k}$ error combinations. However, for a fixed seed, we cover all combinations where the seed itself contains no errors and all k errors are distributed among the remaining k seeds, i.e. $\binom{2k-1}{k}$ error combinations. Thus the fraction of error combinations covered by filtration with exact seeds over the minimal ones is

$$\frac{(k+1)\binom{2k-1}{k}}{\binom{2k}{k}} = \frac{k+1}{2} \quad (4.9)$$

For instance, filtration with exact seeds covers three times more combinations than required when $k = 5$. With approximate seeds we partition the pattern in less seeds and thus we indirectly reduce filter redundancy.

² Here we consider the fraction of redundant error combinations and not the fraction of redundant candidate locations reported by the filter.

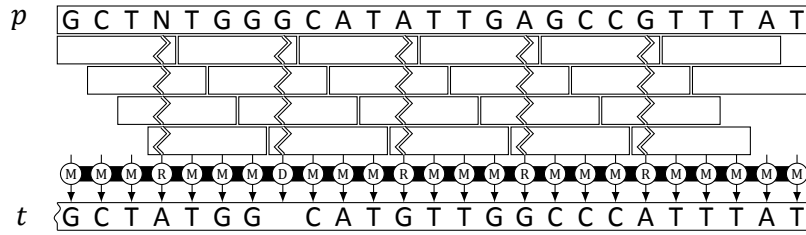
4.3 Contiguous q -grams

q -Gram filters are based on the so-called q -gram similarity measure $\tau_q : \Sigma^* \times \Sigma^* \rightarrow \mathbb{N}_0$, defined as the number of substrings of length q common to two given strings. The following lemma relates q -gram similarity to edit and Hamming distance. It gives a lower bound on the q -gram similarity $\tau_q(x, y)$ of any two strings x, y within edit distance k . This means that $\tau_q(x, y) \geq k$ is a necessary but not sufficient condition for $d_E(x, y) \leq k$.

Lemma 4.3 (The q -gram lemma). [Jokinen and Ukkonen, 1991] Let x, y be two strings s.t. $d_E(x, y) = k$, and assume w.l.o.g. $|x| \leq |y|$ and $|x| = m$. Then x and y have q -gram similarity $\tau_q(m, k) \geq m - q + 1 - kq$.

The first part of the threshold function τ counts the number of q -grams of x (i.e. $m - q + 1$), while the second part counts how many q -grams can be covered by k errors (kq , i.e. at most q per error). Figure 4.3 illustrates. Note how the threshold function τ depends only on the parameters q, m, k and not on any specific q -gram.

Figure 4.3: Filtration with q -grams.



Lemma 4.3 itself does not give us a direct solution to approximate string matching. Indeed, it considers the edit distance between two arbitrary strings, while in approximate string matching the pattern can match any substring of the text. More precisely, if the pattern approximately matches any substring s of t , then in the case of k -mismatches s must have length m ; in the case of k -difference, the length of s must be within $m - k$ and $m + k$. The dot plot representation helps us to visualize this concept: k -mismatches occurrences cover one single diagonal of the dot plot, while k -difference occurrences are enclosed inside a parallelogram of side $2k + 1$.

Therefore, we can design an online filtration algorithm scanning the text and counting how many q -grams of the pattern fall into each parallelograms. Only the parallelograms exceeding the threshold $\tau_q(m, k)$ have to be verified with an online method, e.g. standard DP. Alternatively, to speed up the filtration phase, we can count the q -grams with the help of a substring index.

Which is the biggest q -gram length yielding lossless filtration given m and k ? In order to satisfy lemma 4.3, the q -gram threshold must be greater than zero, i.e. it must hold $\tau_q(m, k) \geq 1$. Thus, by substituting τ , we obtain $q \leq \lfloor \frac{m}{k+1} \rfloor$, analogously to equation 4.3 of seed filters.

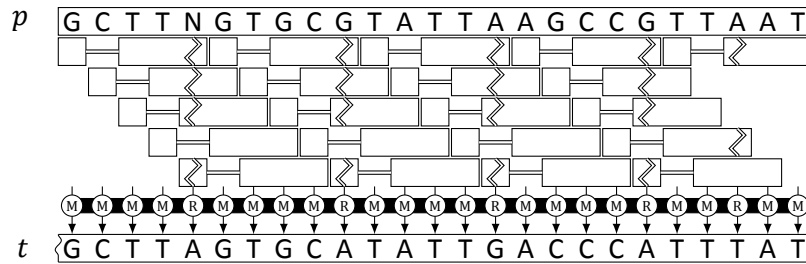
4.4 Gapped q -grams

In section 2.5.3 we introduced the q -gram similarity measure as the number of substrings of length q common to two given strings. We now generalize this similarity measure to consider the number of common subsequences³ of length q whose symbols are taken from a fixed set Q of positions.

Definition 4.1. We call Q -gram a finite sequence Q of natural numbers starting with the unit element, i.e. $Q \subset \mathbb{N}$ and $1 \in Q$. We denote by $w(Q)$ the *weight* of Q as the cardinality of the set $|Q|$, and by $s(Q)$ the *span* of Q as the maximum element of the set Q .

In literature, Q -grams are visualized as words over the alphabet $\{1, *\}$ or $\{\#, -\}$. We adopt the former notation and represent the Q -gram by the word $w \in \{1, *\}^{s(Q)}$ such that $w_j = 1$ iff $j \in Q$. Figure ?? shows an example of Q -gram.

Figure 4.4: Filtration with gapped q -grams.



The first thing we remark is that, compared to contiguous q -grams, we obtain a higher threshold, as mismatches do not cover don't care positions. The q -gram lemma (??) does not provide us anymore with a tight threshold, but only with a lower bound. Note that, as in the q -gram lemma, the threshold depends only on Q and parameters m, k . Indeed, the pattern of covered q -grams does not depend on the text or pattern sequences but only on their transcript, i.e. on the position of the mismatches in the pattern.

Gapped q -grams raise hard combinatorial questions. Given a gapped q -gram, (i) does it yield a full-sensitive filter for k -mismatches? If so, either (ii) which is the maximum q -gram threshold t that guarantees full-sensitivity? or (iii) which is the maximum error k for which full-sensitivity is guaranteed? If the answer to question ?? is negative and the filter is lossy, (iv) how many false negatives our filter discards? Considering filtration efficiency, (v) how many false positives our filter produces? If we take the weight as a simplified criterion predicting filtration efficiency, (vi) which is the maximum weight lossless shape?

Question ii has been first considered in [Burkhardt and Karkkainen, 2001; Kucherov *et al.*, 2005], the more general questions i and vi have been introduced in [Nicolas and Rivals, 2005], while we consider here for the first time questions iii-v. With the aim of elucidating these questions, we first introduce simple characteristic functions to formally

³ A subsequence is a non-contiguous sequence of symbols of a given string.

define transcripts detected by gapped q -grams. Afterwards, we recapitulate known results for questions i-vi and give new exact and approximate solutions.

4.4.1 Characteristic functions

Consider an arbitrary transcript σ as a m -dimensional vector over \mathbb{B} , where $|\sigma|_0$ indicates the Hamming distance of the transcript. Let $\mathbb{B}_k^m \subset \mathbb{B}^m$ be the set containing all transcripts σ such that $|\sigma|_0 = k$.

Definition 4.2. A Q -gram *occurs* at position i in a similarity σ iff $\forall j \in Q \sigma_{i+j} = 1$. Fixed a Q -gram threshold t , the Q -gram detects σ iff it occurs at least t times in σ .

Boolean functions

Let $T_Q^m : \mathbb{B}^m \rightarrow \mathbb{B}$ denote a *boolean function* such that $T_Q^m(\sigma)$ is true iff the Q -gram occurs at least one time in a similarity σ of length m . We define such boolean function as the disjunction

$$T_Q^m(\sigma) = \bigvee_{i=1}^{m-s(Q)+1} \bigwedge_{j \in Q} \sigma_{i+j} \quad (4.10)$$

where each *clause* of T_Q^m represents a single possible occurrence of Q in σ . We define an analogous boolean function for a Q -gram family F as the disjunction

$$T_F^m(\sigma) = \bigvee_{Q_i \in F} T_{Q_i}^m(\sigma) \quad (4.11)$$

By definition, T_Q^m and T_F^m are *monotone nondecreasing* boolean functions in *disjunctive normal form (DNF)*. Since all monotone boolean functions in DNF are minimal, T_Q^m and T_F^m are *minimal*.

In general, (Q, t) detects σ iff σ satisfies at least t clauses of T_Q^m .

Pseudo-boolean functions

Let the function $t_Q^m : \mathbb{B}^m \rightarrow \mathbb{N}_0$ be the boolean function T_Q^m acting on \mathbb{N}_0 . We defined such *pseudo-boolean function* as

$$t_Q^m(\sigma) = \sum_{i=1}^{m-s(Q)+1} \prod_{j \in Q} \sigma_{i+j} \quad (4.12)$$

Here $t_Q^m(\sigma)$ counts how many times a Q -gram occurs in a similarity σ of length m . It is useful to define the complementary function \bar{t}_Q^m , counting how many times a Q -gram does not occur in a similarity σ , as

$$\bar{t}_Q^m(\sigma) = m - s(Q) + 1 - t_Q^m(\sigma) \quad (4.13)$$

Analogously, we define a pseudo-boolean function for a Q -gram family F

$$t_F^m(\sigma) = \sum_{Q_i \in F} t_{Q_i}^m(\sigma) \quad (4.14)$$

along with its complementary function

$$\bar{t}_F^m(\sigma) = \sum_{Q_i \in F} (m - s(Q_i) + 1) - t_F^m(\sigma) \quad (4.15)$$

The above functions expose important properties which will let us devise approximate solutions. *Nondecreasing monotonicity* of functions t_Q^m and t_F^m follow from nondecreasing monotonicity of their boolean counterparts T_Q^m and T_F^m . Consequently \bar{t}_Q^m and \bar{t}_F^m are *monotone nonincreasing*. From definition ??, function t_Q^m is *supermodular*, thus it follows that \bar{t}_Q^m is *submodular*. Since super and submodular functions are closed under non-negative linear combination, functions t_F^m and \bar{t}_F^m are respectively super and submodular.

4.4.2 Full-sensitivity

NON DETECTION [Nicolas and Rivals, 2005]. Does a given gapped q -gram yield a full-sensitive filter for k -mismatches?

Problem definition

Instance A Q -gram, two integers m, k with $0 < k < m$.

Question Does it exist a similarity $\sigma \in \mathbb{B}_k^m$ such that $T_Q^m(\sigma)$ is false?

Hardness results

NON DETECTION is *strongly* NP-complete [Nicolas and Rivals, 2005]. Nicolas and Rivals introduce an intermediate problem, called SOAPY SET COVER. They reduce EXACT COVER BY 3-SETS to SOAPY SET COVER and SOAPY SET COVER to NON DETECTION. Strong NP-completeness implies that no *FPTAS* nor any *pseudo-polynomial* algorithm for it exist, under the assumption that $P \neq NP$.

Our FPRAS solution

Describe FPRAS.

4.4.3 Optimal threshold

Which is the highest Q -gram threshold t that guarantees full-sensitivity? This problem has been introduced in [Burkhardt and Karkkainen, 2001].

Problem definition

Instance A Q -gram, two integers m, k such that $0 < k < m$.

Solution The largest integer t^* such that NON DETECTION for $(Q, t^*), m, k$ answers *no*.

Recalling Q -gram pseudo-boolean functions 4.12, we can define the optimal threshold problem as the minimization of a supermodular function subject to linear constraints

$$\begin{aligned} \min \quad & t_Q^m(\sigma) \\ \text{w.r.t.} \quad & \\ & \sigma \in \mathbb{B}_k^m \end{aligned} \tag{4.16}$$

Exact DP solution

Optimal threshold is fixed-parameter tractable (FPT) in the span of the q -gram shape. Burkhardt and Karkkainen give a DP algorithm computing the optimal threshold in time $O(m \cdot k \cdot 2^{s(Q)})$ [Burkhardt and Karkkainen, 2001]. Kucherov *et al.* give an extension for Q -gram families in [Kucherov *et al.*, 2005].

All possible assignments, i.e. $\mathbb{B}^s(Q)$, for the first clause $\bigwedge_{j \in Q} \sigma_j$ of the boolean function T_Q^m are considered and all satisfying assignments for it, i.e. $\phi(Q)$, are computed. Clause Q_2 is considered next...

Our exact ILP solution

We reduce this problem to *maximum coverage* [?] and solve it with the following ILP

$$\begin{aligned} \max \quad & |c|_1 \\ \text{w.r.t.} \quad & \\ & \sigma \in \mathbb{B}_k^m \\ & c \in \mathbb{B}^{m-s(Q)+1} \\ & \sigma_i \geq c_j \end{aligned} \tag{4.17}$$

where variable c_j indicates the truthfulness of the j -th clause in T_Q^m . Given the ILP solution c^* , we obtain the optimal threshold $t^* = |c^*|_1$.

Our APX solution

We reduce the complementary optimal threshold problem to the maximization of a submodular function subject to linear constraints

$$\begin{aligned} \max \quad & \bar{t}_Q^m(\sigma) \\ \text{w.r.t.} \quad & \\ & \sigma \in \bar{\mathbb{B}}_k^m \end{aligned} \tag{4.18}$$

where the complementary optimal threshold is $\bar{t}^* = m - s(Q) + 1 - t^*$.

We compute an approximate solution via deepest descent. Our greedy algorithm for complementary OPTIMAL THRESHOLD has an APX-ratio of $1 + 1/e$ [?]. The same *absolute error* applies to OPTIMAL THRESHOLD.

4.4.4 Maximum error

Which is the maximum error k^* for which full-sensitivity is guaranteed?

Problem definition

Instance A Q -gram, an integer $m > 0$.

Solution The largest integer k^* such that NON DETECTION for Q, m, k^* answers *no*.

Recalling pseudo-boolean functions 4.12, we define our problem as the minimization of a linear function subject to submodular constraints

$$\begin{aligned} \min \quad & |\sigma|_1 \\ \text{w.r.t.} \quad & \\ & \sigma \in \mathbb{B}^m \\ & \bar{t}_Q^m(\sigma) \leq 0 \end{aligned} \tag{4.19}$$

Our ILP solution

We reduce our problem to MINIMUM SET COVER [?], solve it with the following ILP

$$\begin{aligned} \min \quad & |\sigma|_1 \\ \text{w.r.t.} \quad & \\ & \sigma \in \mathbb{B}^m \\ & b \in \mathbb{B}^{m-s(Q)+1} \\ & A\sigma \geq b \end{aligned} \tag{4.20}$$

where the value A_{ij} of the coefficient matrix A is defined as

$$A_{ij} = \begin{cases} 1 & \text{if } i - j + 1 \in Q \\ 0 & \text{if } i - j + 1 \notin Q \end{cases} \tag{4.21}$$

and find the maximum error for which full-sensitivity is guaranteed as $k^* = |\bar{\sigma}^*|_1$ given the solution σ^* to the ILP.

Note that contiguous q -grams provide an interesting special case of this ILP. If A has the *consecutive ones property*, it is *totally unimodular*. The *polytope* defined by a totally unimodular coefficient matrix is *integral*. Hence the optimal solution of the relaxed LP is also the optimal solution of the original ILP.

Our APX solution

Again, we compute an approximate solution via deepest descent. APX-ratio of $H_{w(Q)}$ [?].

4.4.5 Specificity

How many false positives our filter produces?

Problem definition

Instance A Q -gram, two integers m, k such that $0 < k < m$.

Solution The number of false positives produced by the Q -gram.

False positives are true points of the boolean function 4.10 which have weight inferior to $m - k$ and satisfy more than t clauses of $T_{Q,t}^m$. Hence we define the function FP_k^m counting the number of false positives of filter (Q, t) in instance (m, k) as

$$FP_k^m(Q, t) = \sum_{\sigma \in \mathbb{B}_k^m} T_{Q,t}^m(\sigma) \quad (4.22)$$

Our FPRAS solution

We reduce counting false positives to counting the number of true assignments to a boolean function in DNF. The latter problem can be approximated via importance sampling. ? introduces a *RPTAS* approximating the number of true points of a DNF.

4.4.6 Optimal gapped q -grams

Introduced in [Nicolas and Rivals, 2005].

Problem definition

Instance A finite set S of similarities.

Solution A Q -gram that detects all similarities of S .

Measure The weight $w(Q)$ of the Q -gram.

Given a set of similarities, find the Q -gram of maximum weight detecting all similarities. This applies to the DNA Homology Search Framework as well.

Hardness and inapproximability results

Nicolas et al. [Nicolas and Rivals, 2005] perform an approximation preserving reduction from MAXIMUM INDEPENDENT SET. MWLS is NP-hard and APX-hard within $(|S|)^{0.25-\epsilon}$ unless $P = NP$. If $S = \mathbb{B}_k^m$, $|S| = \binom{m}{k}$.

Branch-and-bound search

Burkhardt et al. [Burkhardt and Karkkainen, 2001] bounding criterion. If $Q_1 \subseteq Q_2$, then $t_{Q_2}(m, k) \leq t_{Q_1}(m, k)$. Such bounding criterion allows to discard parts of the search space which do not solve the considered (m, k) instance.

4.5 Verification methods

4.5.1 Banded Myers' bit-vector algorithm

4.5.2 Increased bit-parallelism using SIMD instructions

Part II

READ MAPPING

5.1 High-throughput sequencing data

5.1.1 Read sequences

Illumina

Illumina / Solexa.

Ion Torrent

Life Technologies / Ion Torrent.

Other technologies

Roche / 454 Life Sciences.

SOLiD

5.1.2 Phred base quality scores

Phred base quality scores have been introduced in [Ewing *et al.*, 1998; Ewing and Green, 1998] to assess the quality of sequencing single bases in capillary reads. Instead of directly discarding low-quality regions present in capillary reads, the tool Phred calls each base and annotates it with a quality score encoding the probability that it has been wrongly called. As this method has been widely accepted, base callers annotate reads issued of all sequencing technologies with Phred base quality scores.

To formally define Phred base quality scores, let us fix the alphabet $\Sigma = \{A, C, G, T\}$, and consider a known donor genome g over Σ and a read r sequenced at location l from the template $g_{l \dots l+|r|-1}$. We define the base calling error ϵ_i at position i in the read r , as the probability ϵ_i of miscalling a base r_i instead of calling its corresponding base g_{l+i-1} in the donor genome. Therefore, we define the Phred base quality Q_i at position i as:

$$Q_i = -10 \log_{10} \epsilon_i. \quad (5.1)$$

Given the above, the probability $p(r_i | g_{l+i-1})$ of calling the base r_i in the read r , given

the donor genome base g_{l+i-1} , is:

$$p(r_i|g_{l+i-1}) = \begin{cases} 1 - \epsilon_i & \text{if } g_{l+i-1} = r_i \\ \frac{\epsilon_i}{|\Sigma|-1} & \text{if } g_{l+i-1} \in \Sigma \setminus \{r_i\} \end{cases} \quad (5.2)$$

and assuming i.i.d. base calling errors, it follows that the probability $p(r|g, l)$ of observing the read r , given the donor genome template $g_{l \dots l+|r|-1}$, is:

$$p(r|g, l) = \prod_{i=1}^{|r|} p(r_i|g_{l+i-1}) \quad (5.3)$$

5.2 Data analysis paradigms

The goal of secondary analysis is to reconstruct the original sequence of the donor genome. The *reference-guided* assembly plan assumes a prior knowledge of a reference genome similar to the donor. Reads are thus mapped (i.e. aligned) to the reference genome w.r.t. a given scoring scheme and threshold. The scoring scheme should account for eventual genomic variation, as well as for any sequencing artefacts. An alignment of optimal score for a read implies its *original location* on the reference genome. Conversely, no alignment within the score threshold implies too many sequencing errors, too much genetic variation, or sample contamination. A problem arises in presence of co-optimal or close sub-optimal alignments: the read cannot be mapped confidently.

The problem of confidently mapping high-throughput sequencing reads comes from the non-random nature of genomic sequences. Genomes evolved through multiple types of duplication events, including whole-genome duplications [?] or large-scale segmental duplications in chromosomes [?], transposition of repetitive elements as short tandem repeats (microsatellites) and interspersed nuclear elements (LINE, SINE) [?], proliferation of repetitive structural elements such as telomeres and centromeres [?]. As a result of these events, for instance, about 50 % of the human genome is composed of repeats.

Repeats present in general technical challenges for all *de novo* assembly and sequence alignment programs [Treangen and Salzberg, 2011]. Due to repetitive elements, a non-ignorable fraction of high-throughput sequencing reads cannot be mapped confidently. In general, the shorter the reads, the higher the challenges due to repeats. I quantify this phenomenon more precisely in section 5.3. Here I focus on analysis strategies to deal with *multi-reads*, i.e. reads that cannot be mapped confidently as they align equally well to multiple locations.

It is not evident how to treat *multi-reads*. According to Treangen and Salzberg, common strategies to deal with multi-reads are (i) to discard them all, (ii) to randomly pick one best mapping location, (iii) to consider all or up to k best mapping locations within a given distance threshold. A *de facto* standard strategy emerged over the last years, combining strategies i and ii. The read mapper randomly picks one best mapping location and complements it with its *mapping quality*, i.e. the probability of the mapping location being correct (see section ??). Subsequently, downstream analysis tools apply a mapping quality score cutoff to discard reads not mapping confidently to any location. The other

popular strategy adopted by analysis tools is to consider all mapping locations within an edit distance threshold. In this case, it is not clear whether downstream analysis tools consider equally all mapping locations regardless of their distance.

In the light of these facts, I define two broad paradigms for the secondary and tertiary analysis of HTS data: *best-mapping* and *all-mapping*. The best-mapping paradigm considers a single mapping location per read along with its confidence, while the all-mapping paradigm considers a comprehensive set of mapping locations per read. It goes without saying that read mapper and downstream analysis tools must agree on a common paradigm. Thus these paradigms are valid not only for read mappers but also for any downstream analysis tool, e.g. variant callers. Read mapping and variant calling are indeed tightly coupled steps within reference-based HTS pipelines.

5.2.1 Best-mapping

As said, best-mapping methods rely on one single mapping location per read. In order to maximize recall, best-mappers often adopt complex scoring schemes taking into account gaps and base quality values, and at the same time implement sophisticated heuristics to speed up the search. Best-mappers should always complement any mapping location with its mapping quality. Subsequently, in order to maximize precision, variant calling tools decide whether to consider or discard reads not mapping confidently to any location. The GATK [?] and Samtools [?] are popular best-mapping tools to call small variants. In section ??, I show how these methods are limited to the analysis of high mappability regions, as they systematically discard reads belonging to low mappability regions.

Mapping quality score

Mapping quality has been introduced in [Li *et al.*, 2008]. The study considers short reads of length ranging from 30 bp to 40 bp, produced by early Illumina/Solexa and ABI/SOLiD sequencing technologies, whose sequencing error rates were quite high. Given the short lengths and high error rates, a significant fraction of such reads can be aligned to multiple mapping locations, even considering only co-optimal Hamming distance locations.

The key point is that the Hamming distance is not an adequate scoring scheme to guess the correct mapping location of many reads. Li *et al.* claim that: *it is possible to act conservatively by discarding reads that map ambiguously at some level, but this leaves no information in the repetitive regions and it also discards data, reducing coverage in an uneven fashion, which may complicate the calculation of coverage*. However, they do not show in their study what is the effect of relying on mapping quality rather than on mapping uniqueness.

Since base callers output base call probabilities in Phred-scale along with the reads, Li *et al.* propose a novel probabilistic scoring scheme called mapping quality, giving the probability that a given read has been aligned correctly at a given mapping location in the reference genome.

By applying Bayes' theorem, we can derive the posterior probability $p(l|g,r)$, that location l in the reference genome g is the correct mapping location of read r . Assuming

uniform coverage, each location $l \in [1, |g| - |r| + 1]$ has equal probability of being the origin of a read in the donor genome, thus the prior probability $p(l)$ is simply:

$$p(l) = \frac{1}{|g| - |r| + 1} \quad (5.4)$$

Therefore, recalling $p(r|g, l)$ from equation 5.3, the posterior probability $p(l|g, r)$ equals the probability of the read r originating at location l normalized over all possible locations in the reference genome:

$$p(l|g, r) = \frac{p(r|g, l)}{\sum_{i=1}^{|g|-|r|+1} p(r|g, i)} \quad (5.5)$$

which in Phred-scale becomes:

$$Q(l|g, r) = -10 \log_{10}[1 - p(l|g, r)] \quad (5.6)$$

Computing the exact mapping quality as in equation 5.6 requires aligning each read to all positions in the reference genome. On one hand, this computation would not be practical, indeed the vast majority of a reference genome is discarded when mapping reads by means of filtering and fully-indexed methods. On the other hand, the contribution of discarded locations to the sum in equation 5.5 can be neglected. Therefore, equation 5.5 is approximated using only relevant mapping locations found by the read mapper.

Mapping quality has been initially used in [Li *et al.*, 2008] and [Li *et al.*, 2009a] to maximize variant calling confidence by discarding reads whose best mapping location is below a given mapping quality threshold. This measure has been widely accepted: nowadays it is computed by most popular read mappers and used by almost all variant calling tools e.g. the Genome Analysis ToolKit (GATK) [DePristo *et al.*, 2011].

Nonetheless, some important objections can be moved against mapping quality. First, the mapping quality score is derived under the unlikely assumption of the reference genome being equal to the donor genome. In other words, mapping quality considers only errors due to base miscalls and disregards genetic variation; thus the risk is to prefer mapping locations supported by known low base qualities rather than by true but unknown SNVs. Second, mapping quality is nonetheless strongly correlated to mapping uniqueness, as discussed in section 5.3; it is easy to see that the mapping probability in equation 5.5 is diluted in presence of a large number of co-optimal mapping locations. Third, mapping quality tends to become less relevant as base calls improve, due to advances of sequencing technologies, and thus degenerates in a shallow measure of uniqueness.

5.2.2 All-mapping

All-mapping analysis methods consider a comprehensive set of locations per read. Almost all read mappers in this category adopt edit distance, the simplest scoring scheme, and report all mapping locations within an error threshold, absolute or relative w.r.t. to the length of the reads. Variant calling algorithms based on all-mapping have the potential to detect a wider spectrum of genomic variation events than in best-mapping. For

instance, variant callers based on the all-mapping paradigm detect CNVs [?], and SNVs in homologous regions [?]. A practical challenge of all-mapping is represented by reporting and handling huge sets of mapping locations.

5.3 Limits of high-throughput sequencing

Due to repetitive elements, a non-ignorable fraction of high-throughput sequencing reads cannot be mapped confidently. Which regions of a model organism's genome cannot be resequenced confidently by a high-throughput sequencing technology? And how accurate is downstream analysis on these low confidence regions? Two recent studies [Derrien *et al.*, 2012; Lee and Schatz, 2012] answer these questions. Below, I report their key ideas and most relevant findings.

5.3.1 Genome mappability

In [Derrien *et al.*, 2012], *genome mappability* is defined for a given q -gram length, a distance measure i.e. the Hamming or edit distance, and a distance threshold k . Given a genomic sequence g , the (q, k) -frequency $F_k^q(l)$ of the q -gram $g_{l...l+q-1}$ at location l in g denotes the number of occurrences of the q -gram in g and its reverse complement \bar{g} . The (q, k) -mappability $M_k^q(l)$ is the inverse (q, k) -frequency, i.e. $M_k^q(l) = F_k^q(l)^{-1}$ with $M_k^q : \mathbb{N} \rightarrow]0, 1]$. Note that $M_k^q(l)$ can be seen as the prior probability that any read of length q originating at location l will be mapped correctly. The values of (q, k) -frequency and mappability obviously vary with the distance threshold k . Nonetheless, under any distance measure, it holds that the q -gram at location l is unique up to distance k iff $M_k^q(l) = 1$ and repeated otherwise.

Unique mappability determines which fraction of a genome can be analyzed according to strategy i (i.e. discarding non-unique reads, see section 5.2). Derrien *et al.* quantify the *unique mappability* of whole human, mouse, fly, and worm genomes. Mimicking typical Illumina read mapping setups, they consider q -grams of length 36, 50 and 75 bp, and Hamming distance 2. They find out that about 30 % of the whole human genome is not unique w.r.t. $(36, 2)$ -mappability. At $(75, 2)$ -mappability, 17 % of the human genome is not yet unique. This last result is quite optimistic, as typical mapping setups call for 3–4 edit distance errors in order to map a significant fraction of the reads. Table shows some results extrapolated from [Derrien *et al.*, 2012].

To estimate resequencing accuracy at a single location, Derrien *et al.* consider the mappability of all possible q -grams spanning it. They define *pileup mappability* P_k^q at position i as the average mappability of all q -grams spanning position i , i.e.:

$$P_k^q(i) = 1/q \sum_{j=i}^{i+q-1} M_k^q(j) \quad (5.7)$$

Derrien *et al.* find out in their own resequencing studies that *low pileup-mappability regions are more prone to show a high value of heterozygosity than those with high mappability* [Derrien *et al.*, 2012]. Variant callers ideally call a locus heterozygous whenever its

Table 5.1: Mappability of model genomes. Data extrapolated from [Derrien et al., 2012].

	H.sapiens (hg19)	M.musculus (mm9)	D.mel (dm3)
Repeats content [%]	45.25	42.33	26.50
Uniqueome (36 bp, 2 msm) [%]	69.99	72.07	68.09
Uniqueome (50 bp, 2 msm) [%]	76.59	77.06	69.44
Uniqueome (75 bp, 2 msm) [%]	83.09	81.65	71.00

consensus alignment column, consisting of piled up reads, contains two distinct bases. This situation tends to arise whenever the consensus alignment contains reads originating from similar yet distinct regions.

5.3.2 Genome mappability score

Genome mappability score (GMS) [Lee and Schatz, 2012], analogously to pileup mappability, estimates single-locus resequencing accuracy for a specific sequencing technology. Instead of considering the inverse q -gram frequency, Lee and Schatz use mapping quality (see subsection 5.2.1) to estimate the probability that a read originating at a given position can be mapped correctly. Subsequently, they derive average mapping probability of any read spanning a location l of a reference genome g as¹:

$$p(l|g) = \sum_{r \in \mathcal{R}(l)} \frac{p(l|g, r)}{|\mathcal{R}(l)|} \quad (5.8)$$

which in Phread-scale becomes:

$$Q(l|g) = \sum_{r \in \mathcal{R}(l)} \frac{1 - 10^{-\frac{Q(l|g, r)}{10}}}{|\mathcal{R}(l)|} \quad (5.9)$$

Thus, fixed a genomic sequence g , they define the genome mappability score $GMS(l)$ in percentual value:

$$GMS(l) = 100 Q(l|g) \quad (5.10)$$

Lee and Schatz proceed as follow to compute GMS. They first simulate reads from all genomic locations, having length and error profiles similar to those issued by actual sequencing technologies. Subsequently, they compute mapping quality scores by mapping all simulated reads with BWA (see section ??). Then, as just explained, they compute GMS at any location by averaging the quality scores. Finally, they define *low GMS* regions as those locations for which $GMS(l) \leq 10$, and *high GMS* otherwise. Table ?? shows performance of various sequencing technologies on the whole human genome (data extrapolated from [Lee and Schatz, 2012]).

¹ Equation 3 in [Lee and Schatz, 2012] is not precise, please consider equation 5.8 instead.

Table 5.2: Human genome mappability score of various sequencing technologies. Data extrapolated from [Lee and Schatz, 2012].

Sequencing technology	Read length [bp]	Error rate [%] (msm, ins, del)	Low GMS [%]	High GMS [%]
Illumina-like	100	(0.10, 0.00, 0.00)	10.51	89.49
Ion Torrent-like	200	(0.04, 0.01, 0.95)	9.35	90.65
Roche/454-like	800	(0.18, 0.54, 0.36)	8.91	91.09
PacBio-like	2000	(1.40, 11.47, 3.43)	100.0	0.00
PacBio EC-like	2000	(0.33, 0.33, 0.33)	8.61	91.39

Lee and Schatz simulate an Illumina-like resequencing study. They measure variant calling accuracy by GMS for the popular combination of best-mapping tools BWA and SAMtools [?]. They find out that at $30 \times$ sequencing coverage accuracy tends to 100 % in high GMS regions, while it levels off to 25 % in low GMS regions. Their analysis *shows that most SNP detection errors are false negatives, and most of the missing variations are in regions with low GMS scores* [Lee and Schatz, 2012]. These are the limits of *de facto* standard tools for the analysis of high-throughput sequencing data.

5.4 Popular read mappers

Following the boom of NGS technologies, recent bioinformatics research has produced dozens of tools to perform read mapping. Two surveys [Li and Homer, 2010; Fonseca *et al.*, 2012] try to help bioinformaticians to extricate themselves from the jungle of read mapping tools. The survey by Li and Homer first classifies read mapping algorithms by data structure: those based on hash tables and those based on suffix/prefix trees. However, the adopted data structure is often an implementation detail, indeed most algorithms covered in the survey fit into both classes. The survey primarily considers the application of SNP calling; in the considered setup, tools enumerating a comprehensive set of locations always lag behind those designed to report only one location per read. The survey by Fonseca *et al.* catalogs read mappers by the features exposed to the user. It considers supported input–output formats, rate of errors and variation, number and type (i.e. local or semi-global read alignments) of mapping locations reported. After this exhaustive catalog, the survey concludes that the choice of a read mapper *involves application-specific requirements such as how well it works in conjunction with downstream analysis tools (i.e. variant callers)*.

Read mapping and variant calling are indeed tightly coupled steps within reference-based HTS analysis pipelines. Secondary and tertiary analysis methods are based on one of the two following paradigms: best-mapping and all-mapping. In the light of the above consideration, the most important feature of a read mapper is the number of mapping locations reported, followed by their type, while the other features are mostly of technical

relevance. Most read mappers are specifically designed to fit one paradigm, while others are versatile enough to work well in both cases.

The rest of this section presents most popular read mapping tools. Among them, BWA [??], Bowtie [??] and Soap [?] are prominent tools designed for best-mapping, while mr(s)Fast [??], RazerS [??], SHRiMP [??] are designed for best-mapping. Grosso modo, most prominent best-mappers recursively enumerate substrings on a suffix/prefix tree of the reference genome via backtracking algorithms. Backtracking alone is impractical as its time complexity grows exponentially with the number of errors considered, hence best-mappers apply heuristics to reduce and prioritize enumeration. Conversely, all-mappers are based on filtering algorithms for approximate string matching. They quickly determine, often with the help of an index, locations of the reference genome candidate to contain approximate occurrences, then verify them with conventional methods. Their efficiency is bound to filtration specificity and thus deteriorates with increasing error rates and genome lengths. Finally, the most recent tools GEM [?], Masai [Siragusa *et al.*, 2013], and Yara, fit both best and all-mapping paradigms. They speed up best-mapping by stratifying mapping locations by edit distance and prioritizing filtration accordingly. In addition to that, they also speed up all-mapping by means of more specific filters based on backtracking.

5.4.1 Bowtie

Bowtie [Langmead *et al.*, 2009] is a mapper designed to have a small memory footprint and quickly report a few good mapping locations for early generation Illumina/Solexa and ABI/SOLiD short reads of length up to 50 bp. It achieves the former goal by indexing the reference genome with an FM-index and the latter goal by performing a greedy depth-first traversal on it.

The greedy depth-first traversal visits first the subtree yielding the least number of mismatches and stops after having found a candidate (not guaranteed to be optimal when $k > 1$). In addition, Bowtie speeds up backtracking by applying case pruning, a simple application of the pigeonhole principle. However this technique is mostly suited for $k = 1$ and requires the index of the forward and reverse text.

Bowtie can be configured to search by strata, however the search time increases significantly while the traversal still misses a large fraction of the search space due to seeding heuristics. Main practical drawbacks of the tool are too many cryptic options.

Bowtie 2 [Langmead and Salzberg, 2012] has been designed to quickly report a couple of mapping locations for recent Illumina/Solexa, Ion Torrent and Roche/454 reads, usually having lengths in the range from 100 bp to 400 bp.

This tool uses an heuristic seed-and-extend approach, collecting seeds of fixed length, partially overlapping, and searching them exactly in the reference genome using an FM-index. Candidate locations to verify are chosen randomly, to avoid uncompressing large CSA intervals and executing many DP instances. Each mapping location is verified using a striped vectorial dynamic programming algorithm, implemented using SIMD instructions, previously introduced by [Farrar, 2007] and extended to compute end-to-end alignments.

Bowtie 2 can be configured to report end-to-end or local alignments, scored using a tunable affine scoring scheme. For this reason, it is believed to be good at reporting alignments containing indels. However, its completely heuristic filtration method, independent of the scoring scheme, makes it hard to believe what it promises.

5.4.2 BWA

BWA-backtrack [Li and Durbin, 2009] is designed to map Illumina/Solexa reads up to 100 bp and report a few best end-to-end alignments. The program performs a greedy breadth-first search on an FM-index of the reference genome. Nodes to be visited are ranked by edit distance score: the best node is popped from a priority queue and visited, its children are then inserted again in the queue. The traversal considers indels using a more involved 9-fold recursion. Backtracking is sped up by adopting a more stringent pruning strategy that nonetheless takes some preprocessing time and requires the index of the reverse reference genome.

BWA performs paired-end alignments by trying to anchor both paired-end reads and verifying the corresponding mate, within an estimated insert size, using the classic DP-based Smith-Waterman algorithm. Consequently, the program in paired-end mode aligns reads at a slower rate than in single-end mode. The program is not fully multi-threaded, therefore BWA scales poorly on modern multi-core machines.

BWA-SW [Li and Durbin, 2010] is designed to map Roche/454 reads, which have an average length of 400 bp. It is an heuristic version of BWT-SW, designed to report a few good local alignments.

This version of BWA adopts a double indexing strategy: it indexes all substrings of one read in a DAWG. It performs Smith-Waterman of all read substrings directly on the FM-index, by backtracking as soon as no viable alignment can be obtained. As in BWA-backtrack, the traversal proceeds in a greedy fashion. In addition, BWA-SW implements some seeding heuristics to limit backtracking and jump in the reference genome to verify candidate locations whenever this becomes favorable.

This version of BWA does not support paired-end reads, presumably because it was meant for Roche/454 reads.

5.4.3 Soap

Soap 2 [Li *et al.*, 2009b] is very similar to Bowtie: it has been designed to produce a very quick but shallow mapping of Illumina/Solexa reads up to 75 bp with no more than 2 mismatches and no indels. However, its underlying algorithm is based on the so-called bi-directional (or 2-way) BWT. The tool support paired-end mapping but at a slower alignment rate. Practical drawbacks are the lack of native output in the de-facto standard SAM format and is closed source. Soap 3 [Liu *et al.*, 2012] is algorithmically similar to Soap 2 but targets only NVIDIA CUDA accelerators.

5.4.4 SHRiMP

SHRiMP 2 TODO.

5.4.5 RazerS

RazerS [Weese *et al.*, 2009] has been designed to report all mapping locations within a fixed hamming or edit distance error rate. It is based on a full-sensitive q -gram filtration method (SWIFT semi-global) combined with the Myers edit distance verification algorithm. On demand, the SWIFT filter can be configured to become lossy within a fixed loss rate. The lossy filter becomes more stringent and produces a lower number of candidates to verify, thus improving the overall speed of the program. All in all, the SWIFT filter is very slow while not highly specific.

RazerS 3 [Weese *et al.*, 2012] is a faster version featuring shared-memory parallelism, a faster banded-Myers verification algorithm, and a faster filtration scheme based on exact seeds that however turns out to be very weak on mammal genomes. Because of this, RazerS 3 is one-two orders of magnitude slower than Bowtie 2 and BWA-backtrack on mammal genomes.

All RazerS versions index the reads and scan the reference genome. One positive aspect of this strategy is that no preprocessing of the reference genome is required. However, other mapping strategies beyond all-mapping, e.g. mapping by strata, cannot be efficiently implemented. Moreover, the program exhibit an high memory footprint as it must remember the mapping locations of all input reads until the whole reference genome has been scanned.

5.4.6 mr(s)Fast

The tools mrFast [Ahmadi *et al.*, 2012] and mrsFast [Hach *et al.*, 2010] are designed to report all mapping locations within a fixed absolute number errors, respectively under the hamming and edit distance, given Illumina/Solexa reads of length ranging from 50 bp to 125 bp. Similarly to RazerS 3, they are based on a full-sensitive filtration method using exact seeds, which turns out to be very weak on mammal genomes.

The peculiarity of their underlying method is a cache-oblivious strategy to mitigate the high cost of verifying clusters of candidate locations. In addition, mrsFast computes the edit distance between one read and one mapping location in the reference genome with an antidiagonal-wise vectorial dynamic programming algorithm, implemented using SIMD instructions.

These tools are as slow as RazerS 3 and appealing for nothing more than all-mapping. They lack multi-threading support and exhibit various bugs. Furthermore, they only accept reads of fixed length and produce files of impractical size.

5.4.7 GEM

The GEM mapper [Marco-Sola *et al.*, 2012] is a flexible read aligner for Illumina/Solexa, ABI/SOLiD, and Ion Torrent reads. It is full-sensitive and can be configured either as an

all-mapper, as a best/unique-mapper, or to search by strata.

GEM uses a combination of state of the art approximate string matching methods, e.g. approximate seeds and suffix filters. The program indexes the reference genome with an FM-index, tries to find an optimal filtration scheme per read, and verifies candidate locations using Myers algorithm. Paired-reads are either mapped independently and then combined, or left/right are mapped and their mates verified using an online strategy.

Unfortunately the tool lacks direct SAM output, it is not open source, and provides many obscure parameters.

	platform				strategy			method			index	
	Illumina	Ion	454	SOLiD	best	strata	all	alignment	optimal	algorithm	type	reference reads
Bowtie	≤ 50	✓	✗	✓	✓	✓	•	mismatches	✗	backtracking	FM-index	✓
Bowtie 2	≥ 75	✓	✓	✗	✓	•	•	local	✗	exact seeds	FM-index	✓
BWA	≤ 100	✗	✗	✗	✓	✗	•	indels	✗	backtracking	FM-index	✗
BWA-SW	✗	✓	✓	✗	✓	✗	✗	local	✗	backtracking	FM-index	✓
Soap 2	≤ 75	✗	✗	✗	✓	✓	•	mismatches	✗	backtracking	FM-index	✗
RazerS	≥ 50	✗	✗	✗	•	•	✓	indels	✓	q -grams	q -gram index	✓
RazerS 3	≥ 50	✓	✗	✗	•	•	✓	indels	✓	exact seeds	q -gram index	✓
SHRiMP 2	✓	✓	✓	✓	✓	•	•	local	✗	q -grams	q -gram index	✗
mrsFast	≤ 75	✗	✗	✗	•	✗	✓	mismatches	✓	exact seeds	q -gram index	✓
mrFast	≤ 125	✗	✗	✗	•	✗	✓	indels	✓	exact seeds	q -gram index	✓
GEM	✓	✓	✗	✓	✓	✓	✓	indels	✓	apx seeds	FM-index	✗
Masai	✓	✗	✗	✗	✓	•	✓	indels	✓	apx seeds	generic	✓
Yara	✓	✓	✗	✗	✓	✓	✓	indels	✓	apx seeds	generic	✗

In this chapter we present our first attempt to engineer an efficient all-mapper. When we started this project, in October 2011, the fastest all-mappers (mrFast and RazerS 3) were two order of magnitude slower than prominent best-mappers (Bowtie and BWA). On one hand, all-mappers were using filtration based on exact seeds, which is fine for short reference genomes but becomes too weak for mammal genomes; clearly, a stronger filtration method would have been beneficial. On the other hand, best-mappers were based on heuristic backtracking, which was becoming inadequate to map reads of increasing length. After a thorough literature review, we came out with a novel read mapping method combining seed-based filtering with backtracking, that we published in [Siragusa *et al.*, 2013].

In the engineering section, we see how our filtration method works, which data structures we adopt for indexing, and how we perform seed extension. In particular, our filtration method is based on exact or approximate seeds: by employing approximate seeds instead of exact seeds, we obtain a stronger filter for long reference genomes, which is still non-heuristic and quasi full-sensitive. We find approximate seeds by backtracking the index of the reference genome. Moreover, we speed up the backtracking phase by searching all seeds simultaneously, with the help of an additional index and the multiple backtracking algorithm. Lastly, we improve our method to perform best-mapping in a more efficient way.

Our method is packaged in a C++ tool nicknamed *Masai*, which stands for *multiple backtracking of approximate seeds on a suffix array index*. Masai is part of the SeqAn library, it is distributed under the BSD license and can be downloaded from <http://www.seqan.de/projects/masai>.

In the evaluation section, we extensively compare Masai with popular read mappers, both on simulated and real datasets. Compared to all-mappers mrFast and RazerS 3, Masai is an order of magnitude faster and has comparable sensitivity. In addition, Masai as a best-mapper is 2–4 times faster and more accurate than Bowtie 2 [Langmead and Salzberg, 2012] and BWA [Li and Durbin, 2009]. Finally, we discuss the limitations of Masai that led us to engineer Yara, yet another read aligner.

6.1 Engineering

We start by giving an outline of the read mapping method of Masai. Later, we give a detailed explanation of each mapping step, explaining and motivating relevant engineering choices that led us to the final implementation.

Masai requires an index capable of simulating a top-down traversal of the suffix trie of the reference genome. We give to the user the possibility to choose among various indices (see section 6.1.2). Similarly to all read mappers relying on an index of the reference genome, we index the reference genome only once, store it on disk and reuse it for all subsequent read mapping jobs.

At mapping time, Masai requires two parameters to be provided: a maximum number of errors per read and a minimum seed length. Default parameters work well for actual Illumina reads, otherwise the user has to parametrize adequately the tool for optimal performance. Nonetheless, independently of the chosen parameterization, filtration is guaranteed to be quasi full-sensitive (see section 6.1.1).

We partition all reads (and their reverse complements) in non-overlapping seeds; subsequently we arrange all seeds in a conceptual *trie*. Using our *multiple backtracking* algorithm, we backtrack simultaneously all indexed seeds in the suffix trie of the reference genome. We perform seed extension on all hits reported by the multiple backtracking algorithm; we extend both ends of each seed using a banded version of *Myers bit-vector algorithm* [?] (details in section 6.1.3).

6.1.1 Filtration

Our original intent was to improve the speed of our all-mapper RazerS [Weese *et al.*, 2009] while preserving full-sensitivity under the edit distance. RazerS was based on a q -gram filter; we were aware that gapped q -grams could have brought a huge speedup, but we could not see any straightforward generalization of gapped q -grams to the edit distance. At the same time, we experienced that weaker but quicker filtration using exact seeds was more advantageous than filtration using q -grams (indeed, a typical Illumina read mapping setup requires only moderate error rates, in the range of 4–6 %). Thus RazerS 3 [Weese *et al.*, 2012] went back to filtration with exact seeds (similarly to mr-Fast). Nonetheless, we wanted to improve again filtration specificity, as the runtime of RazerS 3 on mammal genomes became dominated by verifications, and we knew that to improve filtration specificity we had to increase the seed length, as these two things are strongly correlated.

While reviewing past literature in the field of approximate string matching, we rediscovered the works of Myers, Navarro and Baeza-Yates on approximate seeds, providing stronger filtration than exact seeds while preserving full-sensitivity under the edit distance. Their idea is to partition the pattern into $s \leq k + 1$ non-overlapping seeds, which obviously can be longer than exact seeds but have to be searched within distance $\lceil k/s \rceil$ (see section ??).

Following [Navarro and Baeza-Yates, 2000], we decided to find approximate seeds by backtracking the suffix trie of the reference genome (in section 6.1.2 we recall our engi-

neering work to find approximate seeds efficiently). For simplicity, we decided to find approximate seeds only under the hamming distance. For this reason, when resorting to approximate seeds, Masai does not attain strict full-sensitivity under the edit distance. Nonetheless, in section ?? we show that such implementation detail sacrifices less than 1% sensitivity.

Then, we slightly improved the filtration lemma of [Navarro and Baeza-Yates, 2000]: we search $(k \bmod s) + 1$ seeds within distance $\lfloor k/s \rfloor$ and the remaining seeds within distance $\lfloor k/s \rfloor - 1$. To prove full-sensitivity it suffices to see that, if none of the seeds occurs within its assigned distance, the total distance must be at least $s \cdot \lfloor k/s \rfloor + (k \bmod s) + 1 = k + 1$. Hence all approximate occurrences will be found.

Finally, we chose to parameterize our filter by the seed length rather than by the number of seeds. Clearly, these two parameterization are dual: if we choose the number of seeds to be s , the minimum seed length l has to be $\lfloor |r|/s \rfloor$; vice versa, if we fix the minimum seed length to l , the number of seeds s has to be $\lfloor |r|/l \rfloor$. Nonetheless we prefer the latter, as the minimum seed length gives us a direct estimate of the expected number of verifications produced by the filter. The resulting filter is flexible, indeed by increasing l filtration becomes more specific at the expense of a higher filtration time.

The optimal seed length l depends on the reference genome as well as on read length and the absolute number of errors. We experimentally evaluated filtration with exact and approximate seeds (see section ??). When mapping current Illumina reads on short to medium length genomes, exact seeds are still more efficient than approximate seeds. Conversely, on larger genomes (e.g. mammalian genomes) approximate seeds outperform exact seeds by an order of magnitude.

Best-mapping

Masai is a tool designed primarily to perform all-mapping rather than best-mapping. In best-mapping, Masai simply reports the first optimal mapping location encountered per read. Clearly, this policy makes sense if the edit distance is effective at identifying original mapping locations. Section ?? shows that Masai is competitive in best-mapping with tools using more complex scoring schemes. Nonetheless, Masai's best-mapping method is ad-hoc and limited. In best-mapping, Masai does not produce mapping qualities, it does not even support paired-end and mate-pair protocols. The reader is thus referred to the next chapter (section 7.1) for the complete description of an efficient best-mapping method that, in standard scenarios, is an order of magnitude faster than all-mapping.

6.1.2 Indexing

Within the SeqAn library, we initially disposed of two indices capable of simulating a top-down suffix trie traversal: the enhanced suffix array (ESA) [?] and the lazy suffix tree (LST) [?]. To improve the efficiency of Masai, we implemented a generic top-down traversal for some additional indices, namely the suffix array (SA) [Manber and Myers, 1990], the q -gram index, and various flavours of the full-text minute index (FM-index) [Ferragina and Manzini, 2001]. Below we discuss the performance of these indices in our

specific application, while we refer the reader to chapter 3 for their extensive explanation.

Indexing the reference genome

We initially chose the ESA over LST because of better construction times. Indeed, we dispose of a linear time construction algorithm for the ESA (an adaptation of the DC7 algorithm [?] to multiple sequences [Weese, 2013] for the generalized SA, followed by the algorithms proposed in [?]), while our LST construction algorithm takes quadratic time (using the radix sort based *wotd*-algorithm [?]). Apart from that, both our ESA and LST implementations require 13 bytes per base pair and exhibit comparable query speed. Thus, for the human reference genome (GRCh38), we had a suffix trie constructed in about 1.5 hours and consuming 39 GB of memory (see figure ??).

At this point, Masai required high-end hardware to process large reference genomes. Therefore, thinking of a space-time trade-off, we designed a generic suffix trie top-down traversal for the SA (see section ??); indeed, the SA consumes only 5 bytes per base pair but is theoretically slower than the ESA, as it adds a logarithmic factor to query times. However, with surprise we found out that, within our application, the SA had equal or better performance than the ESA (see figure ??). Ultimately, we brought down the memory footprint of the index from 39 GB to 15 GB but preserved query speed.

We tried to further improve query speed by removing the logarithmic factor introduced by the SA. Therefore, to cut the most expensive binary searches, we put a q -gram index on top of the SA and extended our generic suffix trie top-down traversal accordingly (see section ??). Yet, the q -gram index did not bring significant speedup to our application; indeed, the lookup table turned out to be useful when searching patterns one by one, but not when coupled with our multiple backtracking algorithm as it performs a factorization of the top-down traversal.

Finally, we explored additional space-time trade-offs. We started implementing¹ a generalized FM-index based on a wavelet tree [?]. Our initial FM-index consumed about 1.5 bytes per base pair with a SA sampling of 10 %. Thus the memory footprint of the index went down to 4.5 GB, but Masai became significantly slower (less than twice as slow though).

In definitive, we prefer the SA as it provides a good compromise between query speed and memory consumption. Nevertheless, we leave to the user the possibility to choose among the aforementioned data structures.

Indexing the reads

In order to improve index query speed, we designed and implemented an algorithm to search simultaneously many exact or approximate seeds, achieving a speedup of 3–5 times (see section ??). As our multiple search algorithm requires a trie of the seeds, we also engineered an efficient trie implementation.

It was straightforward to reuse our suffix trie implementations to emulate tries. It goes without saying that the easiest way to implement a trie is by means of a partial SA:

¹ Thanks to the master's thesis of Jochen Singer.

we index only the first suffix of each seed in the collection and construct the SA-based trie via quicksort in time $\mathcal{O}(n \log n)$, where n is the number of seeds; then, our top-down traversal based on binary search still works. We adapted the LST in an analogous way: we fill the partial SA as above and then apply the *wotd*-algorithm [?] to construct the trie in linear time.

Quicksorting the SA turned out to be faster than radix sorting the LST but, in our application, the more involved LST data structure payed off at query time (see section ??). Indeed, the LST stores all trie nodes and thus provides node traversal in constant time, while the SA explicitly stores only the leaves and thus internal nodes have to be worked out via binary search. As the memory footprint of the trie is negligible within our application, we chose the LST to perform multiple backtracking of approximate seeds.

When performing multiple backtracking of exact seeds, the LST construction time dominates the overall filtration time (see section ??). Therefore, we decided to resort to the *q-gram index* to emulate a trie in this case: we build a partial *q*-gram index efficiently and in linear time by bucket sort, again considering only the first suffix of each seed in the collection. Such index represents a trie truncated at depth q (which we fixed to 12 in our application). Truncation is only a minor concern: at depth q we continue by applying the single backtracking algorithm on each active node.

6.1.3 Verification

To verify hits reported by the filtration algorithm, we use a banded version of Myers bit-vector algorithm [?]. Myers' algorithm is an efficient DP alignment algorithm [?] for edit distance. Instead of computing DP cells one after another, it encodes the whole DP column in two bit-vectors and computes the adjacent column in a constant number of 12 logical and 3 arithmetical operations. We implemented a bit-parallel version that computes only a diagonal band of the DP matrix and is faster and more specific than the original algorithm by Myers. More details can be found in section ??.

We had already used Myers' algorithm in RazerS 3 [Weese *et al.*, 2012]. However, instead of performing a semi-global alignment to verify a parallelogram surrounding the seed, in Masai we perform a global alignment on both ends of a seed. Given a seed occurring with e errors, we first perform seed extension on the left side within an error threshold of $k - e$ errors. Only if the seed extension on the left side succeeds, we perform a seed extension on the right side within the remaining error threshold. Moreover, we first compute the longest common prefix on each side of the seed and let the global alignment algorithm start from the first mismatching positions. We observed that this approach is up to two times faster than RazerS 3.

6.2 Evaluation

In order to evaluate Masai, we propose three experiments: (i) the Rabema benchmark and (ii) variant detection on simulated data, and (iii) performance on real data.

It should be noted that in this evaluation we are interested on the capability of the

mapper to retrieve the location of a single read without the help of read pairs, which can of course disambiguate mapping locations of the partner.

As references, we use whole genomes of *E. coli* (NCBI NC_000913.2), *C. elegans* (Worm-Base WS195), *D. melanogaster* (FlyBase release 5.42), and *H. sapiens* (GRCh37.p2).

We compare Masai with the best-mappers Bowtie 2, BWA and Soap 2 as well as with the all-mappers RazerS 3, Hobbes, mrFAST and SHRiMP 2. We remark that Bowtie 2, BWA, Soap 2 and SHRiMP 2 rely on scoring schemes taking into account base quality values, while Masai, RazerS 3, Hobbes and mrFAST use edit distance. When relevant, we configured some read mappers with the appropriate absolute number of errors (Masai, mrFAST, Hobbes, Soap 2) or error rate (RazerS 3). In section , we give the exact parameterization for the read mappers considered in our evaluation.

6.2.1 Rabema benchmark on simulated data

We first consider the Rabema benchmark [Holtgrewe *et al.*, 2011] (v1.1) for a thorough evaluation and comparison of read mapping sensitivity. The benchmark contains the categories *all*, *all-best*, *any-best*, *precision*, and *recall*. In the categories *all*, *all-best*, and *any-best* a read mapper has to find all, all of the best, or any of the best edit distance locations for each read. The categories *precision* and *recall* require a read mapper to find the *original* location of each read, which is a measure independent of the used scoring model, e.g. edit distance or quality based. A read is mapped *correctly* if the mapper reports its original location, and it is mapped *uniquely* if the mapper reports only one location. Rabema defines *recall* to be the fraction of reads which were correctly mapped and *precision* the fraction of uniquely mapped reads that were mapped correctly.

Similarly to [Langmead and Salzberg, 2012], we used the read simulator Mason [?] with default profile settings to simulate from each whole genome 100 k reads of length 100 bp having sequencing errors distributed like in a typical Illumina run. We performed the benchmark for an error rate of 5 %, which corresponds to edit distance 5 for reads of length 100 bp. Therefore, we built a Rabema gold standard for each dataset by running RazerS 3 in full-sensitive mode up to edit distance 5. We further classified mapping locations in each category by their edit distance.

For a more fair and thorough comparison, we also consider BWA and Bowtie 2 as all-mappers (Soap 2 cannot be configured accordingly). To this extent, we parametrized these tools to be highly sensitive and output all found mapping locations. Since BWA and Bowtie 2 were not designed to be used as all-mappers, they spent much more time than proper all-mappers, i.e. up to 3 hours in a run compared to several minutes. However, the aim of this experiment is to investigate read mapping sensitivity, therefore we do not report running times. Results for *H. sapiens* are shown in table 6.1.

Best-mappers

Masai shows the best recall values, not losing more than 3.3 % recall on edit distance 5. Conversely, recall values of BWA and Bowtie 2 drop significantly with increasing edit distance and loose up to 15.4 % and 11.5 % on edit distance 5. As expected, Soap 2 turns

Table 6.1: Rabema benchmark results on $100\text{ k} \times 100\text{ bp}$ Illumina-like reads. We show Rabema scores in percent (average fraction of edit distance locations reported per read). Large numbers show total scores in each Rabema category and small numbers show the category scores separately for reads with $\begin{pmatrix} 0 & 1 & 2 \\ 3 & 4 & 5 \end{pmatrix}$ errors.

	method	all	all-best	any-best	precision	recall
best-mappers	Masai	93.26 99.18 98.73 97.93 95.60 85.77 43.60	97.91 97.79 97.88 98.03 97.98 98.20 96.70	99.95 100.00 100.00 100.00 99.98 99.93 98.71	97.79 97.88 97.84 97.79 97.68 97.61 97.93	97.75 97.88 97.84 97.79 97.68 97.56 96.74
	Bowtie 2	92.04 99.18 98.72 96.80 93.44 81.94 40.19	96.16 97.79 97.85 95.80 94.83 93.37 88.86	98.08 100.00 99.96 97.55 96.62 94.93 90.46	96.58 98.01 97.72 95.98 95.19 95.22 94.37	95.94 98.01 97.72 95.55 94.24 92.79 89.52
	BWA	92.18 99.18 98.72 97.81 94.25 80.92 37.65	96.81 97.79 97.87 97.88 96.59 92.63 83.47	98.81 100.00 99.95 99.81 98.55 94.28 85.37	97.50 97.93 97.70 97.37 97.11 97.17 97.57	96.41 97.93 97.69 97.25 95.77 91.98 84.61
	Soap 2	65.93 99.18 95.55 91.34 8.67 0.70 0.00	69.89 97.79 94.74 91.37 8.98 0.79 0.00	71.37 100.00 96.78 93.18 9.21 0.81 0.00	97.69 98.05 97.74 97.73 94.87 84.13 91.67	69.91 98.05 94.62 91.20 11.85 1.41 0.36
all-mappers	Masai	99.90 100.00 100.00 100.00 100.00 99.94 98.58	99.96 100.00 100.00 100.00 100.00 99.93 98.71	99.96 100.00 100.00 100.00 100.00 99.93 98.71	100.00 100.00 100.00 100.00 100.00 100.00 100.00	99.96 100.00 100.00 100.00 100.00 99.93 98.78
	Bowtie 2	95.69 99.98 99.91 99.45 97.99 90.69 55.14	98.85 99.74 99.79 98.61 98.21 97.55 93.84	99.16 100.00 99.98 99.01 98.63 97.94 94.17	99.84 100.00 99.95 99.87 99.64 99.67 99.29	98.54 99.74 99.58 98.27 97.64 96.87 94.40
	BWA	95.89 99.96 99.88 99.49 97.13 87.79 64.11	97.98 98.81 99.01 99.02 97.83 93.95 85.20	98.82 100.00 99.95 99.82 98.56 94.34 85.37	98.12 100.00 100.00 100.00 98.49 98.68 99.56	97.80 99.03 98.96 98.75 97.35 93.43 86.36
	RazerS 3	100.00 100.00 100.00 100.00 100.00 100.00 100.00	100.00 100.00 100.00 100.00 100.00 100.00 100.00	100.00 100.00 100.00 100.00 100.00 100.00 100.00	100.00 100.00 100.00 100.00 100.00 100.00 100.00	100.00 100.00 100.00 100.00 100.00 100.00 100.00
	Hobbes	96.56 99.41 99.00 98.76 97.80 93.20 73.05	97.08 97.23 96.59 97.01 97.38 98.16 97.42	98.01 97.92 97.51 97.96 98.43 99.12 98.46	99.97 99.96 99.97 99.97 99.98 99.95 99.96	96.41 95.49 95.84 96.54 97.03 97.98 97.79
	mrFAST	99.97 100.00 100.00 100.00 100.00 99.99 99.53	99.97 100.00 100.00 100.00 100.00 100.00 99.10	99.97 100.00 100.00 100.00 100.00 100.00 99.13	100.00 100.00 100.00 100.00 100.00 100.00 100.00	99.97 100.00 100.00 100.00 99.99 100.00 99.18
	SHRIMP 2	96.53 99.87 99.82 99.53 98.37 92.58 64.63	99.50 99.34 99.50 99.60 99.64 99.65 98.32	99.85 99.87 99.90 99.91 99.89 99.84 98.57	99.95 100.00 100.00 100.00 99.93 99.89 99.23	99.25 99.35 99.30 99.24 99.30 99.09 98.48

out to be inadequate for mapping reads of length 100 bp at this error rates.

Precision values have less variance than recall values. Masai shows the best precision values with 97.8 %, followed by Soap 2 with 97.7 %, and BWA with 97.5 %. Interestingly, Bowtie 2 shows the worst precision values, losing up to 5.6 % on edit distance 5.

All-mappers

As expected, RazerS 3 shows full-sensitivity and mrFAST loses only a minimal percentage of mapping locations. Overall, Masai does not lose more than 0.1 % of all mapping locations. In particular, Masai is full-sensitive for low-error locations and loses only a small percentage of high-error locations, i.e. its loss is limited to 0.1 % and 1.4 % of mapping locations at edit distance 4 and 5.

Conversely, BWA and Bowtie 2 miss 35 % and 45 % of all mapping locations at edit distance 5 and their recall values as all-mappers do not substantially increase. Likewise, SHRIMP 2 is not able to enumerate all mapping locations, although its recall values are good. Again, Hobbes has the worst performance.

We remark that Masai is not full-sensitive whenever approximate seeds are used, e.g. on *H. sapiens*. Indeed, Masai loses 0.1 % overall sensitivity in respect to RazerS 3. In general, RazerS 3 should be used when full-sensitivity is required, i.e. for read mappers benchmarking. However, our results show that Masai can replace RazerS 3 or mrFAST as an all-mapper in practical setups.

6.2.2 Variant detection on simulated data

The second experiment analyzes the theoretical performance of Masai and other read mappers in genomic variation pipelines. Similarly to [?], we consider simulated reads containing sequencing errors, SNPs and indels, such that each read has an edit distance of

Table 6.2: Variant detection results on $5\text{ M} \times 100\text{ bp}$ Illumina-like reads. We show the percentages of found origins (recall) and fraction of unique reads mapped to their origin (precision) classed by reads with s SNPs and i indels (s, i).

		(0,0)		(2,0)		(4,0)		(1,1)		(1,2)		(0,3)	
method		prec.	recl.	prec.	recl.	prec.	recl.	prec.	recl.	prec.	recl.	prec.	recl.
best-mappers	Masai	98.2	98.2	97.6	97.5	96.8	96.8	97.8	97.2	97.9	97.9	97.2	97.2
	Bowtie 2	97.6	97.3	94.6	92.0	92.6	82.5	95.3	93.3	93.5	92.3	96.1	95.4
	BWA	98.2	97.9	97.6	95.3	94.9	85.1	97.4	90.9	97.1	80.3	96.3	66.5
	Soap 2	98.1	82.9	97.4	31.0	0.0	0.0	90.6	6.2	0.0	0.0	0.0	0.0
all-mappers	Masai	100.0	100.0	100.0	99.9	100.0	100.0	100.0	99.3	100.0	100.0	100.0	100.0
	RazerS 3	100.0	100.0	100.0	100.0	100.0	100.0	100.0	100.0	100.0	100.0	100.0	100.0
	Hobbes	99.9	99.9	99.9	99.9	100.0	100.0	100.0	99.8	100.0	93.6	99.6	90.5
	mrFAST	100.0	99.9	100.0	100.0	100.0	100.0	100.0	100.0	100.0	100.0	100.0	100.0
	SHRiMP 2	100.0	99.4	100.0	99.7	100.0	99.7	100.0	99.5	100.0	99.2	100.0	99.6

at most 5 to its genomic origin. Reads are grouped according to the number of contained SNPs and indels, where class (s, i) consists of all reads with s SNPs and i indels. We say that a read is mapped *correctly* if a mapping location is reported within 10 bp of its genomic origin; it is considered to map *uniquely* if only one location is reported by the mapper. For each class we define *recall* to be the fraction of reads which were correctly mapped and *precision* the fraction of uniquely mapped reads that were mapped correctly.

We simulated 5 million Illumina-like reads of length 100 bp from the whole human genome using Mason. We mapped the reads with each tool and measured its sensitivity in each class. Table 6.2 shows the results of each read mapper by class.

Best-mappers

Among best-mappers, Masai shows the highest precision and recall in all classes. In particular, Masai does not loose more than 3.2 % recall in class (4,0), whether Bowtie 2 and BWA loose respectively 17.5 % and 14.9 % and Soap 2 is not able to map any read.

Interestingly, we observe that recall values of Bowtie 2, BWA and Soap 2 are negatively correlated with the amount of genomic variation. For instance, in the Rabema benchmark, Bowtie 2 looses respectively 7.2 % and 11.5 % of mapping locations at distance 4 and 5, but in class (4,0) of this experiment it looses 17.5 % recall. We observe a similar trend for BWA and Soap 2. The low performance of Soap 2 is also due to its limitation to at most 2 mismatches and no support for indels.

All-mappers

Looking at all-mappers results, Masai shows 100 % precision and recall in all classes, except for classes (2,0) and (1,1) where it looses only 0.1 % and 0.7 % recall. Masai is therefore roughly comparable to the full-sensitive read mappers RazerS 3 and mrFAST. SHRiMP 2 shows 100 % precision in all classes but looses between 0.3 % and 0.8 % recall in each class. Hobbes has the lowest performance among all-mappers: it appears to have problems with indels, indeed it looses 9.5 % recall in class (0,3).

6.2.3 Performance on real data

In the last experiment we focus on comparing read mappers performance on real data. We mapped the first 10 M \times 100 bp reads from an Illumina lane of *E. coli* (ERR022075, Genome Analyzer IIx), *D. melanogaster* (SRR497711, HiSeq 2000), *C. elegans* (SRR065390, Genome Analyzer II), and *H. sapiens* (ERR012100, Genome Analyzer II). Whenever possible we configured the tools to map the reads within edit distance 5.

We measured mapping times on a cluster of nodes with 72 GB RAM and 2 Intel Xeon X5650 processors running Linux 3.2.0. For an accurate running time comparison, we ran the tools using a single thread and used local disks for I/O. We measured running times, peak memory consumptions, mapped reads and Rabema any-best scores.

We cannot measure precision and recall values as real reads have unknown origins. Therefore, for this evaluation, we adopt the commonly used measure of percentage of *mapped reads*, i.e. the fraction of reads for which the read mapper reports a mapping location. However, as some mappers report mapping locations without constraints on the number of errors, we also include Rabema *any-best* scores. We recall that the Rabema any-best benchmark assigns a point for a read if the mapper reports at least one mapping location with the optimal (minimum) number of errors; final Rabema any-best scores are normalized by the number of reads.

Results for *C. elegans* and *H. sapiens* are shown in table 6.3.

Best-mappers

On the *C. elegans* dataset, Masai is 7.7 times faster than Bowtie 2, 8.2 times faster than BWA and 1.5 times faster than Soap 2. On the *H. sapiens* dataset, Masai is 2.6 times faster than Bowtie 2, 3.6 times faster than BWA but 2.1 times slower than Soap 2.

On one end, Soap 2 is not able to map a consistent fraction of reads because of its limitation to 2 mismatches. On the other end, Bowtie 2 reports more mapped reads than Masai but, taking any-best scores into account, it reports less mapping locations than Masai. In fact, Bowtie 2 uses a scoring scheme based on quality values and does not impose a maximal error rate threshold. On the *C. elegans* and *H. sapiens* datasets, Bowtie 2 misses respectively 22.0 % and 20.7 % of reads mappable at edit distance 5.

All-mappers

On the *C. elegans* dataset Masai is 2.0 times faster than RazerS 3, 10.9 times faster than Hobbes, 6.3 times faster than mrFAST and 50.1 times faster than SHRiMP 2. Hobbes constantly crashes and maps less reads than all other mappers in this category.

On the *H. sapiens* dataset Masai is 11.9 times faster than RazerS 3, 14.6 times faster than mrFAST, and 7.6 times faster than Hobbes. We note that the current version of Hobbes constantly crashes and maps only half of the reads. SHRiMP 2 is not able to map the *H. sapiens* dataset within 4 days.

Likewise for Bowtie 2, also SHRiMP 2 does not impose a maximal error rate threshold and reports more mapped reads than Masai. However, its Rabema any-best score is inferior to Masai. This could be due to the use of a different scoring scheme where two

Table 6.3: Performance on real data using $10\text{ M} \times 100\text{ bp}$ Illumina reads.

Rabema any-best: in large we show the percentage of reads mapped with the minimal number of errors (up to 5%) and in small the percentage of reads that were mapped with $\begin{pmatrix} 0 & 1\% & 2\% \\ 3\% & 4\% & 5\% \end{pmatrix}$ errors.

Mapped reads: in large we show the percentage of mapped reads and in small the cumulative percentage of reads that were mapped with $\begin{pmatrix} 0 & 1\% & 2\% \\ 3\% & 4\% & 5\% \end{pmatrix}$ errors.

Remarks: SHRiMP 2 is not able to map the *H. sapiens* dataset within 4 days; Hobbes constantly crashes and is not able to map completely nor the *C. elegans* nor the *H. sapiens* dataset.

dataset		SRR065390 C. elegans				ERR012100 H. sapiens			
		time	memory	Rabema any-best	mapped reads	time	memory	Rabema any-best	mapped reads
method		[min:s]	[Mb]	[%]	[%]	[min:s]	[Mb]	[%]	[%]
best-mappers	Masai	3:10	2936	100.00	89.49	22:35	19711	99.99	93.76
	Bowtie 2	24:14	135	99.21	92.58	57:41	3180	99.45	96.72
	BWA	25:53	325	99.33	89.33	80:58	4475	99.54	93.53
	Soap 2	4:37	748	95.98	85.95	11:11	5357	95.66	89.73
all-mappers	Masai	10:49	2821	100.00	89.49	307:16	20130	100.00	93.76
	RazerS3	21:18	11489	100.00	89.49	3653:03	17298	100.00	93.77
	Hobbes	117:46	3885	89.77	80.34	2319:27	71685	59.02	55.35
	mrFAST	67:41	875	99.99	89.49	4462:25	929	99.98	93.75
	SHRiMP 2	541:20	2735	98.51	91.91	–	–	–	–

mismatches cost less than opening a gap. Anyway, this hypothesis does not explain why SHRiMP 2 does not report some mapping locations at distance 0.

6.2.4 Filtration efficiency

Here we assess the contribution of approximate seeds and multiple backtracking on run-time results. To this intent we performed all-mapping with Masai on each previously considered dataset, this time using either exact or approximate seeds in combination with either single or multiple backtracking. Table 6.4 shows the results. Filtration time consists of the time spent to index the seeds (in case of multiple backtracking) and to perform backtracking. Candidates reports the number of candidate locations reported by the filter for which seed extension is subsequently performed. In bold we show the optimal combination of seeding and backtracking that we used to parameterize Masai.

Since we concentrate on filtration, we do not consider the time spent performing seed extensions and I/O, i.e. loading the reference genome and its index, loading the reads, writing the results. Such time is independent of any combination of seeding or backtracking and can be extrapolated by subtracting bold filtration times of table 6.4 from respective Masai all-mappers times of table 6.3 and table ??.

On *E. coli*, *D. melanogaster* and *C. elegans* approximate seeds reduce the number of candidates respectively by 2.1 times, 9.9 times, and 4.3 times. Nevertheless we still prefer exact seeds as filtration dominates the total runtime. Multiple backtracking on exact seeds compared to single backtracking speeds up filtration by 2.9 times on *E. coli*, and

3.8 times on *D. melanogaster* and *C. elegans*. Without the contribution of multiple backtracking Masai would not be faster than RazerS 3, the second fastest all-mapper.

Approximate seeds become effective on *H. sapiens*, where they reduce the number of candidates by 10.8 times. On *H. sapiens* seed extensions largely dominate the total runtime, therefore we prefer approximate seeds. Multiple backtracking on approximate seeds provides a speed-up of 3.2 times over single backtracking. The combination of the two methods makes Masai an order of magnitude faster than any other all-mapper.

Table 6.4: Masai filtration efficiency results for all-mapping. Filtration time is given as [min:s] and includes seeds indexing time.

organism	dataset	seeding	backtracking	filtration time	candidates
E. coli	ERR022075	exact	single	3:55	69.17 M
E. coli	ERR022075	exact	multiple	1:20	69.17 M
E. coli	ERR022075	approximate	single	38:42	33.08 M
E. coli	ERR022075	approximate	multiple	9:00	33.08 M
D. melanogaster	SRR497711	exact	single	8:15	1020.28 M
D. melanogaster	SRR497711	exact	multiple	2:11	1020.28 M
D. melanogaster	SRR497711	approximate	single	100:18	102.78 M
D. melanogaster	SRR497711	approximate	multiple	20:48	102.78 M
C. elegans	SRR065390	exact	single	8:25	1065.70 M
C. elegans	SRR065390	exact	multiple	2:11	1065.70 M
C. elegans	SRR065390	approximate	single	102:02	246.65 M
C. elegans	SRR065390	approximate	multiple	21:33	246.65 M
H. sapiens	ERR012100	exact	single	55:54	294943.86 M
H. sapiens	ERR012100	exact	multiple	41:52	294943.86 M
H. sapiens	ERR012100	approximate	single	165:45	27396.01 M
H. sapiens	ERR012100	approximate	multiple	52:15	27396.01 M

6.3 Discussion

Masai consists of three important algorithmic methods: (i) approximate seeds, (ii) multiple backtracking and (iii) greedy filtration. Approximate seeds are of paramount importance to obtain very specific yet full-sensitive filtration; their adoption speeds up Masai by one order of magnitude. Multiple backtracking further speeds up the filtration phase by 3–5 times on a (enhanced) suffix array index; this technique makes Masai twice as fast. Greedy filtration prioritizes analysis of optimal mapping locations; because of this method, Masai in best-mapping is an order of magnitude faster than in all-mapping.

Is the edit distance sufficient to perform best-mapping? Both Rabema benchmark and variant detection results show that Masai has constantly better accuracy than other best-mappers relying on more complex scoring schemes. In particular, the Rabema benchmark results show that Rabema any-best values are tightly bound to recall values. Hence,

the edit distance is a pertinent and adequate scoring scheme for best-mapping. Vice versa, best-mappers using scoring schemes based on quality values show a generalized and substantial loss of mapping accuracy. This is likely due to the heuristics on which these tools rely. To sum up, it is better to stick to edit distance and guarantee full-sensitivity rather than to adopt an involved scoring scheme and explore the alignment space heuristically, hence partially.

How many mapping locations do heuristic best-mappers miss? By looking at precision and recall values on simulated data, or at Rabema any-best values on real data, it can be deduced that Bowtie 2, BWA and Soap 2 miss up to 20 % of reads mappable at 5 % error rate. Yet, it is not evident how these results affects variant calling pipelines.

Summing up, Masai as an all-mapper is an order of magnitude faster and thus a valid alternative to tools like RazerS 3 and mrFast. Computational requirements of all-mapping now become close to those of best-mapping: Masai as an all-mapper is only 4 times slower than BWA, despite reporting two orders of magnitude more mapping locations. Masai as a best-mapper is 2–4 times faster and more accurate than Bowtie 2 [Langmead and Salzberg, 2012] and BWA [Li and Durbin, 2009]. The achieved speedup is huge when RazerS 3 has to be used as a best-mapper: in this scenario, Masai is roughly 200 times faster!

Despite the good results, Masai is not being widely used. This is mainly because it lacks some commonly requested features, including: parallelization via multi-threading, low memory footprint, direct support of paired-end or mate-pair protocols, computation of mapping qualities, automatic parameterization. Because of initial inexperience and unclear (or wrong) goals, I neglected these requirements while designing the tool. The next chapter introduces *Yara*, yet another read aligner, a tool fulfilling these requirements.

Yara (Yet another read aligner) is an exhaustive, non-heuristic read mapper, capable of quickly reporting all stratified mapping locations within a given error rate. *Yara* offers parallelization via multi-threading, has a low memory footprint by using the FM-index, directly supports paired-end or mate-pair protocols, computes accurate mapping qualities, does not require ad-hoc parameterization and works on Illumina or Ion Torrent reads.

7.1 Engineering

7.1.1 Ad-hoc filtration

Specific yet rapid filtration is fundamental in the design of an efficient read mapping tool. Read mappers like RazerS3 [Weese *et al.*, 2012] and mrFast [Ahmadi *et al.*, 2012] are designed around naïve filtration with exact seeds. This filtration method is always very quick, however it is not specific enough on long, repetitive reference genomes like the human genome. Masai [Siragusa *et al.*, 2013] circumvents this problem by enforcing a minimum seed length, whose optimal value must be tuned for a specific reference genome, and eventually resorting to approximate seeds in order to guarantee full-sensitivity. This filtration method speeds up Masai by an order of magnitude but is still rough: it needs external parametrization, lacks flexibility and is suboptimal in practice.

Yara applies an ad-hoc filtration scheme *per read*. Under any fixed filtration scheme, the number of verifications per read is not uniform: within a typical mapping, most reads produce very few verifications and are easily mappable, while a few others are problematic and often not even confidently mappable to one single location. Consequently, any fixed filtration scheme turns out to be too weak for some reads yet too strong for others, thus suboptimal in practice. An ad-hoc filtration scheme per read improves filtration efficiency by optimizing the ratio between filtration speed and specificity. *Yara* thus automatically chooses an ad-hoc filtration scheme per read, without requiring manual parameterization by the user.

Ad-hoc filtration works as follows. *Yara* initially applies filtration with exact seeds to all reads. The tool counts the number of verifications to be performed for each read, thus decides if it is worth proceeding with the verification phase or alternatively applying a stronger filtration scheme. This decision depends on fine-tuned internal verification thresholds. Under standard Illumina setups, exact seeds provide efficient filtration for

up to 70–80 % of the reads; on the remaining reads, a filtration scheme using 1- or 2-approximate seeds works better. Thus, Yara starts with the quickest filtration scheme and becomes more specific whenever it pays off to do so.

7.1.2 Stratified filtration

All-mapping methods consider a set of relevant mapping locations per read. Yet, this definition leaves open what relevant means. In all-mapping under the edit distance, the user defines relevant mapping locations by imposing a distance threshold. Despite being sound, this definition does not work well in practice. On the one hand a very low threshold leaves a consistent fraction of the reads unmapped, on the other hand a moderate threshold produces a deluge of mapping locations for some reads. In practice, at 5 % error rate, Illumina reads map to hundreds of mapping locations on the human genome. It is questionable whether all these locations are relevant for the downstream analysis. Thus, a finer definition of all-mapping relevance is necessary in practice.

Stratification of mapping locations yields an equally sound yet practical definition of all-mapping under the edit distance. The *e*-stratum

$$S(r, e) = \{(i, j, e) : d_E(g_{i...j}, r) = e\} \quad (7.1)$$

denotes the set of all mapping locations of a read r at edit distance e from the reference genome g . According to the above definition, conventional all-mapping under the edit distance defines the set

$$S(r, 0) \cup S(r, 1) \cup \dots \cup S(r, k) \quad (7.2)$$

as relevant mapping locations within an *absolute* error threshold k . Stratified all-mapping refines this definition by considering only mapping locations being co-optimal, or sub-optimal up to a certain degree. Formally, if the distance of any optimal mapping location for read r is

$$e^* = \min \{e \in [0, k] : S(r, e) \neq \emptyset\} \quad (7.3)$$

stratified all-mapping considers mapping locations

$$S(r, e^*) \cup \dots \cup S(r, \min \{e^* + l, k\}) \quad (7.4)$$

within a *relative* error threshold l to be relevant.

Yara significantly improves the runtime of stratified all-mapping over conventional all-mapping. Obviously, the most straightforward way to achieve stratified all-mapping consists into performing conventional all-mapping and subsequently filtering out any irrelevant mapping location. For instance, RazerS 3 implements this method and gets no speedup. Another naïve method consists into applying up to k rounds of conventional all-mapping, with filtration schemes for thresholds going from 0 to $\min \{e^* + l, k\}$. It is easy to see that also this method performs redundant computation: the total work for any read mapping at distance greater or equal to k corresponds to the sum of all k filtration schemes.

The following stratified all-mapping method, adopted by Yara, guarantees not to perform more work than conventional all-mapping. Indeed, the key idea is to simply reduce any filtration scheme full-sensitive within distance k to be full-sensitive within distance $\min\{e^* + l, k\}$. Given any filtration scheme full-sensitive within distance k , with s seeds having thresholds $\mathbb{k} = (k_1, \dots, k_s)$, any subset consisting of $s^* < s$ seeds with thresholds $\mathbb{k}^* = (k_1^*, \dots, k_{s^*}^*)$ is full-sensitive within distance $\min\{e^* + l, k\}$ if it satisfies

$$s^* + \sum \mathbb{k}^* > \min\{e^* + l, k\}. \quad (7.5)$$

The proof is analogous to that one given in section ??.

Example 7.1. Let $k = 5$ be the absolute threshold, and $l = 0$ be the relative threshold, restricting relevant locations to co-optimal ones. A read r maps at distance 1, i.e. $|S(r, 0)| = 0$, $|S(r, 1)| > 0$ thus $e^* = 1$. Given the filtration scheme $\mathbb{k} = (1, 1, 1)$, any subset full-sensitive up to distance $\min\{e^* + l, k\} = 1$ finds all relevant mapping locations, i.e. all subsets of \mathbb{k} are: $(0, 0, -)$, $(0, -, 0)$, $(-, 0, 0)$, $(1, -, -)$, $(-, 1, -)$, $(-, -, 1)$ are full-sensitive. Thus, verification of all candidates, produced by *any* two exact seeds or one 1-approximate seed, yields all mapping locations in the 1-stratum of r .

In addition, Yara implements a simple greedy strategy to minimize the number of verifications to find all relevant stratified mapping locations. As candidate locations can be verified in any order, Yara chooses the ordering of seeds producing the minimum number of verifications. The tool first finds all seeds and ranks them by number of candidate locations produced. Then it processes all candidate locations, from the least to the most frequent seed, until it explores l strata from the first non-empty one, or until it attains the absolute distance threshold k .

Yara performs best-mapping by means of stratified filtration. Best-mapping requires one primary mapping location along with its confidence. Under the edit distance, without any further assumptions, any co-optimal location is equally likely to be correct. Thus, Yara performs stratified all-mapping with a relative threshold $l = 0$, picks one random co-optimal location, and subsequently estimates its mapping quality using all found mapping locations (see section 7.1.4). Because of this method, Yara in best-mapping is an order of magnitude faster than in conventional all-mapping.

7.1.3 Paired-end and mate-pair protocols

Paired-end and mate-pair protocols are the sequencing protocols of choice of Illumina instruments. Reads are sequenced in pairs from both ends of the same insert. Properly paired reads are expected to map within the insert size adopted in the sequencing protocol. The lack of any proper pair of mapping locations signals a potential structural variation, e.g. a long indel or an inversion. Thus, the added information of an expected insert size allows a read mapper to map read pairs to their original locations more confidently than in the single-end protocol. Nonetheless, a read mapper should report equally important unpaired mapping locations.

In the paired-end or mate-pair workflows, Yara maps paired reads independently, exactly as in the single-end workflow, and reports all relevant mapping locations per read. However, in addition to the single-end workflow, Yara implements a finer strategy to choose primary mapping locations. For any reads pair, among all pairs of co-optimal mapping locations, the tool selects the one with minimal deviation from the expected insert size. Since Yara outputs all relevant mapping locations, the choice of primary locations can be always corrected a posteriori.

7.1.4 Mapping qualities

Yara computes mapping qualities using the number of mapping locations stratified by error rate.

7.1.5 Indexing

Yara uses an efficient FM-index specialization for the DNA alphabet, based on interleaved rank dictionaries (see section ??). This interleaved FM-index exhibit a fourfold speedup over the first FM-index implementation bundled with Masai. Surprisingly, the interleaved FM-index is also faster than any other index, both in exact and approximate search (see figure ??). Moreover, this index consumes only 1.23 bytes per base pair with a SA sampled at 10 %, thus its memory footprint is 3.7 GB for the human genome. Under these terms, there is no indexing space-time trade-off: the FM-index always provides the most convenient suffix trie implementation.

Yara does not use multiple search algorithms of section ?? to search seeds on the FM-index. These algorithms work according to a *cache-friendly* memory access pattern, which holds for forward search but not for backward search. Using forward search, navigation in a suffix trie becomes less expensive as it proceeds towards bottom nodes. Indeed, navigation towards a child node involves the computation of a subinterval of the current suffix array interval; such computation accesses memory locations within the current interval, that have good chances to be in the cache. Conversely, using backward search, navigation becomes more expensive as it proceeds deeper in the trie; navigation downwards involves the computation of intervals outside of the current one, unlikely to be in the cache as they are accessed less often than top intervals. As multiple backtracking factorizes the navigation of top nodes, it pays off with forward search rather than with backward search. Hence, on the FM-index, it is always faster to search exact queries in a naïve way and approximate queries simply sorted in lexicographical order (see figure ??).

7.2 Evaluation

The evaluation consists of three experiments: (i) accuracy on simulated data, (ii) Rabema benchmark on simulated and real data, and (iii) throughput on real data. In each experiment, I compare Yara in best-mapping with GEM, Bowtie 2 and BWA, while in all-mapping with GEM, RazerS 3, and Hobbes 2.

7.2.1 Experimental setup

Read mappers parametrization

In appendix B.2, I give the exact parametrization of each read mapper considered in the evaluation. Whenever possible, I configured the tools with the appropriate error rate (Yara, GEM, RazerS 3) or absolute number of errors (Hobbes 2). When processing paired-end reads, I provided the tools with appropriate insert size information.

Infrastructure

All tools run on a desktop computer running Linux 3.10.11, equipped with one Intel Core i7-4770K CPU @ 3.50 GHz, 32 GB RAM and a 2 TB HDD @ 7200 RPM. For maximum throughput, all tools run using eight threads. For accurate running time comparisons, I disabled Intel Turbo Boost; therefore, real throughputs might be slightly lower than the measured ones.

Datasets

The reference in all experiments is the human whole genome (GRCh38).

The simulated data consists of 1 M Illumina-like 2×100 bp paired-end reads, simulated from the reference genome using Mason [?]. The mean insert size is $INS = 175$ and the deviation $ERR = 225$.

The real data is a publicly released sequencing run (SRA/ENA id: ERR161544) by the Beijing Genome Institute; the genomic DNA used in this study came from an anonymous male Han Chinese individual who has no known genetic diseases. This dataset consists of 2×100 bp whole genome sequencing reads, produced by an Illumina HiSeq 2000 instrument. BWA reports mean insert size $INS = 178$ and deviation $ERR = 200$.

7.2.2 Accuracy on simulated data

I introduce an *accuracy benchmark* to measure read mappers accuracy of finding the *original* location of simulated reads. This benchmark considers for each read only the *first primary mapping location* encountered while scanning the SAM file [?] produced by each tool; this policy mimics the behavior of de-facto standard *best-mapping analysis pipelines*, e.g. the GATK [DePristo *et al.*, 2011]. This accuracy benchmark counts a simulated read as *correctly mapped* if the found mapping location corresponds to its original location, it computes the *recall* of each tool as the fraction of correctly mapped reads and the *precision* as the fraction of mapped reads that are correct; for a thorough evaluation, it also classes all simulated reads by the *error rate* of their original locations, then computes recall and precision within each error rate class.

I repeated this experiment twice: first providing the simulated reads as unpaired, then as paired-end with additional insert size information. Results are shown in table 7.1.

Table 7.1: Accuracy results on the human whole genome. The left panel shows the results of mapping 1 M Illumina-like 2×100 bp reads as unpaired; the right panel shows the results of mapping the same reads as paired-end, providing additional insert size information. Big numbers show total scores, while small numbers show marginal scores for the reads at $\begin{pmatrix} 0 & 1 & 2 \\ 3 & 4 & 5 \end{pmatrix}$ % error rate.

		hiseq_hg19_like_se						hiseq_hg19_like_pe									
		H. sapiens SE						H. sapiens PE									
tool		recall			precision			recall			precision						
best	Yara	97.67	97.70 97.32	97.62 97.76	97.57 97.03	97.67	97.70 97.32	97.62 97.82	97.57 97.19	98.50	98.55 97.90	98.42 98.51	98.28 97.61	98.55 97.90	98.42 98.56	98.28 97.77	
	Gem	97.65	97.69 96.54	97.56 96.86	97.56 97.20	97.65	97.69 96.56	97.56 96.91	97.56 97.20	98.50	98.54 97.49	98.48 97.71	98.34 98.43	98.50 97.49	98.48 97.71	98.34 98.43	
	Bowtie 2	97.56	97.70 94.27	97.61 94.68	95.60 95.80	97.59	97.70 95.13	97.61 95.44	96.01 96.35	98.46	98.50 97.58	98.47 96.59	98.08 97.53	98.50 97.74	98.47 96.96	98.12 98.17	
	BWA	97.53	97.69 90.86	97.58 76.53	97.28 68.01	97.64	97.69 96.30	97.58 95.80	97.35 97.40	98.39	98.54 91.56	98.47 77.06	98.19 68.34	98.50	98.54 97.05	98.47 96.47	98.26 97.87
all	Yara	97.67	97.70 97.18	97.61 97.50	97.61 96.95	97.67	97.70 97.18	97.61 97.55	97.61 97.11	98.50	98.55 97.90	98.42 98.56	98.27 97.61	98.50	98.55 97.90	98.42 98.62	98.27 97.77
	Gem	97.65	97.70 96.59	97.57 96.86	97.58 97.20	97.65	97.70 96.59	97.57 96.91	97.58 97.20	98.50	98.53 97.41	98.45 97.66	98.35 98.43	98.50	98.53 97.41	98.45 97.66	98.35 98.43
	Hobbes 2	98.34	98.38 97.56	98.29 97.76	98.20 97.77	90.00	89.63 91.83	90.68 94.01	91.74 95.18	89.22	89.10 89.41	89.46 87.33	89.99 84.09	89.92	89.60 91.92	90.47 93.72	91.53 96.41
	RazerS 3	91.00	90.52 94.01	91.90 96.11	93.14 96.87	91.00	90.52 94.01	91.90 96.11	93.14 96.87	94.13	93.95 95.40	94.48 96.38	94.95 92.75	94.17	93.98 95.53	94.51 96.79	94.99 97.74

7.2.3 Rabema benchmark on simulated and real data

The *Rabema benchmark* [Holtgrewe *et al.*, 2011] (v1.1) measures read mappers sensitivity of finding *relevant* mapping locations of simulated or real reads. This experiment considers the Rabema benchmark category *all* for all-mappers and *all-best* for best-mappers. In the category *all*, Rabema counts as relevant, for each read, all mapping locations within a maximal error rate; in the category *all-best* it considers just co-optimal mapping locations. Rabema computes the *sensitivity* of each tool as the fraction of relevant mapping locations found per read. Analogously to the accuracy benchmark, Rabema classes mapping locations by their *error rate*, then computes sensitivity within each error rate class. The benchmark reports percentual scores normalized by the number of reads.

I applied the Rabema benchmark both on simulated and real data, within an error rate of 5 %. Therefore, I built a Rabema gold standard for each dataset by running RazerS 3 in full-sensitive mode up to 5 % error rate. I provided unpaired reads to each tool as the Rabema benchmark by definition does not consider paired-end reads. Results are shown in table 7.2.

7.2.4 Throughput on real data

This experiment complements the sensitivity evaluation on real data provided by the Rabema benchmark. The goal of this experiment is to determine if read mappers are able to sustain sequencing throughput of the instrument or constitute a potential bottle-

Table 7.2: Rabema benchmark results on the human whole genome. The left panel shows the results of mapping 1 M Illumina-like 2×100 bp simulated reads; the right panel shows the results of mapping 1 M Illumina 2×100 bp real reads. Big numbers show total Rabema scores, while small numbers show marginal scores for the mapping locations at $\binom{0 \ 1 \ 2}{3 \ 4 \ 5}$ % error rate.

		hiseq_hg19_like						ERR161544					
		H. sapiens						H. sapiens					
tool		all		all-best		any-best		all		all-best		any-best	
best	Yara	92.09	100.00 97.99 85.94 40.28 10.10 2.56	100.00	100.00 100.00 100.00 100.00 99.94 99.71	100.00	100.00 100.00 100.00 100.00 99.94 99.83	90.49	100.00 94.64 75.66 50.19 30.86 14.27	99.99	100.00 100.00 100.00 99.96 99.88 99.40	99.99	100.00 100.00 100.00 99.96 99.90 99.53
	Gem	93.71	100.00 98.73 90.88 61.29 31.48 15.01	99.99	100.00 99.99 99.95 99.84 99.23 97.97	100.00	100.00 100.00 99.98 99.95 99.71 98.39	93.25	100.00 96.64 84.54 72.12 55.35 31.75	99.94	100.00 99.98 99.91 99.71 99.48 94.16	99.95	100.00 99.99 99.97 99.84 99.77 95.12
	Bowtie 2	90.98	98.86 96.87 83.98 38.88 9.79 2.47	97.60	97.67 97.81 95.73 94.89 95.59 95.64	99.88	100.00 99.99 97.74 96.83 97.14 97.72	88.40	98.58 92.21 70.69 44.59 25.30 9.41	95.82	97.17 95.00 87.74 81.88 76.13 64.68	99.57	100.00 99.94 97.33 94.98 90.74 81.12
	BWA	90.93	98.86 96.87 84.84 37.15 7.77 1.73	97.59	97.67 97.82 97.70 91.33 76.10 67.27	99.88	100.00 99.99 99.88 93.38 77.51 68.61	88.40	98.58 92.22 71.29 44.08 24.74 9.45	95.90	97.17 94.99 89.67 82.49 75.82 65.10	99.68	100.00 99.99 99.56 96.06 90.95 82.74
all	Yara	99.82	100.00 100.00 100.00 99.99 99.56 96.27	100.00	100.00 100.00 100.00 100.00 99.94 99.71	100.00	100.00 100.00 100.00 100.00 99.94 99.83	99.83	100.00 100.00 100.00 99.98 99.72 97.17	99.99	100.00 100.00 100.00 99.96 99.88 99.43	99.99	100.00 100.00 100.00 99.97 99.89 99.54
	Gem	95.27	100.00 99.04 94.93 70.97 48.00 34.47	99.75	100.00 99.06 99.61 99.64 99.20 97.88	100.00	100.00 100.00 99.99 99.98 99.71 98.39	95.18	100.00 98.13 92.41 80.50 67.39 47.99	99.65	100.00 98.32 98.97 99.03 99.02 93.72	99.95	100.00 99.98 99.97 99.82 99.76 95.10
	Hobbes 2	99.91	100.00 100.00 100.00 100.00 99.89 98.04	100.00	100.00 100.00 100.00 99.99 100.00 99.91	100.00	100.00 100.00 100.00 100.00 100.00 100.00	—	—	—	—	—	—
	RazerS 3	100.00	100.00 100.00 100.00 100.00 100.00 100.00	100.00	100.00 100.00 100.00 100.00 100.00 100.00	100.00	100.00 100.00 100.00 100.00 100.00 100.00	100.00	100.00 100.00 100.00 100.00 100.00 100.00	100.00	100.00 100.00 100.00 100.00 100.00 100.00	100.00	100.00 100.00 100.00 100.00 100.00 100.00

neck in the data analysis pipeline. The Illumina HiSeq 2500 in a six days run produces¹ up to 800 Gbp as 2×100 bp paired-end reads. The experiment measures read mapping throughput in *giga base pairs per hour* (Gbp/h); under this measure the maximum throughput of the Illumina HiSeq 2500 is 5.56 Gbp/h.

For an accurate throughput estimation, best-mappers processed 10 M Illumina 2×100 bp reads, while for all-mappers it was sufficient to process 1 M reads. For a fair comparison, best-mappers produced a SAM file as expected by de-facto standard best-mapping pipelines, while all-mappers output a file in native format (SAM for Yara and Hobbes 2, custom for Gem and RazerS 3).

¹ According to the specifications at http://res.illumina.com/documents/products/datasheets/datasheet_hiseq2500.pdf for high output run mode with dual flow cell.

Table 7.3: Read mapping throughput on the human whole genome. All tools run using 8 threads on a desktop computer equipped with an Intel Core i7-4770K CPU. The left panel shows the results of mapping 2×100 bp Illumina HiSeq 2000 reads as single-end; the right panel shows the results of mapping the same reads as paired-end. The maximum throughput of an Illumina HiSeq 2500 is 5.56 Gbp/h.

	tool	ERR161544 100 bp		ERR161544 2x100 bp	
		throughput	memory	throughput	memory
		[Gbp/h]	[Mb]	[Gbp/h]	[Mb]
best	Yara	12.59	5072	11.39	5093
	Gem	8.19	4438	13.35	4430
	Bowtie 2	6.60	3326	6.69	3370
	BWA	4.36	4579	3.77	4759
all	Yara	1.27	5549	1.34	6210
	Gem	0.84	5356	1.64	4733
	Hobbes 2	–	–	–	–
	RazerS 3	0.10	19065	0.17	9139

APPENDIX

A Dictionary search and join

A

Dictionary search is a restriction of string matching. Given a set of database strings \mathbb{D} and a query string q , the approximate dictionary search problem is to find all strings in \mathbb{D} within distance k from q . Note that usually the query string q has length similar to strings in \mathbb{D} , as $||d| - |q|| \leq k$ is a necessary condition for $d_E(d, q) \leq k$.

A.1 Online methods

The problem can be solved by checking whether $d_E(d, q) \leq k$ for all $d \in \mathbb{D}$. Answering the question whether the distance $d_E(d, q) \leq k$ is an easier problem than computing the edit distance $d_E(d, q)$: a band of size $k + 1$ is sufficient.

Lemma A.1. *The k -differences global alignment problem can be solved by computing only a diagonal band of the DP matrix of width $k + 1$, where the leftmost band diagonal is $\lfloor \frac{m-n+k}{2} \rfloor$ cells left of the main diagonal (see Figure ??).*

Proof. Indirect. Assume that a cell outside the band is part of a global alignment with at most k errors. If the cell is left of the band, the traceback that starts in the top left corner would go down at least $c = \lfloor \frac{m-n+k}{2} \rfloor + 1$ cells. Then it needs to go right at least $n - m + c$ cells to end in the bottom right corner. Hence it contains at least $n - m + 2c > n - m + 2 \frac{m-n+k}{2} = k$ errors. The assumption that the cell is right of the band can be falsified analogously. \square

Figure A.1: DP table representing the match of $p = \dots$ in $t = \dots$

ϵ	C	G	C	A	N	A	T	A	T	C	A	G								
ϵ	0	1	2	3	4	5	6	7												
C	0	1	2	3	4	5	6	7	8											
G	0	1	2	3	4	5	6	7	8	9										
C	0	1	2	3	4	5	6	7	8	9	10									
A		0	1	2	3	4	5	6	7	8	9	10								
N			0	1	2	3	4	5	6	7	8	9	10							
A				0	1	2	3	4	5	6	7	8	9	10						
T					0	1	2	3	4	5	6	7	8	9	10					
A						0	1	2	3	4	5	6	7	8	9	10				
T							0	1	2	3	4	5	6	7	8	9	10			
C								0	1	2	3	4	5	6	7	8	9	10		
A									0	1	2	3	4	5	6	7	8	9	10	
G										0	1	2	3	4	5	6	7	8	9	10

A.2 Indexed methods

Using a radix tree \mathcal{D} we can find all strings in \mathbb{D} equal to a query string q , in optimal time $\mathcal{O}(|q|)$ and independently of $||\mathbb{D}||$.

Algorithm A.1 Exact dictionary search on a radix trie.

```

1: procedure EXACTSEARCH( $x, p$ )
2:   if  $p = \epsilon$  then
3:     report  $\mathbb{E}(x)$ 
4:   else if  $\exists c \in \mathbb{C}(x) : \text{label}(c) = p_1$  then
5:     EXACTSEARCH( $c, p_{2..|p|}$ )

```

Figure A.2: Exact dictionary search on a suffix trie.



A.3 Filtering methods

Filtering methods of section 2.5.3 can be directly applied to solve the dictionary search problem. Database strings satisfying the filtering condition can be verified with algorithm ??.

B Read mappers parameterization

B.1 Masai evaluation

In the following, I give the exact parameterization of each read mapper considered in the evaluation of section ??.

Masai Version 0.5 was used. In order to use Masai as an all-mapper, we passed the argument `-all`, otherwise the argument `-any-best` is used by default. We set the maximal edit distance using the parameter `-e`. We configured the seed length with the parameter `-seed-length`; on *E. coli*, *D. melanogaster* and *C. elegans* we chose a seed length of 16, while on *H. sapiens* we chose a seed length of 33. We selected the SAM output format with `-os` and enabled CIGAR output with `-oc`.

Bowtie 2 Version 2.0.0-beta6 was used. We used the parameter `-end-to-end` to enforce semi-global read alignments. For the Rabema experiment we used the parameter `-k 100`.

BWA Version 0.6.1-r104 was used. For the Rabema experiment we passed the parameter `-N` to `aln` and `-n 100` to `samse`.

Soap 2 Version 2.1 was used.

RazerS 3 Version 3.1 was used. We mapped with indels using the pigeonhole filter (default) and set the error rate through the parameter `-i`, e.g. `-i 95` to map within an error rate of 5 %. We selected the native or SAM output format with `-of 0` or `-of 4`.

Hobbes Version 1.3 was used. We built the index using the recommended q -gram length 11. Since we focus on edit distance, we used the 16 bit bit-vector version. We enabled indels with `-indels` and set maximal edit distance using the parameter `-v`. For resource measurement we used the output without CIGAR, for analyzing the results we enabled CIGAR output using `-cigar`.

mrFAST Version 2.1.0.6 was used. We set maximal edit distance using the parameter `-e`.

SHRiMP 2 Version 2.2.2 was used.

B.2 Yara evaluation

In the following, I give the exact parameterization of each read mapper considered in the evaluation of section 7.2. Below, MIN and MAX are placeholders for minimal and maximal insert size, while INS is the mean insert size and ERR its allowed deviation, i.e. $INS = (MIN + MAX) / 2$, $ERR = (MAX - MIN) / 2$.

Yara Version 1.0 was used. To perform all-mapping, we passed the argument `-all`; by default, the tool runs as a best-mapper. We set the error rate using the parameter `-e`. In paired-end mode, the parameters used were `-library-length INS -library-error ERR`. The number of threads was set with the parameter `-t`.

GEM Version 1.376 was used. We set the error rate using the parameters `-m` and `-e`, then we disabled adaptive mapping using the parameter `-quality-format ignore`. In best-mapping, to analyze only the best stratum, we passed the argument `-s 0`; in all-mapping, to analyze all strata, we passed `-d all -D all -s all -max-big-indel-length 0`. In single-end mode, we passed the parameter `-expect-single-end-reads`; in paired-end mode, we passed `-paired-end-alignment`, along with `-min-insert-size MIN -max-insert-size MAX`, and `-map-both-ends` to select the workflow mapping both reads independently. The number of threads was selected using the parameter `-t`.

Bowtie 2 Version 2.2.1 was used. We used the parameter `-end-to-end` to enforce semi-global read alignments. In paired-end mode, we used the parameters `-minins MIN -maxins MAX`. The number of threads was selected using the parameter `-p`.

BWA Version 0.7.7-r441 was used. We used the parameter `-t` to select the number of threads in the `aln` step; the `sampe` and `samse` steps were performed using one thread since BWA does not offer any parallelization here.

Hobbes 2 Version 2.1 was used. We built the index using the recommended q -gram length 11. We enabled edit distance with `-indels` and set the distance threshold using the parameter `-v`. In paired-end mode, we used the parameters `-pe -min MIN -max MAX`. Multi-threading was enabled using `-p`.

RazerS 3 Version 3.2 was used. We set the error rate through the parameter `-i`, e.g. `-i 95` to map within an error rate of 5 %. We passed the option `-rr 100` to set the recognition rate to 100 % and `-m 1000000` to output all mapping locations per read. In paired-end mode, the parameters used were `-library-length INS -library-error ERR`. The number of threads was set with the `-tc` parameter.

C Declaration

I declare that this thesis is my own work and has not been submitted in any form for another degree or diploma at any university or other institute of tertiary education. Information derived from the published and unpublished work of others has been acknowledged in the text and a list of references is given.

Enrico Siragusa
August 3, 2014

BIBLIOGRAPHY

- Ahmadi, A., Behm, A., Honnalli, N., Li, C., Weng, L., and Xie, X. (2012). Hobbes: optimized gram-based methods for efficient read alignment. *Nucleic Acids Res.*, **40**(6), page e41.
- Baeza-Yates, R. A. and Gonnet, G. H. (1999). A fast algorithm on average for all-against-all sequence matching. In *SPIRE/CRIWG*, pages 16–23. IEEE.
- Baeza-Yates, R. A. and Navarro, G. (1999). Faster approximate string matching. *Algorithmica*, **23**(2), pages 127–158.
- Bauer, M. J., Cox, A. J., and Rosone, G. (2013). Lightweight algorithms for constructing and inverting the bwt of string collections. *Theoretical Computer Science*, **483**, pages 134–148.
- Burkhardt, S. and Karkkainen, J. (2001). Better filtering with gapped q-grams. In *CPM*, volume 1, pages 73–85. Springer.
- Burrows, M. and Wheeler, D. J. (1994). A block-sorting lossless data compression algorithm.
- Crochemore, M., Grossi, R., Kärkkäinen, J., and Landau, G. M. (2013). A constant-space comparison-based algorithm for computing the burrows–wheeler transform. In *Combinatorial Pattern Matching*, pages 74–82. Springer.
- DePristo, M. A., Banks, E., Poplin, R., Garimella, K. V., Maguire, J. R., Hartl, C., Philippakis, A. A., del Angel, G., Rivas, M. A., Hanna, M., *et al.* (2011). A framework for variation discovery and genotyping using next-generation dna sequencing data. *Nature genetics*, **43**(5), pages 491–498.
- Derrien, T., Estellé, J., Marco Sola, S., Knowles, D. G., Raineri, E., Guigó, R., and Ribeca, P. (2012). Fast computation and applications of genome mappability. *PLoS ONE*, **7**(1), page e30377.
- Elias, P. (1975). Universal codeword sets and representations of the integers. *Information Theory, IEEE Transactions on*, **21**(2), pages 194–203.
- Ewing, B. and Green, P. (1998). Base-calling of automated sequencer traces using phred. ii. error probabilities. *Genome research*, **8**(3), pages 186–194.

- Ewing, B., Hillier, L., Wendl, M. C., and Green, P. (1998). Base-calling of automated sequencer traces using phred. i. accuracy assessment. *Genome research*, **8**(3), pages 175–185.
- Faro, S. and Lecroq, T. (2013). The exact online string matching problem: a review of the most recent results. *ACM Computing Surveys (CSUR)*, **45**(2), page 13.
- Farrar, M. (2007). Striped smith–waterman speeds database searches six times over other simd implementations. *Bioinformatics*, **23**(2), pages 156–161.
- Ferragina, P. and Manzini, G. (2000). Opportunistic data structures with applications. In *Foundations of Computer Science, 2000. Proceedings. 41st Annual Symposium on*, pages 390–398. IEEE.
- Ferragina, P. and Manzini, G. (2001). An experimental study of an opportunistic index. In *SODA*, pages 269–278.
- Fonseca, N. A., Rung, J., Brazma, A., and Marioni, J. C. (2012). Tools for mapping high-throughput sequencing data. *Bioinformatics*, **28**(24), pages 3169–3177.
- Gusfield, D. (1997). *Algorithms on strings, trees, and sequences: Computer science and computational biology*. Cambridge University Press, New York, NY, USA.
- Hach, F., Hormozdiari, F., Alkan, C., Hormozdiari, F., Birol, I., Eichler, E. E., and Sahinalp, S. C. (2010). mrsFAST: a cache-oblivious algorithm for short-read mapping. *Nat. Methods*, **7**(8), pages 576–577.
- Hatem, A., Bozda, D., Toland, A. E., and Çatalyürek, Ü. V. (2013). Benchmarking short sequence mapping tools. *BMC bioinformatics*, **14**(1), page 184.
- Holtgrewe, M., Emde, A.-K., Weese, D., and Reinert, K. (2011). A novel and well-defined benchmarking method for second generation read mapping. *BMC Bioinformatics*, **12**, page 210.
- Intel (2011). *Intel® 64 and IA-32 Architectures Optimization Reference Manual*. Intel Corporation.
- Jacobson, G. (1989). Space-efficient static trees and graphs. In *Foundations of Computer Science, 1989., 30th Annual Symposium on*, pages 549–554. IEEE.
- Jokinen, P. and Ukkonen, E. (1991). Two algorithms for approximate string matching in static texts. In *Mathematical Foundations of Computer Science 1991*, pages 240–248. Springer.
- Kärkkäinen, J. and Sanders, P. (2003). Simple linear work suffix array construction. *ICALP*, pages 943–955.
- Knuth, D. (1973). *The Art of Computer Programming. Volume 3, Addison-Wesley*.

-
- Kucherov, G., No  , L., and Roytberg, M. (2005). Multiseed lossless filtration. *IEEE/ACM Transactions on Computational Biology and Bioinformatics (TCBB)*, **2**(1), pages 51–61.
- Kurtz, S. (1999). Reducing the space requirement of suffix trees. *Software-Practice and Experience*, **29**(13), pages 1149–71.
- Langmead, B. and Salzberg, S. L. (2012). Fast gapped-read alignment with Bowtie 2. *Nat. Methods*, **9**(4), pages 357–359.
- Langmead, B., Trapnell, C., Pop, M., and Salzberg, S. L. (2009). Ultrafast and memory-efficient alignment of short DNA sequences to the human genome. *Genome Biol.*, **10**(3), page R25.
- Lee, H. and Schatz, M. C. (2012). Genomic dark matter: the reliability of short read mapping illustrated by the genome mappability score. *Bioinformatics*, **28**(16), pages 2097–2105.
- Li, H. and Durbin, R. (2009). Fast and accurate short read alignment with burrows-wheeler transform. *Bioinformatics*, **25**(14), pages 1754–1760.
- Li, H. and Durbin, R. (2010). Fast and accurate long-read alignment with burrows-wheeler transform. *Bioinformatics*, **26**(5), pages 589–595.
- Li, H. and Homer, N. (2010). A survey of sequence alignment algorithms for next-generation sequencing. *Brief Bioinform.*, **11**(5), pages 473–483.
- Li, H., Ruan, J., and Durbin, R. (2008). Mapping short dna sequencing reads and calling variants using mapping quality scores. *Genome research*, **18**(11), pages 1851–1858.
- Li, H., Handsaker, B., Wysoker, A., Fennell, T., Ruan, J., Homer, N., Marth, G., Abecasis, G., Durbin, R., and 1000 Genome Project Data Processing Subgroup (2009a). The sequence alignment/map format and SAMtools. *Bioinformatics*, **25**(16), pages 2078–2079.
- Li, R., Yu, C., Li, Y., Lam, T.-W., Yiu, S.-M., Kristiansen, K., and Wang, J. (2009b). SOAP2: an improved ultrafast tool for short read alignment. *Bioinformatics*, **25**(15), pages 1966–1967.
- Liu, C.-M., Wong, T., Wu, E., Luo, R., Yiu, S.-M., Li, Y., Wang, B., Yu, C., Chu, X., Zhao, K., *et al.* (2012). Soap3: ultra-fast gpu-based parallel alignment tool for short reads. *Bioinformatics*, **28**(6), pages 878–879.
- Manber, U. and Myers, G. (1990). Suffix arrays: a new method for on-line string searches. In *SODA*, pages 319–327.
- Marco-Sola, S., Sammeth, M., Guig  , R., and Ribeca, P. (2012). The gem mapper: fast, accurate and versatile alignment by filtration. *Nature methods*, **9**(12), pages 1185–1188.

- Morrison, D. R. (1968). Patricia- \square practical algorithm to retrieve information coded in alphanumeric. *J. ACM*, **15**(4), pages 514–534.
- Myers, E. W. (1994). A sublinear algorithm for approximate keyword searching. *Algorithmica*, **12**(4-5), pages 345–374.
- Navarro, G. (2001). A guided tour to approximate string matching. *ACM Comput. Surv.*, **33**(1), pages 31–88.
- Navarro, G. and Baeza-Yates, R. A. (2000). A hybrid indexing method for approximate string matching. *Journal of Discrete Algorithms*, **1**(1), pages 205–239.
- Navarro, G., Baeza-Yates, R. A., Sutinen, E., and Tarhio, J. (2001). Indexing methods for approximate string matching. *IEEE Data Eng. Bull.*, **24**(4), pages 19–27.
- Nicolas, F. and Rivals, E. (2005). Hardness of optimal spaced seed design. In *Combinatorial Pattern Matching*, pages 144–155. Springer.
- Schürmann, K.-B. and Stoye, J. (2007). An incomplex algorithm for fast suffix array construction. *Software: Practice and Experience*, **37**(3), pages 309–329.
- Seward, J. (1996). bzip2 and libbzip2. available at <http://www.bzip.org>.
- Siragusa, E., Weese, D., and Reinert, K. (2013). Fast and accurate read mapping with approximate seeds and multiple backtracking. *Nucleic Acids Res.*
- Treangen, T. J. and Salzberg, S. L. (2011). Repetitive dna and next-generation sequencing: computational challenges and solutions. *Nature Reviews Genetics*, **13**(1), pages 36–46.
- Ukkonen, E. (1993). Approximate string-matching over suffix trees. In *CPM*, pages 228–242.
- Weese, D. (2013). *Indices and Applications in High-Throughput Sequencing*. Ph.D. thesis, Freie Universität Berlin.
- Weese, D., Emde, A.-K., Rausch, T., Döring, A., and Reinert, K. (2009). RazerS-fast read mapping with sensitivity control. *Genome Res.*, **19**(9), pages 1646–1654.
- Weese, D., Holtgrewe, M., and Reinert, K. (2012). RazerS 3: Faster, fully sensitive read mapping. *Bioinformatics*. 10.1093/bioinformatics/bts505.
- Wilkes, M. V. (1995). The memory wall and the cmos end-point. *ACM SIGARCH Computer Architecture News*, **23**(4), pages 4–6.

LIST OF FIGURES

2.1	Example of edit transcript	10
2.2	Example of dotplot	11
2.3	Example of DP table	13
2.4	Example of approximate string matching via DP	15
2.5	Example of suffix trie and suffix tree	16
2.6	Example of generalized suffix trie	16
3.1	Example of suffix array	20
3.2	Example of generalized suffix array	21
3.3	Example of q -gram index	24
3.4	Example of Burrows-Wheeler transform	26
3.5	Example of functions LF and Ψ	27
3.6	Example of BWT inversion	28
3.7	Example of rank dictionaries	30
3.8	Example of rank dictionaries	31
3.9	Top-down traversal runtime	33
3.10	Exact string matching on a suffix tree	34
3.11	Exact string matching runtime	36
3.12	Approximate string matching on a suffix trie.	36
3.13	k -mismatches runtime	37
3.14	Multiple exact string matching runtime	38
3.15	Multiple k -mismatches runtime	39
4.1	Filtration with exact seeds.	42
4.2	Filtration with approximate seeds	44
4.3	Filtration with q -grams.	46
4.4	Filtration with gapped q -grams	47
A.1	Example of k -differences global alignment via DP.	89
A.2	Exact dictionary search on a suffix trie.	90

LIST OF TABLES

5.1	Mappability of model genomes	62
5.2	Human genome mappability score	63
6.1	Masai results in the Rabema benchmark	75
6.2	Masai variant detection results	76
6.3	Masai performance on real data	78
6.4	Masai filtration efficiency results	79
7.1	Yara accuracy results	86
7.2	Yara results in the Rabema benchmark	87
7.3	Yara throughput on real data	88

LIST OF AlgorithmS

2.1	goDOWN(x)	17
2.2	goRIGHT(x)	17
3.1	L(x, c)	22
3.2	R(x, c)	22
3.3	goROOT(x)	22
3.4	goDOWN(x, c)	22
3.5	goDOWN(x)	23
3.6	goRIGHT(x)	23
3.7	L(x, c)	24
3.8	R(x, c)	24
3.9	goROOT(x)	25
3.10	goDOWN(x, c)	25
3.11	EXACTSEARCH(t, p)	25
3.12	goROOT(x)	32
3.13	goDOWN(x, c)	32
3.14	DFS(x, d)	33
3.15	EXACTSEARCH(t, p)	34
3.16	KMISMATCHES(t, p, e)	35
3.17	KDIFFERENCES(t, p, D)	35
3.18	MULTIPLEEXACTSEARCH(t, p)	37
3.19	MULTIPLEKMISMATCHES(t, p, e)	38
A.1	Exact dictionary search on a radix trie.	90

